#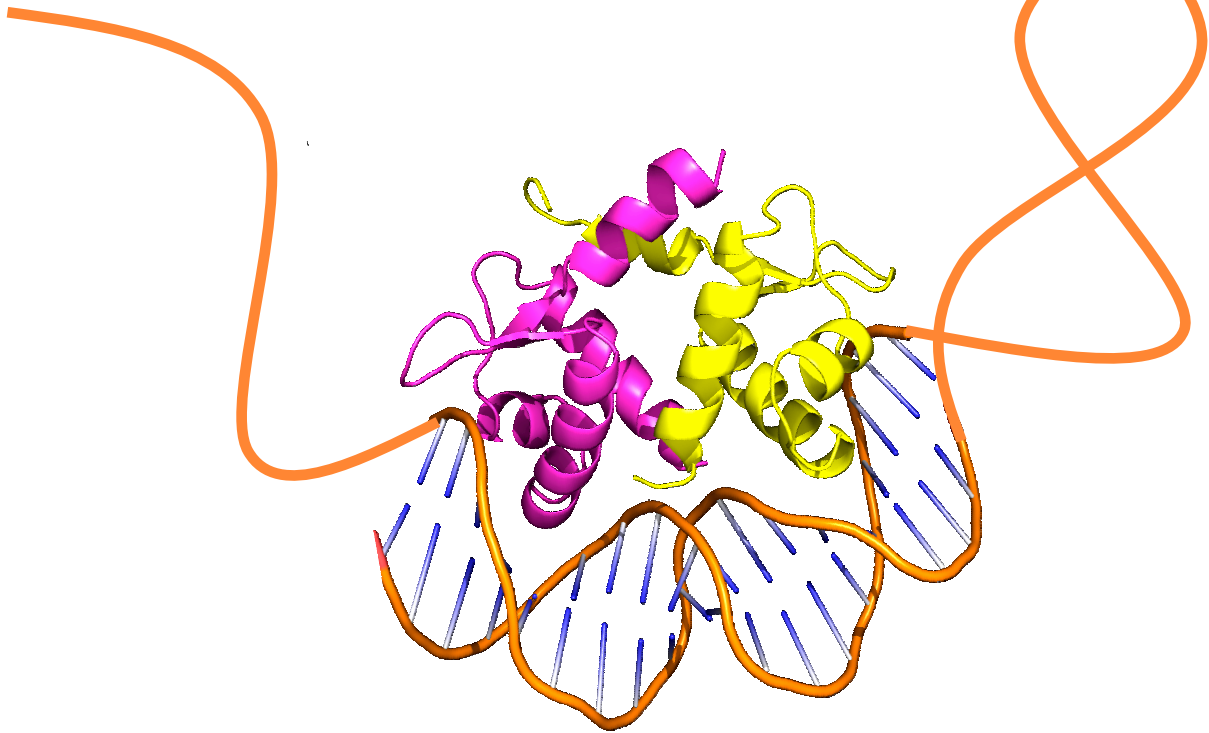 Molecular characterization of the transcriptional regulator TtgV in *Pseudomonas putida* DOT-T1E, a solvent tolerant strain

Sandy Fillet

**CONSEJO SUPERIOR DE INVESTIGACIONES CIENTIFICAS
ESTACIÓN EXPERIMENTAL DEL ZAIDÍN**

eez

CSIC

UNIVERSIDAD DE GRANADA
DEPARTAMENTO DE MICROBIOLOGÍA

Universidad de Granada

Molecular characterization of the transcriptional regulator TtgV in *Pseudomonas putida* DOT-T1E, a solvent tolerant strain

TESIS DOCTORAL

Sandy Fillet

Granada, 2010

Molecular characterization of the transcriptional regulator TtgV in *Pseudomonas putida* DOT-T1E, a solvent tolerant strain

Memoria que presenta la licenciada en Biología, Sandy Fillet, para aspirar al título de Doctora en Microbiología

Fdo.: Sandy Fillet

V°B° El director
Fdo.: Juan Luis Ramos Martín
Doctor en Biología
Profesor de Investigación del C.S.I.C

Universidad de Granada

2010

Esta Tesis Doctoral ha sido realizada en el Departamento de Protección Ambiental de la Estación Experimental del Zaidín, perteneciente al Consejo Superior de Investigaciones Científicas.

This PhD was realized in the Environment Department of the Estación Experimental del Zaidín, part of the Consejo Superior de Investigaciones Científicas.

À ma mère, à mon père,
À Gaëlle, Kinda et Guillaume,
À Mélissa, Imèd et Rayan,

" Nous ne sommes que des grains de sable mais nous sommes ensemble. Nous sommes comme les grains de sable sur la plage, mais sans les grains de sable la plage n'existerait pas. "

Bernard Weber

Indice

Crystal structures of tetrameric TtgV in complex with DNA reveal a novel coopeative binding and induction mechanism

Domain organization of the TtgV repressor: Identification of Glu102 and Arg98 as key residues in interdomain communication

Abbreviations

Abbreviations	meaning
ABC	ATP-binding cassette
AFM	Atomic force microscopy
CL	cardiolipid
cti	*cis*-to-*trans* isomerase
Da	Dalton or g/mol
ΔG	change of Gibbs energy
ΔH	change of enthalpy
ΔS	change of entropy
DSC	Differential Scanning Calorimetry
DTT	Dithiothreitol
HS	Heat Shock
HTH	Helix Turn Helix
IPTG	isopropyl-β-D-thiogalactopyranoside
IR	Inverted Repeat
ITC	Isothermal Titration Calorimetry
K_D	dissociation constant
LB	Luria Bertani medium
MATE	multidrug and toxic-compounds extrusion
MDR	multidrug resistance
MFS	major facilitator superfamily
PE	phosphatidylethanolamine
PG	phosphatidylglycerol
RND	Resistance-Nodulation-Cell-Division
SMR	small multidrug resistance
Ttg	Toluene tolerence gene

Figures' indice

Tables' indice

Introduction

1.   *Aromatic compounds*

Hydrocarbons are composed of hydrogen and carbon atoms, and those that exhibit one or several benzene rings are called aromatic hydrocarbons. These chemicals can be based on a single benzene ring and this set are called monoaromatic hydrocarbons or can be made of several benzene rings and are called Polycyclic aromatic hydrocarbons.. (PAHs). All this set of aromatic compounds is widely distributed in the environment (Sudip *et al*, 2002). Gibson and Subramanian (1984) described that the greatest part of aromatic compounds on the Ecosphere are derived from natural pyrolysis of organic chemicals, although with recent industrialisation and large number of cars a significant fraction of PAHs are from anthropogenic origin. The nature of the aromatic compounds is influenced by the temperature of pyrolysis.

Although catastrophes such as the sunk of the Prestige oil tanker or the recent oil spill in the Golf of Mexico has attracted widely the attention of the public, it should be mentioned that the OCDE has warmed its member states of the relevance of aromatic hydrocarbon pollution due to daily activities. The OCDE considers this a major problem and urged member sates to put attention in this problem and requested measures to deal with these pollutants and their abatement. Problems derived from crude oil pollution had another relevant side that comes from the fact that its composition of varies from one site to another. Crude oils contain multiple hydrocarbons with sulphur, nitrogen and oxygen substituent, the chemical structures can also act as "traps" to capture metal and for this reason lead, nickel and molybdenum have been reported to be a relevant contaminant associated to crude oils. Non substituted hydrocarbons are represented by aliphatic hydrocarbons, naphthalenes and low and high molecular weight polyaromatic hydrocarbons. It should be noted that 17% of aromatic compounds has alkyl lateral chains, of up 6 atoms of carbon (Figure 1)., what make them more resistant to biodegradation.

In soils monocyclic aromatic hydrocarbons like benzene, toluene, ethylbenzene and xylenes are commonly found. These chemicals are among the 50 products with the highest industrial production. Aromatic hydrocarbons are used frequently in a many specialized sectors; however, the main environmental source is the refining of crude petroleum. Benzene, xylenes, toluene and naphthalene are found in paints, glues, paraffin for furniture and many industrial aerosols.
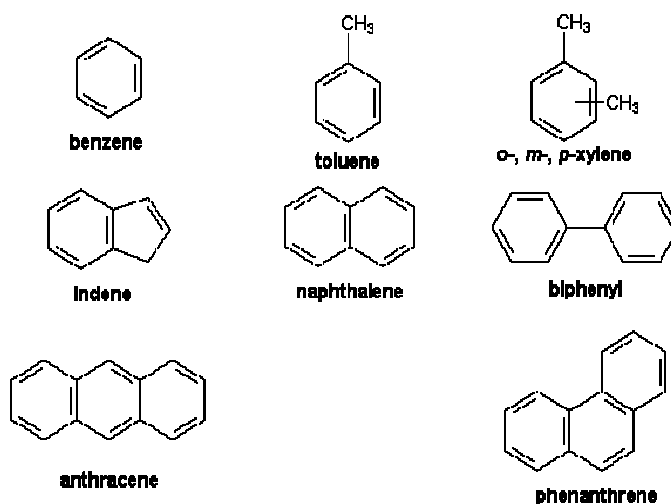
Figure 1. Biochemical structures of some aromatic compounds.

Aromatic hydrocarbons compounds are volatile, what facilitates their dispersion in the atmosphere and in the aquatic medium, they are toxic and noxious for humans and animals. Exposure to high concentrations of aromatic hydrocarbons damage the central nervous system and prolonged exposure at low doses can alter other physical capacities. Because of their toxic, mutagenic and/or carcinogenic properties, these compounds are toxic for –microorganisms, plants,animals and humans. Aromatic compounds toxicity is related to the log P_{ow}, which is the logarithm of the partition coefficient of the compound in a defined mix of octanol-water (Sikkema *et al*, 1995). Compounds having a log P_{ow} below 3, like toluene (P_{ow} 2.69), benzene (P_{ow} 2.13) and styrene (P_{ow} 2.95) are extremely toxic because they accumulate in the cytoplasmic membrane and disorganise its structure, which results in a loss of ions, metabolites, changes the intercellular pH and electrical potential, eventually leading to cell death (De Smet *et al*, 1978; Sikkema *et al*, 1995).

Various physicochemical methods have been used to remove toxic aromatic compounds from the environment; however, they are rather recalcitrant. Isolation of bacteria able to resist and degrade solvents has opened numerous possibilities for the removal of these compounds from the environment. In 1908, Stormer was the first to isolate a strain of *Bacillus hexacarbovorum* able to use toluene and xylenes as a carbon source. Because of the constant exposure to aromatic hydrocarbons at low concentrations, microbes have evolved numerous pathways for their metabolism, and the biodegradation of aromatic chemicals has been integrated by microorganisms into the carbon cycle. In addition, a limited number of Gram negative and Gram positive microorganisms have been identified as tolerantto these toxic chemicals and have been the subject of studies aimed to the understanding of the mechanisms that allow bacteria to overcame the stress imposed by these compounds (Ramos *et al.,* 1995; Isken and de Bont, 1996). A number of strategies have been developed to use microbes as mean of biological treatments -known as bioremediation- so that microbes with bioremediation potential are said that can be prescribed as an "environmental medicine".

Bacteria of the genus *Pseudomonas* are widespread in the environment and are represented by a large number of species (Moore *et al.*, 2009). *Pseudomonas* are Gram negative, rod-shaped and are motile due to the presence of one or several polar flagella, the number of which varies according to the species (Figure 2). The genus *Pseudomonas* presents wide habitat diversity, for example, the most common human pathogen is *Pseudomonas aeruginosa* and it forms biofilms in the human lung (Costerton *et al.,* 1999; Singh *et al.,* 2000), whereas *Pseudomonas syringae* is an insidious plant pathogen (Niepold *et al.,* 1985; Setubal *et al.,* 2005). Plant surfaces are also a preferred environment of *Pseudomonas fluorescens* (Rainey 1999; Preston *et al.,* 2001) and *Pseudomonas putida* (Lee and Cooksey 2000; Ramos-Gonzáles and Ramos, 2005), bacteria of these species, commonly isolated from soil, can be often found localised on the surface of plant roots and even on plant leaves.

Figure 2. TEM image of *Pseudomonas sp.* Their dimensions range between 0,5 and 1,0 μm x 1,5 to 4,0 μm. Magnification of the image : x 3,515. *Photographer: Dennis Kunkel.*

The capacity of *Pseudomonas* to adapt and survive in so many different ecological niches can be explained by their large genomes, which often exceed 6 Mb. The first sequencing project of *Pseudomonas* genome was completed in 2000 with *P. aeruginosa* PAO1 strain (Stover *et al.,* 2000); this revealed that its size was comparable to that of a simple eukaryote like *Saccharomyces cerevisiae.* The sequencing of the soil bacterium *P. putida* KT2440 by a German-American consortium (Nelson *et al.*, 2002) provided significant new understanding on the ubiquitous location in the environment of this group of bacteria. The genome of *P. putida* KT2440 consists of a single circular chromosome of 6,181,863 base pairs, with an average G+C content of 59%, although the G+C range from regions with 43% to region with 69% G+C. The genome structure allowed to identify gene islands, mobile elements, phages and transposons revealing the high capacity that *P. putida* to acquire new genetic information *via* horizontal gene transfer.

A large number of strains of *P. putida* have been isolated based on their ability to use biogenic and xenobiotic compounds. This makes this species very appealing tool for microbiological and biotechnological research, what together with its biochemical characteristics and its ease for genetic manipulation has made this species a model microorganism in bioremediation. *P. putida* is able to colonize the root systems of a large number of plants, establishing and persisting in the rizosphere at a relatively high cell density (Molina *et al.,* 1998; Ramos *et al*, 2002). This species is also able to attach to plant surfaces and form biofilms which facilitates colonization and confer resistance to biotic and abiotic stresses (Yousef-Coronado *et al.,* 2008).

Strains of *P. putida* are a paradigm of metabolically versatile microorganisms that play a relevant role in recycling organic wastes in aerobic and microaerophilic compartments of the environment. Its capacity to survive and adapt to hostile environments is due to its ability to degrade organic chemicals and xenobiotics. Among the unusual properties of *P. putida* is that a number of strains behave as extremophiles because they are solvent-tolerant, examples are *P. putida* DOT-T1E, S12, GM1, or MTB6 that have been described as able to grow in the presence of highly toxic solvents such as *p*-xylene , styrene, octanol, and toluene (Aono *et al*., 1992; Cruden *et al*., 1992; Isken and de Bont, 1996; Kim *et al*., 1998; Ramos *et al*., 1995, Weber *et al*., 1994; Huertas *et al.*, 1998).

In 1995, the laboratory of environmental protection in Granada isolated a strain highly resistant to toluene, which was named *Pseudomonas putida* DOT-T1E. This strain was isolated from a sample taken from a waste water treatment plant in Granada. Initial studies showed that when exposure of this bacterium to 1% (vol/wt) toluene, the number of viable cells decreased by 4 to 5 order of magnitude, but the set of survivors were able to grow colonized the polluted niche (Huertas *et al, 1998).* Under these conditions most microbes are non viable and cannot tolerate this kind of sudden solvent shock.

3.   *Mechanism of solvent tolerance*

Generalities

Pseudomonas putida and other gram negative bacteria use several mechanisms to resist high solvent concentrations. When aromatic compounds are present in the medium, bacteria have to protect themselves from the solvents. The first resistance level takes place at the membrane; contact with solvents induces membrane alterations leading to strong modifications. This impermeabilization is not complete and the solvent that manages to enter the cell provokes an immediate general stress response. This stress response involves the induction of several chaperones that refold proteins denatured by solvent. Another efficient mechanism is the removal of the solvent by efflux pumps that extrude the compounds using energy. A small amount of the internalised solvent can also be degraded by metabolic pathways which allow aromatic compounds to be used as a carbon source (Ramos *et al.*, 2002).

Other bacterial functions are indirectly used to overcome solvent toxicity. For example as a logical consequence of the higher energetic demands, several research groups have observed overexpression of proteins required for energy production (Dominguez-Cuevas *et al.*, 2006; Segura *et al.,* 2005; Volkers *et al*., 2006). One of the most striking examples that have no clear explanation on their role in solvent tolerance is that mutants deficient in flagella assembly are solvent sensitive, it has been suggested that the flagellar transport system may be parasitized by elements involved in the toluene resistance (Segura *et al.,* 2001, Kieboom *et al.,* 2001).

Membrane modification

Gram negative membranes are composed of a phospholipid bilayer which is generally disturbed by the presence of aromatic compounds leading to a characteristic increase in membrane fluidity. Solvent contact with bacterial membranes initiates two different responses: a short-term response consisting of a *cis*-to-*trans* isomerisation of unsaturated fatty acids and a long-term response

changing the saturated-to-unsaturated fatty acid ratio (Pinkart *et al.*, 1997) and phospholipids head group modifications.

In *Pseudomonas*, the three main phospholipid head groups are: phosphatidylethanolamine (PE), phosphatidylglycerol (PG) and cardiolipin (CL). The ratio of these headgroups changes with the growth phase. PG constitutes the most abundant phospholipid in all growth phases, whereas CL accumulates in the stationary phase (Ramos *et al.* 1997; Bernal *et al.*, 2007a). Unsaturated fatty acids forming the phospholipid layer of Gram negative bacteria are synthesised with a *cis* acyl-chain configuration by the cell. In *P. putida* strains, one of the responses to an environmental stress is shifting the double bound to the *trans* configuration through the use of a *cis*-to-*trans* isomerase present in the periplasm (Heipieper *et al.*, 1992; Junker *et al.*, 1999). Bernal and collaborators (2007b) identified the promoters for the *cls* and *cti* genes, encoding cadiolipin synthase and *cis*-to-*trans* isomerase and studied their expression in response to a solvent stress. The *cls* and *cti* genes were expressed constitutively in *P. putida*, while a *cti* mutant exhibited a diminution of membrane rigidity; *cls* mutant had more rigid membranes. Under toluene stress conditions, *cls* and *cls*/*cti* mutants are more sensitive than the wild type; probably due to perturbation in the efflux pump transporters system, whereas *cti* mutant showed a survival equivalent to that of the wild type strain (Bernal *et al.* 2007b). Cls and Cti enzymes present a compensatory role in membrane fluidity but at the level of efflux pump functioning only the cardiolipins are significant.

Other membrane phenomenon such the formation of cyclopropane fatty acids has been proposed to occur in response to environmental stresses (Ramos *et al.* 1997; Bernal *et al.*, 2007a). Cyclopropane fatty acids are the result of a modification of *cis* unsaturated fatty acids involving the addition of a methylene group across the *cis* double bound of unsaturated fatty acids (Grogan and Cronan, 1997; Muñoz-Rojas *et al.*, 2006) (Figure 3). The enzyme catalysing this reaction is the cyclopropane synthase that is expressed in the late-exponential and early-stationary phase of bacterial growth (Grogan and Cronan, 1997). In the *P. putida* genome, two putative cyclopropane synthase genes, *cfaA* and *cfaB*, were found and the one encoded *cfaB* gene has been proposed to be the main cyclopropane synthase in DOT-T1E strain (Pini *et al.*, 2009). Because of the sensitivity of a *cfaB* mutant strain after a toluene shock, *cfaB* seems involved in organic solvent stress (Pini *et al.*, 2009). However, these authors did not report any change in survival when the mutant was compared with the wild type after other type of stress (acid shock, temperature shock, antibiotics shocks, etc) (Pini *et al.*, 2009).

The change of unsaturated fatty acid to cyclopropane fatty acids allows bacteria to counteract the increased membrane fluidity caused by solvent alteration. It allows cells to adapt immediately to new environmental conditions under which denser membrane packaging is a selective advantage.
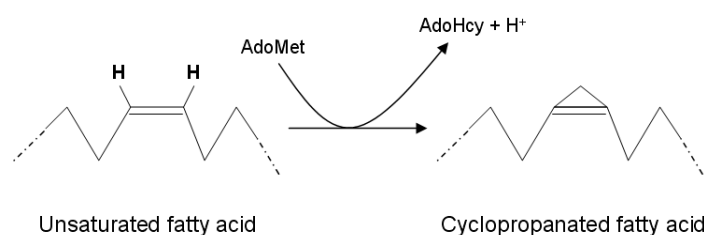
Figure 3. Reaction catalysed by the cyclopropane synthase. (See for details, Pini *et al.,* 2009).

Degradation pathways

Microorganisms have developed a common strategy to degrade aromatic compounds consisting of the incorporation of two hydroxyl groups into the benzenic ring, which destabilizes the aromatic ring structure. Currently, 5 different pathways are known that are able to degrade toluene to catechols: TOL, TOD, TMO, TOM and the TBU pathway. Three of them are present in *Pseudomonas* strains (TOL, TOD and TMO). *P. putida* DOT-T1E is able to degrade toluene into Krebs cycle intermediates via the TOD pathway. All genes implicated in toluene degradation are present in an operon of 10.3 kb (*todXFC1C2BADEGIH*) (Lau *et al.*, 1997; Mosqueda *et al.*, 1999). Mutants in genes of the pathway were as tolerant to solvents as the parental strain, what demonstrated that the degradation pathway is not so relevant in the resistance mechanism (Mosqueda *et al.*, 1999).

Chaperones

Dominguez-Cuevas and collaborators (2006) showed that one major change in response to the addition of the aromatic compounds tested was in genes involved in the so-called Heat Shock (HS) response. First proteomic analysis, permitted to provide evidence of four stress-related protein or chaperones: GroES, Tuf-1, and CspA (Segura *et al.,* 2005). While GroES seems to be related with the protein refolding, CspA2 appears to be involved in protein synthesis under toluene stress. A toluene shock seems to lead to the synthesis of different chaperones contributing to the stabilization of proteins affected by organic solvents, one of them: Tuf-1 could be associated to a periplasmic role. Thanks to microarray assays, several news chaperones involved in the HS response were identified (Dominguez-Cuevas *et al.*, 2006). The HS response leads to an increase in the level of σ^{32}, which sigma factor needs to be stable to be efficient and which is translated in the transcription of σ^{32}–dependent promoters (Dominguez-Cuevas *et al.*, 2006).

Efflux pumps

Efflux pumps are considered the most efficient mechanism of solvent tolerance in Gram negative bacteria. This mechanism consists in pumping excess solvent present in the cell (membrane, periplasm or cytoplasm) to the outer medium. The first studies demonstrating the importance of efflux pumps in solvent tolerance were carried out by Isken and Bont (1996) and Ramos and collaborators (1997) with the isolation of mutants of *P. putida* S12 and DOT-T1E that exhibited impaired functioning of efflux pumps. Numerous studies of these new resistance mechanisms were approached and several efflux pumps identified; as AcrAB, present in *E. coli* K12 strain that is able to expulse antibiotics and solvents using the same transporter (White et al., 1997; Aono, 1998).

Toluene resistance analysis of 19 *Pseudomonas* strains has permitted the determination of 3 different categories of resistance (highly resistant, moderately resistant, and sensitive) (Segura *et al.,* 2003). *P. putida* DOT-T1E, *P. putida* MTB6 and *P. putida* S12 are part of the group of high toluene resistance category; they were able to grow in culture medium with 3% (v/v) solvent in the culture medium. Survival rate after a toluene shock 0,3% of these *Pseudomonas* strains showed that 100% of *P. putida* DOT-T1E, *P. putida* MTB6 and *P. putida* S12 survived if pre-indiced with low concentrations of solvenmts. Segura and collaborators (YEAR) carried out southern hybridization assays and found that the highly resistant strains such as *P. putida* DOT-T1E or *P. putida* MTB6, contain three efflux pumps: TtgABC, TtgDEF and TtgGHI. On the other hand, other *Pseudomonas*

strains classified as moderately resistant (M) included *P. putida* F1 or sensitive (S) like *P. putida* 2440 present in their genome only two or one of this transport systems (Figure 4; Segura *et al.,* 2003). In conclusion, these studies of efflux pump systems of *P. putida* strains allowed the direct correlation of high resistance to solvents with the presence of efflux pumps in the bacterial genome (Segura *et al.,* 2003).

Strains	Tolerance	*ttgABC*	*ttgDEF*	*ttgGHI*
P. putida **DOT-T1E**	**H**	+	+	+
P. putida **MTB6**	**H**	+	+	+
P. putida S12	H	+	-	+
P. putida **F1**	**M**	+	+	-
P. putida MTB5	M	+	+	-
P. putida SMO116	M	+	+	-
P. putida 43	M	+	-	-
P. putida JLR11	M	+	-	-
P. putida **2440**	**S**	+	-	-
P. putida OUS82	S	+	-	-

Figure 4. Identification of homologous efflux pump genes in different *Pseudomonas* sp. strains. The + symbol indicates the presence of the efflux pump corresponding in the *Pseudomonas* genome whereas the symbol – indicates the absence. H, signify Highly resistant; M, Moderately resistant and S, Sensitive. (see for details, Segura *et al.*, 2003).

4. Efflux pumps

MDR systems

Expulsion of toxic compounds is crucial for bacterial survival. Some organisms, like *Pseudomonas*, have the capacity to resist the presence of multiple antimicrobials using multidrug resistance (MDR) efflux systems (Ramos *et al*., 2002; Paulsen, 2003; Ramos *et al.,* 2010). These systems have been the subject of numerous studies because of their importance in bacterial survival, and due to the clinical relevance. To date, drug efflux systems can be divided into 5 groups: the major facilitator super family (MFS), the ATP-binding cassette (ABC), the small multidrug resistance (SMR), the multidrug and toxic-compounds extrusion (MATE) and the resistance/nodulation/cell division (RND) (Figure 5).
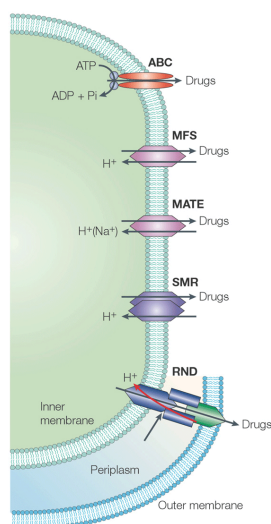
Figure 5. Bacterial drug - and multidrug - efflux pumps found in gram positive and negative bacteria. (See for details Krulwich *et al.,* 2005).

MDR efflux pumps are classified according to the number of components that the pump has (single or multiple), the number of transmembrane-spanning regions that the transporter protein has, the energy source that the pump uses and, the type of substrate that the pump exports. A single organism can express MDR systems from one or more types of efflux pump (Piddock, 2006).

Efflux pumps belonging to the MSF group are found in bacteria, Archaea and eukaryotes. It is a large family that consists of secondary transporters driven by chemiosmotic energy and includes proton/drug antitransporters. QacA is a multidrug exporter from *Staphylococcus aureus,* that provides resistance to monovalent and divalent cationic, lipophilic or antimicrobial compounds via a proton motive force-dependent antiport mechanism (Brown and Skurray, 2001). The *qacA* gene is on a multi-resistance plasmid from a clinical isolate of *S. aureus* and encodes a 514 amino-acid protein with 14 α-helical segments that traverse the cytoplasmic membrane. A number of highly conserved amino acid motifs have been identified within MFS proteins which are likely to be essential for the structure and/or function of these transporters (Paulsen *et al*, 1996).

ABC-type efflux transporters correspond to ATP dependent systems. They have been extensively studied due to their homology with the human multidrug resistance P-glycoprotein ABCB1 which contributes to multidrug resistance in infectious diseases and cancer therapy. P-glycoprotein ABCB1 acts by mediating the energy-dependent extrusion of structurally unrelated chemotherapeutic agents from the cell. LmrA from *Lactococcus lactis* represents the most studied P-glycoprotein ABCB1 homologue, it can functionally substitute ABCB1 in human lung fibroblast and exhibits a substrate specificity similar to the human protein. LmrA consists of six putative transmembrane segments and a nucleotide binding domain. It functions as a homodimer in which the two membrane domains form the solute translocation path across the membrane (Poelarends *et al.,* 2002).

The SMR family is a proton-driven drug efflux pump only found in prokaryotes. A few of these Gram negative multidrug efflux pumps appear to catalyse extrusion across the cytoplasmic membrane. SMR systems are defined by small proteins predicted to span the membrane only four times; the EmrE protein of *E. coli* is one of them. The EmrE transporter confers resistance to a wide variety of toxic cationic hydrophobic compounds such as ethidium bromide, methyl viologen, tetracycline, or tetraphenylphosphonium, as well as other antiseptics and intercalating dyes (Yerushalmi *et al*., 1995). The EmrE protein is one of the smallest transporters known in nature, composed of only 110 amino acids; it appears to constitute a functional unit which is a homodimer. In 2007, elucidation of the high resolution crystal structure of EmrE permitted identification of an antiparallel organization within the dimer (Chen *et al*., 2007).

The MATE group consists of sodium ion-driven drug efflux pumps. NorM from *Vibrio parahaemolyticus* is a member of the MATE family and represents a membrane protein of 456 amino acid residues. Several studies using ethidium like drugs permitted the identification of NorM as the first Na^+/ drug antiporting multidrug efflux pump in the biological world (Morita *et al.* 2000).

RND Pumps

RND family transporters are found only in prokaryotes and catalyse the active efflux of many antibiotics, chemotherapeutic agents and solvents. They use a proton-driven efflux system as an

energy source (Daniels *et al*., 2009). These systems are widely distributed in Gram negative bacteria and thus have to expulse the toxic compound across a double-membrane system. For this reason, members of RND family are multicomponent complex often tripartite: an efflux pump that is located in the inner membrane, an outer membrane channel and a periplasmic "adaptor" protein. This molecular organisation permits bacteria to expulse compounds following two possible pathways: from the periplasm to the external medium or from the cytoplasm to the external medium (Nikaido and Takatsuka, 2009).

The best studied members of the RND family are represented by the AcrAB/TolC from *E. coli* (Koronakis *et al.,* 2000; Tamura *et al.*, 2005; Lobedanz *et al.*, 2007; Murakami *et al.,* 2002; Tamura *et al.*, 2005). Other well study MDR is the OprM-MexA-MexB efflux system from *P. aeruginosa* (Akama *et al.,* 2004; Higgins *et al.,* 2004). Crystallisation of the outer membrane channel, the adaptor protein and the RND pump has permitted the reconstitution of a tripartite structure and allowed a better understanding of the functioning and the mechanism. Assembly of the three sub-units of TolC allowed to observe they form a continuous/undisrupted channel between the inner and outer membranes, which allows the substrates to be expelled (Figure 6). Because most substrates contain a sizable hydrophobic domain, it has been suggested that the entry of substrates occurs from the cytoplasmic membrane/periplasm interface (Murakami, 2008; Nikaido and Takatsuka, 2009).
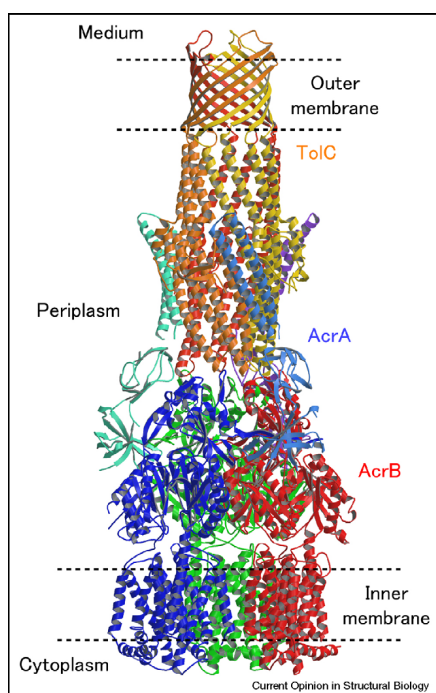
Figure 6. Proposed model of the AcrA–AcrB–TolC complex. Structures of AcrA (Mikolosko *et al.*, 2006) and TolC (Koronakis *et al.,* 2000) are manually docked to AcrB with inspection according to engineered cysteine cross-linking study between AcrB–TolC (Tamura *et al.*, 2005) AcrA–TolC (Lobedanz *et al.*, 2007).

Figure reproduced from Murakami, *Structal Biology*, 2008.

Efflux pumps in *P. putida* DOT-T1E

Pseudomonas putida DOT-T1E genome consists of a circular chromosome of approximately 6 Mb and a medium-sized plasmid of about 130 kb (Molina *et al*., 2010; Segura *et al.* in preparation). This genome encodes 20 RND efflux pumps that can be relevant to tolerance against noxious compounds (Segura *et al.,* in preparation). Three efflux pumps belonging to the RND family have been identified as the main basis of solvent tolerance in *P. putida* DOT-T1E (Rojas *et al.*, 2001). Survival analysis of *P. putida* DOT-T1E revealed that these three efflux pumps are directly involved in toluene resistance since the corresponding triple mutant is hypersensitive to toluene and is unable grow with toluene supplied at low concentrations in the liquid medium (Rojas *et al.*, 2001).

These three RND systems were called Ttg (<u>T</u>oluene <u>t</u>olerance <u>gene</u>): TtgABC, TtgDEF, and TtgGHI. TtgGHI was discovered after TtgABC (Ramos *et* al., 1998; Duque *et al.,* 2001) and TtgDEF by Mosqueda and Ramos (2000) and is very similar to TtgABC. These two efflux pumps permit high level resistance to several solvents such as toluene, styrene, xylenes, ethylbenzene and propylbenzene; whereas TtgDEF is able to expulse only toluene and styrene (Rojas *et al.*, 2001).

It is important to note that the three Ttg efflux pumps are also able to extrude flavonoids and a wide range of antibiotics (Terán *et al.,* 2003; 2006, Guazzaroni *et al.,* 2005). The main role of the TtgABC appears to be the extrusion of antimicrobial agents and is widely distributed in *P. putida* strains (Segura *et al.,* 2003; Godoy et al., 2010); emphasizing the importance of TtgABC efflux pumps role within the solvent-tolerance population. TtgDEF is present only in strains which carry the *tod* pathway for toluene degradation (Mosqueda and Ramos, 2000; Phoenix *et al.,* 2003; Segura *et al.,* 2003). The presence of TtgGHI only in *P. putida* strains able to survive at 0.3% (v/v) toluene shock permits this efflux pump to be classified as a key factor in high level toluene resistance (Segura *et al.,* 2003).

The *ttgABC* and *ttgDEF* operons are located on the chromosome while *ttgGHI* is situated on the ~130 kb plasmid called pGRT1 (Rodríguez-Herva *et al.*, 2007; Molina et al., 2010). This plasmid presents a high stability and is self-transmissible to other *P. putida* strain, thus constituting a valuable tool for biotechnological processes.

5.   *Efflux pumps regulation*

Generalities

Multidrug efflux pumps are often constitutively expressed at low basal level, but the metabolic cost of needless protein production suggests that expression of drug transporter genes will be under some form of stringent regulatory control. Moreover, excessive expression of these pumps could be deleterious, due to a physical disruption of membrane integrity or to an unwanted export of essentials metabolites. Efflux pumps are generally subject to regulation at local level, consisting of examples of both transcriptional repression and activation by proteins encoded adjacent to that for the transporter (Grkovic *et al.,* 2001). Furthermore, some of these transporters have been identified to be regulated also by global regulatory system (Grkovic *et al.* 2001). Most of MDR efflux pumps under the control of a transcriptional regulatory protein are proton dependent and are part of the MFS and RND family (Grkovic *et al.* 2001). MDR transporters regulatory proteins are frequently able to recognize the same array of drugs that are expulsed by the pumps that they regulate. This capacity to bind a combination of a set of drugs, using multiple drug binding sites, provide the pump system with the capacity to expulse a large variety of compounds (Tropel and Van der Meer, 2004)

The most recurrent DNA-binding motif for the binding of regulators to their corresponding promoters is a conserved DNA recognition motif that consists of an α-helix, a turn, and a second α-helix (also called HTH motif). The second helix is known to be the recognition helix involved in the direct contact with the DNA target (Pabo and Sauer, 1992). Generally the HTH-DNA contact takes place in the major groove of the DNA structure. HTH transcriptional regulators have been classified in

families following common 3D structural motifs, conserved regions or primary sequences. At least 17 families of transcriptional regulators have been defined, including some of them using profiles developed specifically, such as: MerR family (Hobman, 2007; Molina-Henares *et al*., 2010), TetR family (Ramos *et al*., 2005), AraC family (Tobes and Ramos, 2002), MarR family (Alekshun *et al.,* 2001), LysR family (Schell, 1993), or IclR family (Molina-Henares *et al*., 2006). Below I will provide details on some transcriptional regulators members of these families known to control efflux pumps.

Regultion by QacR (TetR/CamR family)

QacR is a local transcriptional regulator of the QacA MDR efflux pump system in *Staphylococcus aureus*. The *qac* locus is located on a plasmid which can be transferred to other bacteria to confer resistance to monovalent or bivalent cationic lipophilic antiseptics and disinfectants such as quaternary ammonium compounds (Qac). QacR is a protein of 23 kDa that is a member of the TetR transcriptional regulator family, repressing QacA transcription by blocking the RNA polymerase binding site at the QacA promoter region. QacR is able to bind a wide range of cationic lipophilic drugs such as rhodamine 6G, crystal violet or ethidium. Crystal structures of QacR in complex with DNA or in complex with 6 different effectors had permitted to understand better its mechanism of action (Schumacher *et al.,* 2001 and 2002).

QacR transcriptional regulator binds a 28 pb (IR1) of the promoter region of *qacA* through its HTH domain, making a total of 16 base and 44 phosphate contacts with the recognition helix (α3) on the major groove of the DNA. QacR-DNA structure shows a cooperative binding with a dimer of dimer, each dimer binds to each side of the DNA, half-part of the 28 pb target, which effectively lock the IR1 site into an unwound conformation (Schumacher *et al.,* 2002).

QacR helix α4 through α9 form the drug binding/dimerization domain, in which two amino acids, Tyrosine 92 and Tyrosine 93, act as a structural drug surrogates in absence of effectors. In presence of drug, QacR ligand pocket adopts a bigger arrangement which is ideal for the accommodation of numerous structurally diverse compounds. One drug bound one dimer, so when QacR is in complex with the DNA, two molecules of effector are able bound to two QacR dimers. This binding leads to a coil-to-helix transition of residues 89-93, which extends helix α5 by a turn. The end-result of this structural transition is a rotation of the DNA-binding domain which destabilizes the QacR-DNA complex and releases the DNA. Then the RNA polymerase could bind the promoter region and start the transcription of the MDR transporter corresponding (Schumacher *et al.,* 2001).

Regulation by an IclR member family

IclR family has been identified in wide range of bacterial and archae genomes. Proteins of this family are involved in regulation of diverse catabolic pathways like glyoxylate cycle in Enterobacteriaceae (Sunnarborg *et al.,* 1990) or metabolism of aromatic acids in *E. coli*, *Acinetobacter* or *Pseudomonas* (DiMarco *et al.,* 1993; Gerischer *et al.,* 1998; Arias-Barrau *et al.,* 2004), but also in resistance to toxic compounds (Mosqueda and Ramos 2000; Rojas *et al.,* 2003).

The founding member of this large family is IclR of *Esherichia coli*; it participates in the regulation of the *aceBAK* operon which encodes enzymes involved in the glyoxylate bypass. This bypass permits *E. coli* to grow on acetate as a sole carbon source, but even when *E. coli* is grown in a

rich media, this operon is expressed in order to use acetate accumulated during the exponential phase (Kumari *et al,*. 2000).

Members of the IclR family can be activators, repressors or both; they do not present a clearly consensus sequence in their operators. The target sequence varied following the regulator protein, in the case of the regulator PobR the operator is composed by a palindrome of 8 base pairs separated by one nucleotide (DiMarco *et al.,* 1993; DiMarco and Ornston, 1994); while PcaU presents a sequence of three repetitions of 10 base pairs, two inverted repeats and one direct repeat separated from the other ones by 10 base pairs (Jerg and Gerischer, 2008). The repressor IclR of *E. coli* uses two different modes of transcription repression on its operator *aceBAK* (Yamamoto and Ishihama, 2003). On the DNA target, the presence of three IclR boxes permits two modes for the repression of *aceB* gene. The repression mode I use the competition between IclR and RNA polymerase binding to the *aceB* promoter and, the repression mode II utilizes the dissociation by IclR of the open complex formed at the same promoter (Yamamoto and Ishihama, 2003).

The resolution of the structure of IclR of *Thermotoga maritima* (Zhang *et al.*, 2002) permitted to define some of the structural characteristic of the IclR family members. The N-terminal part is classically represented by a helix-turn-helix DNA binding motif. The N- and C-terminal domains are connected by a linker helix, which participates in protein dimerization through the N-terminal domain. In the case of IclR of *T. maritima* the protein conformation is a tetramer but different oligomeric states of the IclR family like dimers for the regulator PcaU (Popp *et al.*, 2002) have been described. The C-terminal domain structure presents significant structural homology with PAS/GAP domains which are known to bind small molecules (Pellequer *et al.*, 1998).

The C-terminal crystal structure of AllR (another IclR member) helped to identify the effector recognition site, which highlighted the importance of some amino acids forming an hydrophobic patch in the effector binding site (Walker *et al.*, 2006). Lorca and collaborators identified two antagonistic effectors of IclR of *E. coli*: glyoxylate and pyruvate, which are able to bind the C-terminal domain in the same effector binding site of AllR (Lorca *et al.*, 2007). Glyoxylate binding leads to the inactive dimeric state of IclR protein which disturbs the IclR/operator complex, while pyruvate favours the DNA binding by stabilizing the tetrameric active form of IclR (Lorca *et al.*, 2007).

Regulation of TtgABC, TtgDEF and TtgGHI efflux pumps

TtgABC is expressed at a relatively high basal level (Ramos *et al.*, 1998) and, in response to the presence of pump substrates in the culture medium increases its level of expression. The expression of *ttgDEF* and *ttgGHI* operons increased in the presence of solvents in the medium, however, *ttgDEF* has a very low basal level in the absence of its substrate (Duque *et al.,* 2001). The genetic organization of these three efflux pumps is similar: genes encoding for each of the pumps are grouped in operons and divergently from the operons is a gene encoding the regulatory protein of each system (Figure 7).
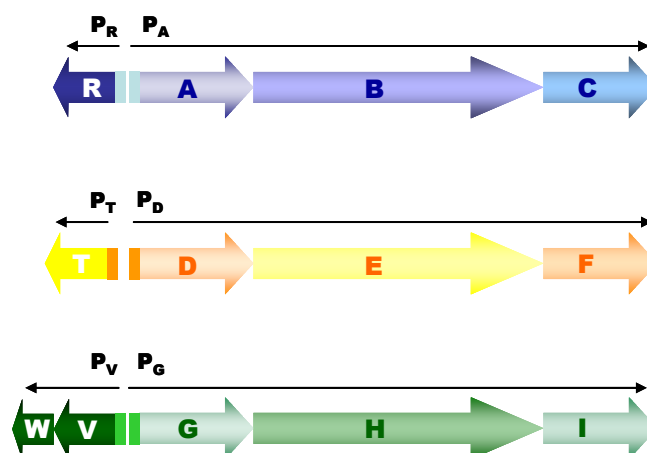
Figure 7. Genetic organization of TtgABC, TtgDEF and TtgGHI efflux pumps in *Pseudomonas putida* DOT-T1E. P_R, P_A, P_T, P_D, P_V, P_G represent each promoter.

For example; divergently to the *ttgABC* genes, is found *ttgR*, encoding the regulator TtgR, a member of the TetR family of transcriptional regulators (Ramos *et al*., 2005). TtgR modulates *ttgABC* transcription in response to antibiotics, aromatic solvents and plant antimicrobials (Terán *et al.,* 2003; 2006). This repressor is of great interest due to its capacity to bind a wide range of compounds. Several studies of TtgR have permitted the resolution of its crystal structure and an increased understanding of its regulatory mechanism (Alguel *et al.,* 2007, Krell *et al*., 2007, Daniels *et al*., 2010). The expression of both *ttgDEF* and *ttgGHI* is controlled by TtgT and TtgV, both belonging to the IclR family. Regulation of these two efflux pumps appears to be more complex because of the capacity to TtgT and TtgV to bind the same promoter regions. TtgW, encoded adjacent to *ttgV*, does not perform a specific role in TtgGHI regulation, since a strain harbouring a knock-out mutation in this gene has the same phenotype as the wild type bacteria. It is interesting to notice that TtgR and TtgV regulate TtgABC and TtgGHI respectively but they also regulate their own expression via auto-control. For TtgT, the intergenic region *ttgT-ttgD* is more extended and presents two independent RNA polymerase binding sites. The negative auto-regulation appreciated by TtgR and TtgV, permit cells to respond quickly to a solvent stress; saving on important energy wastage in the cell.

6.   *TtgV*

TtgV is a protein of 259 amino acids codified by 780 nucleotides; like the majority of *Pseudomonas* genes, *ttgV* nucleotide acids sequence present a high content in G+C (Figure 8). Bioinformatics studies identified TtgV as a cytoplasmic protein with a high percentage of α-helices.

atgaaccaatcagatgaaaatattggcaaggccggggggcatccaggtcatcgccagagcagcctcgatcatgcga
gcgcttggcagtcatccgcacggcttgagcttggcggccattgcgcaactggttgggctgcctcgctccaccgtt
cagagaatcatcaacgctctggaagaagagttcctagtcgaggctttagggcctgccggaggttttcgacttggc
cctgcgcttggccagctaatcaatcaggcgcaaacagacattctttctttggtgaaaccgtacttgcgctcgctg
gctgaggagctggacgagtcggtctgtctggcttctctggccggagaCaaaatctacgtgcttgaccgtatcgtg
tcagagcgagagctgcgggtagtgtttccgattggtattaacgtacccgccgcagcgacggcggccggcaaagtc
ctcttggcagcattacctgacgaaaccctacaagccgcgcttggcgagcagctgccagtattgacctccaacacc
ctaggacgaaaggcgcttgtcaaacaactgagcgaagtgcggcagagtggcgttgccagcgatctggacgagcac
attgatggcgtgtgctcattcgcaacgcttttggatacctacctcgggtattactccctcgcgatcgtaatgccg
agtccagagcgagcaagcagtcagacttgatcaaaaaagctctgctgcagagcaagctgaacatagagcgtgct
atcggccgcgcgtcgaagaaagctccctag

Figure 8. Nucleotide sequence of *ttgV* gene.

TtgV is an IclR family member

The TtgV carboxy terminal part contains a helix-turn-helix (HTH) DNA binding domain (SMART, PROSITE) (Molina-Henares *et al.,* 2006; Krell *et al.,* 2006) (Figure 9A.). Study of 53 IclR members permitted the identification of 3 conserved regions in IclR family members: one comprising the HTH DNA binding domain, another including a small part of the amino terminal region and the central region, and a third one localized in the C-terminal end (Krell *et al.,* 2006) (Figure 9 B.). The most conserved region is from amino acid 151 to the 229 of IclR from *E. coli.* But in general, conserved amino acids are almost extended in all the protein sequence; making us to think that the similarity within the IclR family could be associated more with the 3D structure or protein conformation that the sequence itself.

A.

```
TtgV      -----------------------MNQSDENIGKAGGIQVIARAASIMRALGSHPHGLSLA 37
SrpS      -----------------------MNQSDENVGKAGGIQVIARAASIMRALGSHPHGLSLA 37
TtgT      -----------------------MSDSEESSARHGGIQVIARAASIMRALGSHPQGLSLA 37
SepR      -----------------------MSDSEESSARHGGIQVIARAASIMRALGSHPQGLSLA 37
IclR      MKMISTIQKKETVMVAPIPAKRGRKPAVATAPATGQVQSLTRGLKLLEWIAESNGSVALT 60
TM-IclR   -----------------------------------MNTLKKAFEILDFIVKNPGDVSVS 24
                                              ::  : :. .::  :  .   .::::

TtgV      AIAQLVGLPRSTVQRIINALEEEFLVEALGPAGGFRLGP---ALGQLINQAQTDILSLVK 94
SrpS      AIAQLVGLPRSTVQRIINALEEEFLVEALGPAGGFRLGP---ALGQLINQAQSDILSLVK 94
TtgT      AIAQVVDLPRSTVQRIINALGAEHLVEALGPSGGFRLGP---AFGRLITQAQTDIISLVR 94
SepR      AIAQVVDLPRSTVQRIINALGAEHLVEALGPSGGFRLGP---AFGRLITQAQTDIISLVR 94
IclR      ELAQQAGLPNSTTHRLLTTMQQQGFVRQVGELGHWAIGAHAFMVGSSFLQSR-NLLAIVH 119
TM-IclR   EIAEKFNMSVSNAYKYMVVLEEKGFVLRKKDK-RYVPGYKLIEYGS-FVLRRFNIRDIAH 82
            :*:  .:. *.. : : .:  : :*          :  *       *  :   : ::  :.:

TtgV      PYLRSLAEELDESVCLASLA--GDKIYVLDRIVSERELRVVFPIGINVPAAATAAGKVLL 152
SrpS      PYLRSLAEELEESVCLASLA--GDKIYVLDRIVSERELRVVFPIGINVPAAATAAGKVLL 152
TtgT      PHLIALSEQVYESTCLLSLS--GEKIYVLDRVVAERELRVVFPIGIHVPATAVSGGKVLL 152
SepR      PHLIALSEQVYESTCLLSLS--GEKIYVLDRVVAERELRVVFPIGIHVPATAVSGGKVLL 152
IclR      PILRNLMEESGETVNMAVLDQSDHEAIIIDQVQCTHLMRMSAPIGGKLPMHASGAGKAFL 179
TM-IclR   DHLVDIMKRTGETVHLILKD--GFEGVYIDKVEGEQSIPMVSRLGMKVDLYSTASGKSIL 140
             *   : :.  *:. :      . :   :*::   : : :   :* ::   : ..** :*

TtgV      AALPDETLQAALG-EQLPVLTSNTLGR-KALVKQLSEVRQSGVASDLDEHIDGV-CSFAT 209
SrpS      AALPDETLQAALG-EQLPVFTSNTLRR-KALVKQLSEVRQSGFASDLDEHIDGV-CSFAT 209
TtgT      AELSEEAQQALLP-DPLPVCTPRSVAR-EALLEQLKTIKSGGVADDHDEYIEGL-CSYSV 209
SepR      AELSEEAQQALLP-DPLPVCTPRSVAR-EALLEQLKTIKSGGVADDHDEYIEWL-CSYSV 209
IclR      AQLSEEQVTKLLHRKGLHAYTHATLVSPVHLKEDLAQTRKRGYSFDDEEHALGLRCLAAC 239
TM-IclR   AFVPEKELKEYLKIVELKPKTPNTITNPRVLKRELEKIRKRGYAVDNEENEIGIMCVGVP 200
            * :.::     *    *    *   ::    * .:*   :.  * :  * :*     : *

TtgV      LLDTYLG-YYSLAIVMPSSRASK-QSDLIKKALLQSKLNIERAIGRASKKAP- 259
SrpS      LLDTYLG-YYSLAVVMPSSRASK-QSDLIKKALLQSKQNIERAIGRASKKAP- 259
TtgT      LLDTYLG-HYSVSIVAPNSRATT-RVAEFQQALQACKQNIEVTIGRAPREFAG 260
SepR      LLDTYLG-HYSVSIVAPNSRATT-RVAEFQQALQACKQNIEVTIGRAPREFAG 260
IclR      IFDEHREPFAAISISGPISRITDDRVTEFGAMVIKAAKEVTLAYGGMR----- 287
TM-IclR   IFDHNGYPVAGVSISGVARKFTEEKIEEYSDVLKEKAEEISRKLGY------- 246
           ::.*      .:::    : : :       :      ::     *
```

B.

Figure 9. A, Sequences alignment of several member of the IclR regulator family. B, representation of TtgV domains using SMART programme.

TtgV is a transcriptional repressor

TtgV HTH binding domain is able to recognize the *ttgV-ttgG* intergenic region, including the -10 and -35 boxes of each promoter. DNaseI footprint assays revealed that TtgV protects four DNA helical turns in the P_{ttgG} promoter region, corresponding to positions +13 to -29 and causes an hyper-methylation at the guanine position -14 (Rojas *et al.,* 2003; Guazzaroni *et al.,* 2004) (Figure 10). Hyper-methylation of G -14 suggests that TtgV DNA binding leads to a conformational change of the DNA situating G -14 in a hyper-reactive position. This result was later confirmed using AFM (Atomic Force Microscopy) assays which showed DNA torsion of 57° as a result of TtgV binding to a 716 bp DNA fragment representing the *ttgV-ttgG* intergenic region (Guazzaroni *et al.,* 2007).

TtgV binding prevents RNA polymerase access to the promoter region through physical competition which circumvents *ttgGHI* and *ttgV* gene transcription (Guazzaroni *et al.,* 2004). This is the most commonly used mechanism in repression systems and has been studied in detail in several other systems (Rojo *et al.,* 2001; Teràn *et al.,* 2003; Yamamoto and Ishihama, 2003, Molina-Henares *et al*., 2006). *In vivo* assays permitted the observation that in the presence of aromatic compounds in the culture medium, the *ttgG* promoter increases its activity, especially with 4-nitrotoluene and 1-naphthol (Guazzaroni *et al.,* 2005). These data indicated that binding of effectors to TtgV might induce a conformational change of the repressor which eventually leads to its release from the target DNA. RNA polymerase is then free to bind *ttgG-ttgV* promoter region and initiate *ttgG* and *ttgV* expression.
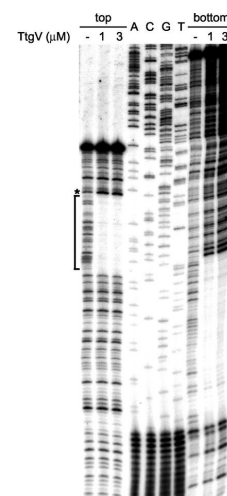
Figure 10. Identification of the TtgV operator in the *ttgG-ttgV* intergenic region by DNase I footprinting. PCR fragments comprising the *ttgG-ttgV* intergenic region were labeled at one 5′ end and incubated without (−) or with a 1 or 3 μM concentration of purified TtgV before being subjected to DNaseI digestion and electrophoresis. The regions protected from DNase I digestion by TtgV are shown in brackets; asterisks indicate hyperactive sites. (See for details *Rojas et al.,* 2003)

It has been shown that the TtgV effector binding domain is able to bind an extensive range of mono and bi-aromatic compounds; such as, toluene, xylenes, benzonitrile, indole, and naphthalenes (Guazzaroni *et al.,* 2004 and 2005). *In vitro* (calorimetric) and *in vivo* (β-galactosidase) data permitted to establish that the efficiency of TtgGHI pump repression is directly correlated with the effector binding affinity. Affinity constants (K_D) for TtgV and various effectors was measured using isothermal titration calorimetry (ITC); in general, the effectors tested bind TtgV with a high affinity (μM range). The ITC analysis also suggested that two molecules of effector bind to a tetramer of TtgV (Guazzaroni *et al.,* 2005).

In order to better understand effector binding Guazzaroni and colleagues studied TtgV effector binding using a three-dimensional model (Guazzaroni *et al.,* 2007a) (Figure 11). In the case of several structurally elucidated MDR regulators, it was observed that effectors enter inside a deep pocket where they can establish van der Waals interactions with hydrophobic amino acids. The TtgV amino acids involved in effector binding were later identified and corroborated via the construction of mutants located in the hypothetical binding pocket. Different amino acids were identified as potentially involved in the binding depending on the nature of the effector. Mutations in the binding pocket showed an increased affinity for bi-aromatic compounds but a defect in mono-aromatic compound binding. Several mutants were constructed but the most relevant were F134A and H200A: they appear to have a key role in the effector binding. Further, DNA-protein ITC studies demonstrated that release of DNA from TtgV is more efficient with a bi-aromatic compound than a monocyclic one. One of the binding pocket mutants, V223A, did notexhibit any deffect in effector binding but curiously, it presented a deficiency release of the DNA, suggesting that this amino acid is part of TtgV signalling pathway between the two domains (effector binding and DNA binding).
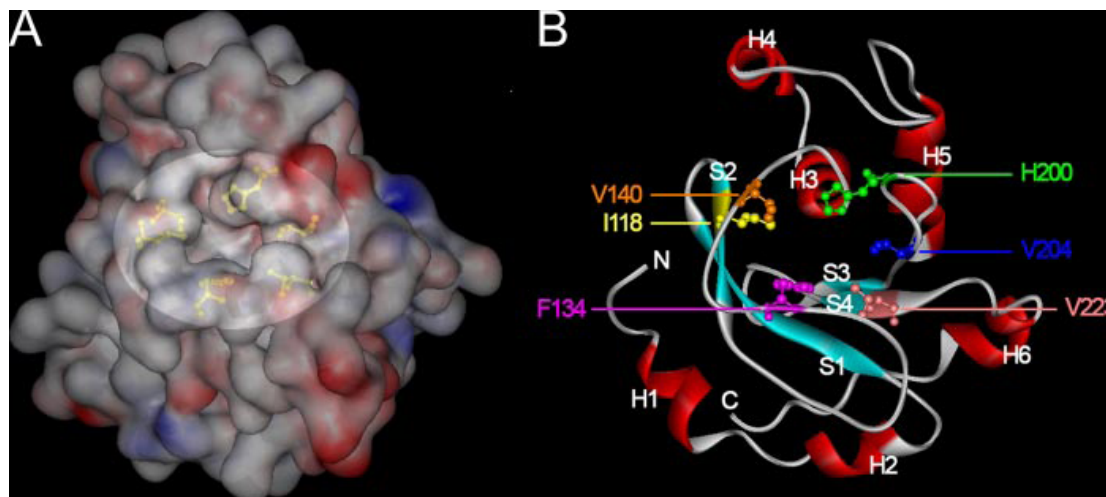
Figure 11. Three dimensional model of the effector binding domain of TtgV. A, a surface plot colored according to electrostatic potential. B, ribbon representation of the model, annotated to show secondary structure elements (H for helix, S for strand) and the mutated amino acids. (See for details Guazzaroni *et al.,* 2007a)

Studies of the oligomeric state of TtgV by ultracentrifugation showed that TtgV is a tetramer in solution with or without 1-naphthol (Guazzaroni *et al*., 2007). The data led to the hypothesis that TtgV binds the DNA target as a tetramer and upon binding of two molecules of effectors is released from the target DNA. Guazzaroni and colleagues proposed the model shown below to explain the mechanism of TtgV repression (Figure 12). While more recent studies have permitted a better

understanding of the TtgV mechanism and its role in *P. putida* DOT-T1E, we would like to explore some aspects still unknown in TtgV protein and other IclR family member.
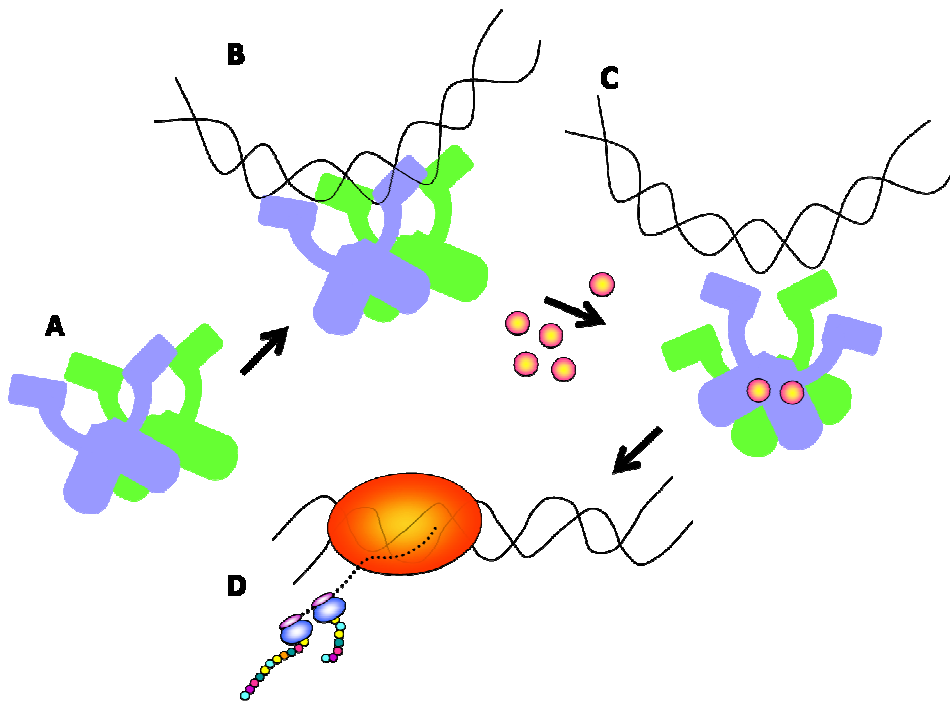
Figure 12. Representation of TtgV functional mechanism. A, TtgV in solution is a tetramer. B, in absence of effector in the medium, TtgV binds its operator sequence and curves the DNA C, in presence of effector in the medium, each dimer of TtgV bindone molecule of effector within the ligand binding domain of TtgV. Binding of effector leads the releasing of the DNA target. D, The promoter region is now available for the RNA polymerase binding. (Figure reproduced from the Dr Guazzaroni's PhD).

The transcriptional regulator TtgV has been the subject of several studies in our laboratory in the last few years. The characterization of its binding to its target DNA, its repression of transcription and its binding to several aromatic compounds with the concomitant release from operators have helped us to understand better why this protein is a key in solvent tolerance of *Pseudomonas putida.*

When I joined the group, interest was on getting inside the physiologic role of TtgV, identification of the binding mode to the DNA target and establishment of the 3D structure of the regulator as a mean to have a model in hands for further exploration of intercommunication of the domain of this repressor. Along these lines, my objectives established were:

- To study the role of TtgV as the major regulator in the toluene resistance in *Pseudomonas putida*
    - Unveiling of the binding of TtgV to the promoters of the *ttgDEF* and *ttgGHI* operons
    - Physiological relevance of TtgV in the cells exposed to toluene

- Details on the binding of TtgV on its two sequences operators
    - Construction of alanine mutants in the recognition helix
    - Biochemical characterization of the interaction of TtgV wild type and its variants mutants to target operators

- Resolution of the TtgV crystal structure free in solution and in complex with its *ttgGHI* operator

- Understanding of the inter-domain communication in TtgV regulator
    - Construction of a set of mutants into the α-helix linker of the two TtgV domains
    - Biophysical studies of the different TtgV mutants

Results

Complexité dans le contrôle de pompe d'efflux : régulation croisée entre les paralogues TtgV et TtgT

Pseudomonas putida DOT-T1E, connues pour sa haute tolérance aux solvants, est pourvues de trois pompes d'efflux de type RND (Nodulation-Cell Division), nommées TtgABC, TtgDEF, TtgGHI et impliquées dans l'extrusion active de solvants. Il a était démontré précédemment que l'expression des opérons *ttgABC* et *ttgGHI* est régulé par deux répresseurs codifiés de manière adjacente, respectivement *ttgR* et *ttgV*. Situé à côté de la troisième pompe d'efflux *ttgDEF* se trouve le régulateur putatif *ttgT*. Dans ce travail, il est démontré que TtgT s'unie à la région promotrice de l'opéron *ttgDEF* et libère l'ADN correspondant, en présence de solvants organiques. Des études *in vitro,* ont révélé que TtgV et TtgT ont la capacité de s'unir au même site opérateur des deux promoteurs *ttgDEF* et *ttgGHI*. Malgré tout, l'affinité de TtgV pour l'opérateur *ttgDEF* est plus grande que celle de TtgT, ce qui, ajouté au fait que le promoteur de TtgV semble être deux fois plus fort que celui de TtgT, explique pourquoi TtgV prend une telle importance dans la régulation des deux pompes d'efflux TtgDEF et TtgGHI. Le remplacement fonctionnel du régulateur TtgT, codifié par le chromosome, par son paralogue TtgV, codifié par un plasmide, illustre un nouveau mode de régulation de pompe d'efflux dont la relevance physiologique est discutée.

Complexidad en el control de bomba de eflujo : regulación cruzada entre los paralogos TtgV y TtgT

Pseudomonas putida DOT-T1E, conocida por su alta resistencia a solventes orgánicos, posee tres bombas de eflujo de tipo RND (Nodulation-Cell Division) llamadas TtgABC, TtgDEF y TtgGHI e implicadas en la extrusión activa de compuestos aromáticos. Anteriormente se había demostrado que la expresión de los operones *ttgABC* y *ttgGHI* está regulada por dos represores codificados de manera adyacente, respectivamente *ttgR y ttgV*. Localizado al lado de la tercera bomba de eflujo *ttgDEF*, se encuentra el gen regulador *ttgT*. En este trabajo, demostramos que TtgT se une a la región promotora del operon *ttgDEF* y se libera del ADN correspondiente, en presencia de disolventes orgánicos. Estudios *in vitro*, han revelado que TtgV y TtgT tienen la capacidad de unirse al mismo sitio operador de los dos promotores *ttgDEF* y *ttgGHI.* Sin embargo, la afinidad de TtgV para su operador en *ttgDEF* es mayor que la de TtgT, lo que, además del hecho que el promotor de TtgV parece ser dos veces mas fuerte que el de TtgT, explicaría porque TtgV tiene una tal importancia en la regulación de las bombas de eflujo TtgDEF y TtgGHI. El reemplazamiento funcional del regulador TtgT, codificado en el cromosoma, por su parálogo TtgV, codificado por un plásmido, ilustra un nuevo modo de regulación de bombas de eflujo cuya la relevancia fisiologica se discute en este capitulo.

Complexity in efflux pump control: cross-regulation by the paralogues TtgV and TtgT

Wilson Terán, Antonia Felipe, Sandy Fillet,
María-Eugenia Guazzaroni, Tino Krell, Raquel Ruiz,
Juan L. Ramos and María-Trinidad Gallegos*
Department of Environmental Protection, Estación
Experimental del Zaidín, Consejo Superior de
Investigaciones Científicas, Granada, Spain.

Summary

***Pseudomonas putida* DOT-T1E, known for its high tolerance to solvents, possesses three Resistance–Nodulation–Cell Division-type (RND) efflux pumps, namely TtgABC, TtgDEF and TtgGHI, which are involved in the active extrusion of solvents. Expression of the *ttgABC* and *ttgGHI* operons was previously shown to be regulated by the adjacently encoded repressors, TtgR and TtgV, respectively. Upstream of the third RND operon, *ttgDEF*, is located a putative regulator gene, *ttgT*. In this study, TtgT is shown to bind to the promoter region of the *ttgDEF* operon, and to be released from DNA in the presence of organic solvents. *In vitro* studies revealed that TtgV and TtgT bind the same operator sites in both the *ttgDEF* and the *ttgGHI* promoters. However, the affinity of TtgV for the *ttgDEF* operator was higher than that of TtgT, which, together with the fact that the *ttgV* promoter seems to be almost twice stronger than the *ttgT* promoter, explains why TtgV takes over in the regulation of the two efflux pump operons. The functional replacement of the cognate, chromosomally encoded TtgT by the plasmid-encoded paralogue TtgV illustrates a new mode of efflux pump regulation of which the physiological relevance is discussed.**

Introduction

Aromatic hydrocarbons have been present in the environment for millions of years as they are the products of the natural pyrolysis of organic material (Dagley, 1971), and are now widely distributed in natural environments. One-ring aromatic compounds such as benzene, xylenes, ethylbenzene and toluene have a logP$_{ow}$ (logarithm of the partition coefficient in *n*-octanol and water) of 2.5–3.5, and

are thus toxic for microorganisms and other living cells because they partition preferentially in the cytoplasmic membrane, disorganizing its structure and impairing vital functions (Sikkema *et al.*, 1995). The toxicity of these compounds depends not only on the inherent toxicity of the solvent but also on the intrinsic tolerance of the microorganisms exposed.

Several mechanisms have been proposed to account for solvent tolerance in Gram-negative bacteria (Ramos *et al.*, 2002). The main passive mechanism involves an increase in cell membrane rigidity via alterations in phospholipid composition. *Cis/trans*-isomerization of unsaturated fatty acids is considered a short-term response, whereas changes in the saturated-to-unsaturated fatty acid ratio are considered a long-term response to solvent exposure (Heipieper and de Bont, 1994; Heipieper *et al.*, 1996; Loffeld and Keweloh, 1996; Junker and Ramos, 1999). The active removal of toxic compounds from the cell membranes to achieve solvent tolerance occurs via mechanisms such as the formation and expulsion of vesicles loaded with toxic compounds that remove the solvents from the cell surface (Kobayashi *et al.*, 2000) and the extrusion of toxic compounds to the external medium in an energy-dependent process mediated by efflux pumps. The latter mechanism was found to be the primary cause of solvent tolerance in several strains resistant to solvents and other toxic chemicals (Inoue and Horikoshi, 1989; Isken and de Bont, 1996; Ramos *et al.*, 1998; Rojas *et al.*, 2003).

In the highly solvent-tolerant *Pseudomonas putida* DOT-T1E strain, three homologous efflux pumps belonging to the Resistance–Nodulation–Cell-Division (RND) family of bacterial transporters (TtgABC, TtgDEF and TtgGHI) contribute to solvent tolerance (Mosqueda and Ramos, 2000; Duque *et al.*, 2001; Rojas *et al.*, 2001). Although these pumps share 70% identity at the protein level, they exhibit significant differences in substrate specificity. TtgABC and TtgGHI extrude antibiotics as well as solvents, and the TtgABC efflux pump has been shown to play a major role in antibiotic resistance in this strain, as a *ttgB* knock-out mutant was shown to be less resistant to a wide variety of antibiotics (Duque *et al.*, 2001; Rojas *et al.*, 2001; Terán *et al.*, 2003). The differential expression of these transporters has been correlated with their individual contributions to the overall survival after a toluene shock (Rojas *et al.*, 2001): the TtgABC and

TtgGHI efflux pumps are both expressed at a relatively high basal level and are responsible for the intrinsic solvent resistance of cells not pre-adapted to the toxic compound. The expression of TtgDEF and TtgGHI increases in response to organic solvents such as styrene and toluene, which is the main cause of the inducible resistance to solvents in pre-exposed *P. putida* DOT-T1E cells. The expression level of TtgABC is enhanced by hydrophobic antibiotics such as chloramphenicol and tetracycline (Terán *et al.*, 2003) but is not altered in response to solvents (Duque *et al.*, 2001). Therefore, the expression of efflux systems responds to the presence of at least one of their substrates in the culture medium, and it has been shown that that this regulation occurs at the transcriptional level (Duque *et al.*, 2001; Rojas *et al.*, 2001; 2003; Terán *et al.*, 2003; Guazzaroni *et al.*, 2004).

Most of the regulatory genes that encode proteins involved in the transcriptional control of RND efflux pumps are located adjacent to the structural genes of the pump. The regulatory genes *ttgR* (Duque *et al.*, 2001) and *ttgV* (Rojas *et al.*, 2003) are located divergently with respect to *ttgABC* and *TtgGHI* respectively. TtgR is a member of the TetR family of transcriptional regulators (Ramos *et al.*, 2005) that modulates transcription of the *ttgABC* operon in response to antibiotics, aromatic solvents and plant antimicrobials (Terán *et al.*, 2003; 2006). TtgV belongs to the isocitrate lyase regulator (IclR) family of transcriptional regulators (Krell *et al.*, 2006; Molina-Henares *et al.*, 2006) and represses expression from the *ttgGHI* operon upon binding to its operator site (located between −29 and +13 in the *ttgG* promoter region) thereby blocking access of the RNA polymerase to the promoter region (Rojas *et al.*, 2003). TtgV binds a wide range of mono- and bicyclic aromatic compounds with K_D in the lower micromolar range. Effector binding to the DNA–TtgV complex leads to the release of TtgV enabling for transcription (Rojas *et al.*, 2003; Guazzaroni *et al.*, 2004; 2005). It has been recently shown that the *ttgGHI* operon and the adjacent *ttgVW* set of regulatory genes are both borne by the pGRT1 megaplasmid. In contrast to their parental strain, mutants lacking pGRT1 were unable to grow in LB medium supplemented with 0.3% (v/v) toluene and, reciprocally, the transfer of the megaplasmid to a toluene-sensitive strain conferred solvent tolerance to the latest (Rodríguez-Herva *et al.*, 2007).

We report here the identification and molecular characterization of a new regulatory gene, *ttgT*, located divergently with respect to the *ttgDEF* operon in the DOT-T1E chromosome. TtgT belongs to the IclR family of repressors and shares 63% sequence identity with TtgV. We demonstrate that both paralogues bind in a similar fashion *in vitro* to the operators located at the *ttgDEF* and *ttgGHI* promoters. This, however, contrasts the *in vivo* situation where TtgV is the dominant repressor of both operons,

and the regulatory activity of TtgT is only detectable in a TtgV-deficient background.

Results

In vivo *expression of the TtgDEF efflux pump is mediated by TtgT and TtgV*

We identified an open reading frame (ORF), located divergently with respect to the *ttgDEF* genes, whose translated product exhibits high identity to several regulators described in different *Pseudomonas* strains, e.g. SepR (99%) from *P. putida* F1, TtgV (63%) from *P. putida* DOT-T1E, SrpS (62%) from strain S12 and TbtR (59%) from *P. stutzeri*. All of these regulators are involved in the transcriptional regulation of RND efflux pumps (Wery *et al.*, 2001; Phoenix *et al.*, 2003; Rojas *et al.*, 2003; Jude *et al.*, 2004). These proteins are members of the IclR family of transcriptional regulators and exhibit a helix–turn–helix (HTH) DNA-binding domain at their N-terminal end, whereas the C-terminal region most likely contains the effector-binding domain (Krell *et al.*, 2006; Molina-Henares *et al.*, 2006).

Mosqueda and Ramos (2000) showed that expression of the *ttgD* promoter was very low in the wild-type DOT-T1E strain but increased about three- to fourfold in response to toluene and styrene. To test whether the putative regulatory gene *ttgT* was involved in expression of the adjacent operon, a null *ttgT* mutant (*P. putida* DOT-T1ET) was constructed (see *Experimental procedures*). A *ttgD::'lacZ* transcriptional fusion (pMPD1) was introduced into *P. putida* DOT-T1E and DOT-T1ET, and β-galactosidase activity was compared in cells growing in the absence and in the presence of different organic solvents (Table 1). In the absence of aromatic hydrocarbons we found a modest twofold increase of the basal *ttgDEF* expression level in the *ttgT* mutant. Also in DOT-T1ET, the pattern of induction was similar to the wild type except that the levels were a little higher (Table 1), increasing up to 10-fold in response to the presence of determined aromatic chemicals (see 1-naphthol in Table 1). These results suggested that another regulator was taking over, as *ttgDEF* expression was still inducible.

We hypothesized that TtgV was the potential additional regulator of the *ttgDEF* operon because TtgT and TtgV share a high degree of sequence identity (63%) and *ttgDEF* and *ttgGHI* expression was shown before to be induced by organic solvents (Mosqueda and Ramos, 2000; Rojas *et al.*, 2001; 2003; Guazzaroni *et al.*, 2004; 2005). To test this hypothesis, we measured β-galactosidase activity from the P*ttgD*::'*lacZ* fusion in a TtgV-deficient background (DOT-T1E-PS61). Results showed that the basal level increased about 10-fold compared with the wild type (Table 1), confirming the involve-

Table 1. Expression from the *ttgD* and *ttgG* promoters in the presence of different compounds.

Promoter fusion/effector	T1E	T1ET	PS61	T1EVT
P$_{ttgD}$::*lacZ*				
–	10	20	100	800
DMSO	10	20	100	800
4-Nitrotoluene	50	70	400	900
Benzonitrile	40	40	600	900
Indole	30	30	500	1000
2,3-Dihydroxy naphthalene	50	70	700	900
1-Naphthol	200	200	1000	1000
m-xylene	20	20	400	900
Toluene	20	20	300	800
Styrene	20	20	700	700
P$_{ttgG}$::*lacZ*				
–	400	500	1500	2500
1-Naphthol	2000	2000	3000	3000
Benzonitrile	2000	2000	3000	3000

β-Galactosidase activity from the *ttgD* (pMPD1 plasmid) and *ttgG* (pANA96) promoters was determined in cultures of *P. putida* DOT-T1E (wild type), DOT-T1ET (*ttgT*-null mutant), DOT-T1E-PS61 (*ttgV*-null mutant) or T1EVT (*ttgT*- and *ttgV*-null mutant) grown in the absence (–) and in the presence of 1 mM of the indicated chemicals. Results are the mean of five to eight different experiments, with standard deviations below 15% of the given value.

ment of TtgV in *ttgDEF* repression. We extended these assays by measuring β-galactosidase activity in *P. putida* DOT-T1E cells grown in the absence or in the presence of 1 mM monocyclic and bicyclic organic compounds that are known TtgV effectors (Table 1 and Table S1). We found that the best TtgV effectors induced high level expression from P$_{ttgD}$: 1-naphthol led to a 20-fold increase, and 4-nitrotoluene, 2,3-dihydroxy naphthalene and benzonitrile induced four- to fivefold increases in activity (Table 1). Interestingly, some induction of *ttgDEF* expression was still observed in the *ttgV* mutant strain in response to different organic compounds confirming that TtgT plays a detectable role in the expression of *ttgDEF* *in vivo*. To verify this we created the double mutant DOT-T1EVT in which *ttgDEF* basal level increased 80-fold and, more interestingly, no significant induction of *ttgDEF* expression was detected in the presence of inducers (Table 1). This is consistent with the notion that TtgT and TtgV are the only regulatory proteins involved in *ttgDEF* induction by organic solvents.

In vivo data showed that relative contribution of TtgT and TtgV to the *ttgDEF* expression depended on the molecule used as inducer (Table 1). Although the repressing effect of TtgV seems to be dominant with most of the effectors, in the presence of 1-naphthol and 4-nitrotoluene, TtgT and TtgV appear to contribute similarly to the induction of P$_{ttgD}$ as, in their presence, expression was 10- and 4-fold above the basal level, respectively, in both *ttgT* and *ttgV* mutants. However, in the presence of benzonitrile, 2,3-dihydroxy naphthalene, indole, styrene or naphthalene, the induction of P$_{ttgD}$ expression in the wild-type strain was greater than

in the *ttgT* mutant, but lower than in the *ttgV* mutant. Therefore, in the presence of those chemicals, TtgT seems to play a more significant role than TtgV in the derepression of *ttgDEF*, probably by recognizing and/or responding better than TtgV to those molecules.

Is TtgT involved in the regulation of ttgGHI expression?

The *ttgGHI* operon was shown previously to be under the control of TtgV (Rojas *et al.*, 2003). To verify whether TtgT repressed *ttgGHI* expression, and to compare the effects of TtgT and TtgV on the *ttgGHI* promoter, we measured β-galactosidase activity of a *ttgG::′lacZ* transcriptional fusion (pANA96) in *P. putida* DOT-T1ET, DOT-T1E-PS61 and DOT-T1EVT. The deletion of *ttgT* alone had little effect on the expression of *ttgGHI*; however, the loss of only *ttgV* or *ttgT* together with *ttgV* led to 3.8- and 6.3-fold increases, respectively, in *ttgGHI* expression. Therefore the effect of TtgT on *ttgGHI* expression is not obvious when TtgV is present but becomes relevant in its absence.

We measured the level of induction of P$_{ttgG}$ in the above mutant backgrounds in response to 1-naphthol, benzonitrile (Table 1) and other aromatic compounds (Table S2). In the *ttgT* mutant the levels were almost identical to those observed in the wild-type strain; in the *ttgV*-null mutant *ttgGHI* expression increased twofold in response to these aromatics. However, in the double mutant DOT-T1EVT, no significant further induction of *ttgGHI* expression was detected (Table 1), showing that TtgT and TtgV are the only regulatory proteins involved in the induction of *ttgGHI* by organic solvents.

Binding of TtgT and TtgV to their operator sites

As TtgT and TtgV have been shown to repress *ttgDEF* expression, comparative binding studies of TtgT and TtgV to the P$_{ttgD}$ promoter were carried out in order to estimate binding affinity. Initial experiments using electrophoretic mobility shift assays (EMSA) revealed that TtgT and TtgV specifically bound to a DNA fragment from +35 of *ttgT* to +86 of *ttgD*, corresponding to the *ttgT-ttgDEF* intergenic region. Binding was specific, as only excess unlabelled intergenic DNA but not excess non-specific DNA was able to compete with labelled DNA for TtgT and TtgV binding (not shown). Assays with increasing protein concentrations demonstrated that TtgV bound to the *ttgT-ttgDEF* intergenic region with higher affinity than TtgT. Indeed, while about 0.1 μM of TtgV retarded approximately 90% of target DNA, a similar effect was only achieved using a 15 times higher TtgT concentration (Fig. 1).

In order to corroborate the greater significance of TtgT in the induction of *ttgDEF* by benzonitrile, 2,3-dihydroxy naphthalene, indole, styrene or naphthalene (Table 1), we carried out EMSAs with purified TtgT and TtgV on the
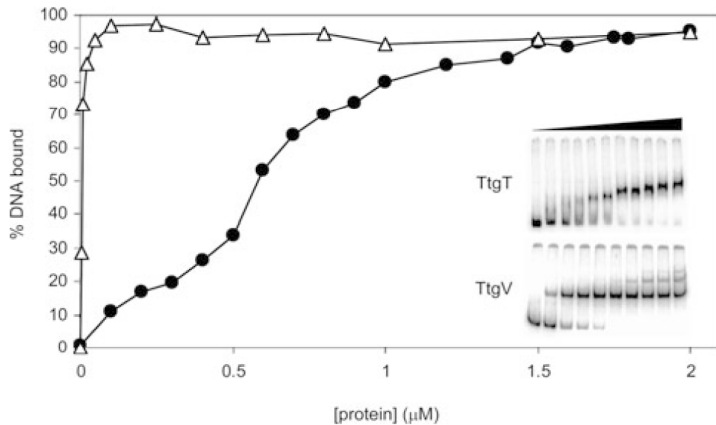
Fig. 1. Electrophoretic mobility shift assays of TtgT and TtgV with the *ttgT-ttgDEF* intergenic region. Binding reactions were carried out as described in *Experimental procedures*. The 295 pb fragment containing the *ttgT-ttgDEF* intergenic region (1 nM) was incubated without protein or with increasing concentrations (from 0.005 to 2 μM) of His₆-tagged TtgT (●) or TtgV (△). As protein concentration increased the percentage of DNA bound also increased. Results shown in the graphic are the mean of six different experiments; standard deviations were below 10% of the given values. Representative EMSAs are also shown in the figure. TtgT concentrations are 0, 0.2, 0.4, 0.6, 0.8,1, 1.2, 1.4, 1.6, 1.8 and 2.0 μM and TtgV concentrations are 0, 0.005, 0.01, 0.02, 0.05, 0.1, 0.25, 0.5, 0.75 and 1 μM.

ttgT-ttgD intergenic region in the presence of some of those chemicals to analyse if they were able to release the proteins from their operator DNA (Fig. 2). It is worth to note that accurately comparing DNA-bound TtgT and TtgV responses to those effectors is hindered by the different affinity of both proteins for their target DNA. Nonetheless, it came clear that, in the presence of 1-naphthol, 2,3-dihidroxy naphthalene and 4-nitrotoluene, TtgT and TtgV were released from their operator site; however, TtgT appeared to respond to styrene better than TtgV as it was released from the DNA whereas TtgV remained bound.

In summary, the effector-mediated release of TtgV from the *ttgD* promoter appeared similar in overall characteristics to the interaction of TtgV with the *ttgGHI* promoter (Guazzaroni *et al.*, 2005). It is interesting to note that TtgT not only recognized 1-naphthol, 2,3-dihydroxy naphthalene and 4-nitrotoluene when bound to the *ttgDEF* promoter as TtgV, but also styrene (Fig. 2). These results are in agreement with *in vivo* determinations of β-galactosidase activity, as the compounds that showed the highest induction level of the P*ttgD* promoter *in vivo* (1-naphthol, 4-nitrotoluene) also released TtgV and TtgT from their operator site most efficiently in the *in vitro* experiments (Table 1, Fig. 2). Furthermore, compounds which failed to induce *ttgDEF in vivo* (i.e. *p*-isopropylbenzoate, tetracycline and chloramphenicol) did not release TtgT and TtgV from the target operator *in vitro* (not shown).

To define the TtgT and TtgV operator site within the *ttgT-ttgD* intergenic region, DNase I footprint assays were performed in the absence and in the presence of the two proteins (Fig. 3A). TtgT and TtgV protected both strands of a single 42 bp segment within the *ttgT-ttgD* intergenic region that covered the +1 transcription initiation site and the −10 and −35 regions of the *ttgDEF* promoter (from −37 to +5 in the top strand and from −37 to +3 in the bottom strand; Fig. S2). To characterize the binding region in

greater detail, DMS methylation protection assays were carried out (Fig. 3B). We observed that Gs at positions −2, −3 and −23 were protected in the top strand, and Gs at +1, −12, −19, −31 and −32 were protected in the bottom strand, suggesting that they might directly contact TtgT and TtgV. These data are consistent with the results of DNase I footprinting, as the protected Gs are located within the proposed binding site defined by DNase I footprint. Together these results indicate that TtgT and TtgV recognize the same sequence in the *ttgT-ttgD* intergenic region but with different affinity (Figs 1 and 3).

To further study the role of TtgT in the regulation of *ttgGHI*, footprint assays were carried out using different protein concentrations. TtgT bound with lower affinity
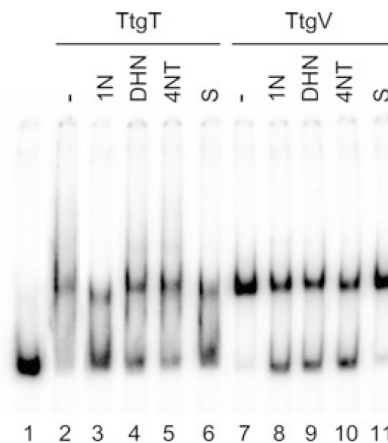
Fig. 2. Electrophoretic mobility shift assays of TtgT and TtgV with the *ttgT-ttgDEF* intergenic region in the presence of different effectors. Binding reactions were carried out as described in *Experimental procedures*. The 295 pb fragment containing the *ttgT-ttgDEF* intergenic region (1 nm) was incubated without protein (lane 1) and with 100 nm of TtgT (lanes 2–6) or TtgV (lanes 7–11), in the absence (lanes 2 and 7) or in the presence of 2 mM of the following effectors: 1-naphthol (1N); 2,3-dihydroxy naphthalene (DHN); 4-nitrotoluene (4NT) and styrene (S).
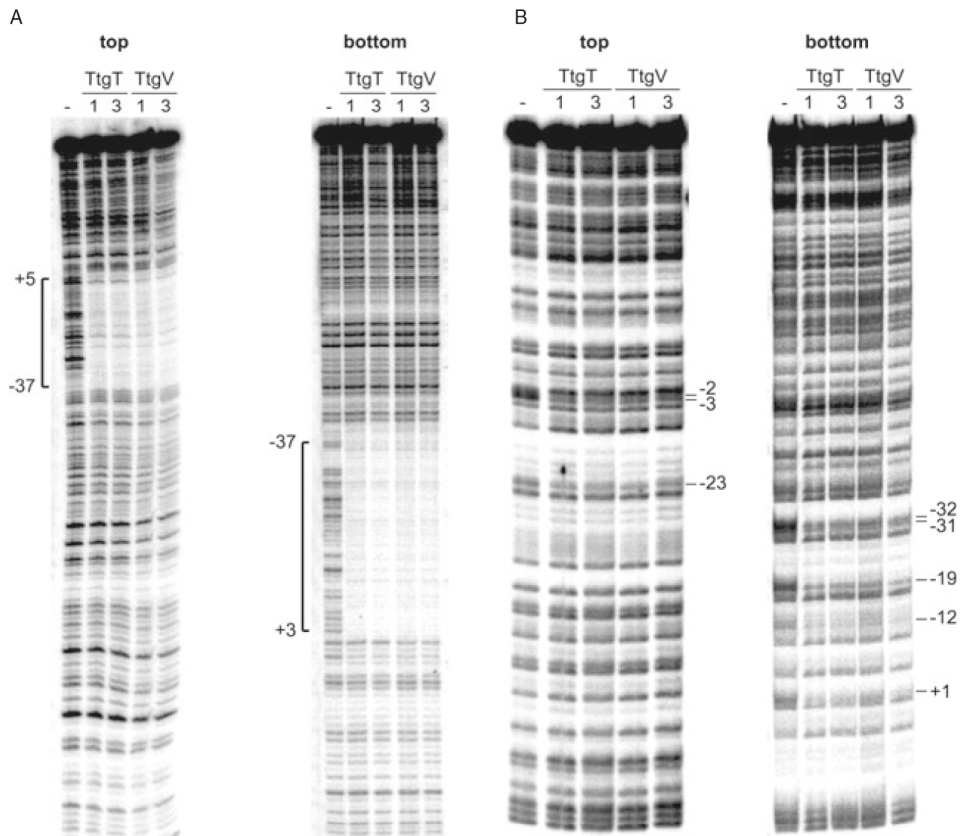
Fig. 3. DNase I and DMS footprints of the *ttgT-ttgDEF* intergenic region.
A. DNase I footprint assays of the *ttgT-ttgDEF* intergenic region were carried out as described in *Experimental procedures*, in the absence (–) and in the presence of TtgT and TtgV (1 and 3 μM). The regions protected by TtgT and TtgV in the top and bottom strands are indicated with respect to the *ttgDEF* transcriptional start point.
B. *In vitro* methylation protection assay of the *ttgDEF* promoter region. PCR fragments comprising the *ttgT-ttgDEF* intergenic region were labelled at one 5′ end and incubated without (–) and with 1 and 3 μM purified TtgV or TtgT before treatment with DMS. The positions of the Gs that are protected from methylation by the repressor are indicated.

(Fig. 1) and protected both strands of a single 42 bp segment within the *ttgV-ttgG* intergenic region that covered the +1 transcription initiation site and the –10 and –35 regions of the *ttgGHI* promoter and the –35 region of the *ttgV* promoter (Fig. 4). To characterize the binding region in greater detail, DMS methylation protection assays were carried out (Fig. 4); the results showed that Gs at positions +6, –15 and –27 were protected in the top strand, Gs at +10, –3, –4, –11 and –23 were protected in the bottom strand, and G –14 was hyper-reactive. Surprisingly, the DNase I-protected region and the DMS methylation pattern of TtgT were similar to those obtained previously for the binding of TtgV (Rojas *et al.*, 2003; Guazzaroni *et al.*, 2004), which indicates that TtgT and TtgV recognize the same sequence in the *ttgV-ttgG* intergenic region in a similar fashion.

TtgT and TtgV exhibit 63% sequence identity and this is particularly significant in their DNA-binding domains, where very few differences are detected. The most dramatic discrepancy within the predicted HTH motif for both proteins is at residue 44: a Gly in TtgV and an Asp in TtgT. In order to test whether amino acid variance in the HTH domain of TtgT versus TtgV accounted for the binding differences, the mutant protein TtgVG44D was produced and EMSAs were carried out using the *ttgT-ttgD* and *ttgV-ttgG* intergenic regions (Fig. S1). Interestingly, the binding affinity of TtgVG44D to the P$_{ttgD}$ promoter region was comparable to that of TtgV. In contrast, the affinity of TtgVG44D for P$_{ttgG}$ DNA was comparable to that of TtgT but inferior to TtgV as the amount of DNA-bound protein (at 100 nM) was 60%, 23% and 15% for TtgV, TtgVG44D and TtgT respectively. This means that TtgT binds to the operator site located at the *ttgGHI* promoter with lower affinity than TtgV; in fact, the estimated binding affinity of TtgVG44D for the P$_{ttgG}$ promoter is more similar to that of TtgT. Therefore, Gly44 seems to be a key residue for the

Fig. 4. DNase I and DMS footprints of the *ttgV-ttgGHI* intergenic region with TtgT. DNase I and DMS footprint assays of the *ttgV-ttgGHI* intergenic region were carried out as described in *Experimental procedures*, in the absence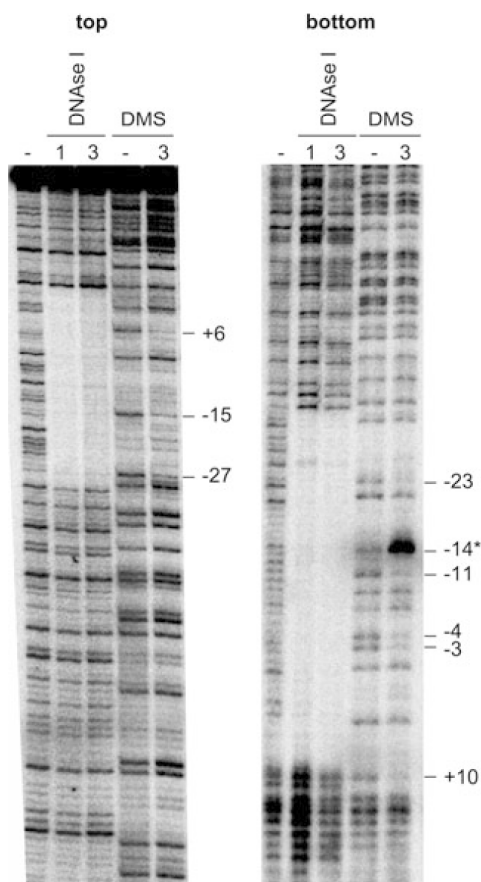 and in the presence of TtgT (1 and 3 μM). The region protected from DNase I by TtgT in the top and bottom strands is indicated with respect to the *ttgGHI* transcriptional start point. The positions of the Gs that are protected from methylation by the repressor are also indicated; G −14 was hyper-reactive to DMS, not protected.

binding to P*ttgG* as TtgV exhibits an increased binding affinity for that operator compared with that of TtgT. This suggests that differences between the HTH domains of both proteins may be critical and could account for their different binding to the two operator sites. Further studies are needed to investigate the exact role of single residues in binding affinity and recognition of both operator sites.

Study of ttgT *and* ttgV *expression*

Rojas *et al*. (2003) demonstrated that TtgV was the repressor of *ttgGHI* and *ttgV* promoters, and showed that the TtgV operator was located within the *ttgV-ttgG* intergenic region that overlaps the −10 and −35 regions of both promoters. We analysed the expression of *ttgV* in the wild-type as well

as in *ttgT*- and/or *ttgV*-deficient backgrounds in the presence of different compounds (Table 2). P*ttgV* basal expression in the wild-type strain was relatively high (about 500 Miller units), and this level increased in the mutant backgrounds lacking *ttgT* or *ttgV* (600 and 1000 Miller units respectively), which indicates that P*ttgV* is repressed by both proteins. Also, in the *ttgT* and *ttgV* mutant strains P*ttgV* was induced by the same compounds that induced P*ttgG*, demonstrating that the two promoters are co-regulated (Rojas *et al*., 2003; Guazzaroni *et al*., 2005). Furthermore, *ttgV* expression levels were high (about 2700 Miller units) and constitutive in the *ttgV/ttgT* double mutant, which is consistent with TtgT and TtgV being the only proteins that modulate *ttgV* expression in response to solvents.

The transcription initiation point of *ttgT* was mapped in *P. putida* DOT-T1E and DOT-T1ET grown in the absence or presence of toluene and styrene (not shown). Independently of the growth conditions, *ttgT* was transcribed from a single promoter whose −10 and −35 regions exhibit low similarity to promoters recognized by the σ^{70} RNA polymerase (Table 2, Fig. S2). The location of *ttgT* and *ttgDEF* start sites indicates that the promoters of the divergently transcribed operons do not overlap, in contrast to the other two homologous efflux pump systems of *P. putida* DOT-T1E, *ttgABC-ttgR* and *ttgGHI-ttgV* (Duque *et al*., 2001; Rojas *et al*., 2003). Analysis of *ttgT* expression levels revealed constitutive expression (about 300 Miller units) regardless of growth conditions (i.e. the presence or absence of organic solvents) or backgrounds (i.e. DOT-T1E, DOT-T1ET, DOT-T1E-PS61 and DOT-T1EVT). These findings are evidence that the *ttgT* gene is not subject to a process of negative autoregulation (Table 2).

The genes encoding the two repressors are therefore differentially expressed. While *ttgT* is always expressed at

Table 2. Expression of *ttgT* and *ttgV* promoters in different backgrounds.

Promoter fusion/effector	T1E	T1ET	PS61	T1EVT
P*ttgT*::*lacZ*				
–	300	300	300	200
Benzonitrile	400	350	300	250
Indole	350	350	350	250
2,3-Dihydroxy naphthalene	300	300	300	200
1-Naphthol	350	350	300	250
P*ttgv*::*lacZ*				
–	500	600	1000	3000
Benzonitrile	2000	2000	2000	2500
Indole	1500	1500	2500	2500
2,3-Dihydroxy naphthalene	2000	1500	2000	3000
1-Naphthol	2000	2500	2500	3000

β-Galactosidase activity from the *ttgT* (pMPT1 plasmid) and *ttgV* (pANA95 plasmid) promoters were determined in cultures of *P. putida* DOT-T1E, DOT-T1ET, DOT-T1E-PS61 or DOT-T1EVT grown in the absence of effectors (–) or with 1 mM of the indicated chemicals. Results are the mean of eight different experiments, with standard deviation below 15% of the given value.
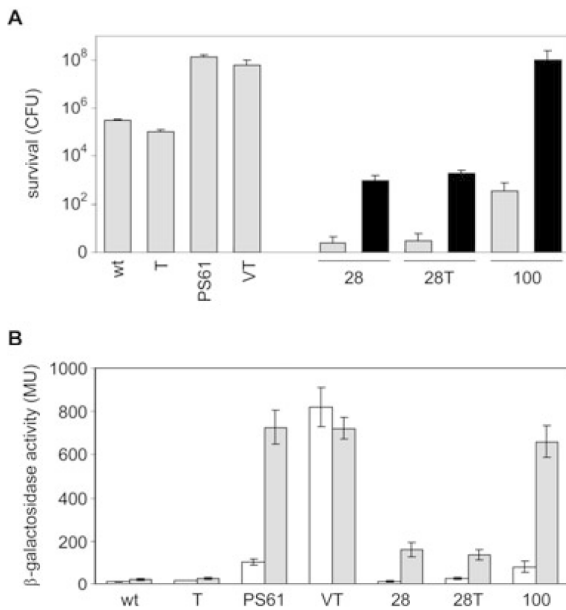
A

B

Fig. 5. Impact of TtgT and TtgV loss on solvent tolerance and on *ttgDEF* expression.
A. Survival of *P. putida* DOT-T1E and mutants after a sudden styrene shock. Cells were grown in LB medium until they reached an OD_{660} of 0.7. The cultures were then split into two halves and 0.3% (v/v) styrene was added to one half and the other was used as a control. The survival was calculated counting the number of viable cells as colony-forming units (cfu ml^{-1}). The strains used were DOT-T1E (wild type), DOT-T1ET (*ttgT*-null mutant), DOT-T1E-PS61 (*ttgV*-null mutant), DOT-T1EVT (*ttgT*- and *ttgV*-null mutant), DOT-T1E28 (*ttgH*-null mutant, therefore lacking the TtgGHI efflux pump), DOT-T1E28T(*ttgT*- and *ttgH*-null mutant, therefore lacking TtgT and TtgGHI), DOT-T1E-100 (defective in the pGRT1 megaplasmid, therefore lacking TtgV and TtgGHI). When indicated (dark bars), cultures were pre-induced with styrene in the gas phase previous to the shock.
B. Induction of the P_{ttgD} promoter by styrene in DOT-T1E mutants. β-Galactosidase activity from the *ttgD* promoter (pMPD1 plasmid) was determined in cultures of *P. putida* DOT-T1E, DOT-T1ET, DOT-T1E-PS61, DOT-T1EVT, DOT-T1E28, DOT-T1E28T and DOT-T1E-100 grown in the absence (white bars) and in the presence of 1 mM of styrene (dark bars). Results are the mean of five different experiments, with the indicated standard deviation.

the same level, *ttgV* basal levels are higher than those of *ttgT* and this difference increases under inducing conditions (Table 2). Also, P_{ttgT} did not appear to be regulated, while *ttgV* expression is controlled by both TtgT and TtgV. The dominance of TtgV over TtgT in the regulation of *ttgDEF* and *ttgGHI* is therefore due to two parameters: its superior affinity and its higher cellular protein levels under inducing conditions.

Biological significance of the TtgDEF efflux pump and the TtgT regulator

Our results show that the main regulator of the *ttgDEF* operon is TtgV and not the expected local repressor TtgT.

The *ttgGHI* operon and the adjacent *ttgV* regulatory gene have been shown to be located on a plasmid that is lost at low frequency, inflicting a toluene-sensitive phenotype (Rodríguez-Herva *et al.*, 2007). In order to analyse the biological role of TtgT and compare it with that of TtgV, we studied its influence on solvent tolerance. To this end, the survival to a sudden styrene shock [0.3% (v/v)] was determined in cells that were not pre-exposed to the solvent (Fig. 5A). The survival of the wild-type strain and the *ttgT* mutant was similar [about 10^5 colony-forming units (cfu) ml^{-1}]. In contrast, the survival of the *ttgV* and *ttgT/ttgV* mutants was significantly higher (around 10^8 cfu ml^{-1}), probably due to the derepression of *ttgGHI* expression in the absence of TtgV. To avoid the super-resistant phenotype originating from *ttgGHI* derepression, survival to styrene shocks was analysed in strains lacking the TtgGHI efflux pump (Fig. 5A). The survival of DOT-T1E28, a strain lacking TtgGHI, was extremely low (lower than 10 cfu ml^{-1}) as compared with that of the wild type; however, pre-adaptation raised the survival rate to 500 cfu ml^{-1}. This is in agreement with previous observations showing that the TtgGHI efflux pump plays a major role in the extrusion of a wide range of toxic aromatic hydrocarbons in *P. putida* DOT-T1E from a quantitative point of view (Rojas *et al.*, 2003; Segura *et al.*, 2003). In DOT-T1E-100, a strain deficient in the pGRT1 plasmid (Rodríguez-Herva *et al.*, 2007), and therefore lacking TtgGHI and TtgV, the survival was about 300 cfu ml^{-1}. However, the pre-adaptation of these cells to styrene resulted in a survival rate of 10^8 cfu ml^{-1}, indicating that, in the absence of the pGRT1 plasmid, TtgDEF plays an important role in the adaptative response to solvents and TtgT exerts its regulatory role in the absence of TtgV. In order to determine the specific role of TtgT in solvent tolerance, we compared the survival of DOT-T1E28 with its isogenic *ttgT* mutant (DOT-T1E28T) and, surprisingly, the behaviour was similar in cells non-pre-exposed and pre-exposed to the solvent. This, together with the observation that pre-adaptation of DOT-T1E-100 cells to styrene resulted in maximal survival, indicates that TtgT controls the survival of cells long time exposed to solvents.

Complementary studies were carried out to analyse the expression of the P_{ttgD} promoter in a strain lacking the pGRT1 plasmid (DOT-T1E-100, Fig. 5B). Wild-type and mutant strains lacking TtgT, TtgV, TtgGHI or combination of them were used as controls (see Table 1). In the wild-type DOT-T1E strain, expression of the *ttgD* promoter was very low, but increased twofold in response to styrene. In the mutant DOT-T1ET, the pattern of induction was similar to that of the wild type although the levels were a little higher. In a TtgV-deficient background, the already high basal level increased sevenfold in the presence of the inducer, a response most likely mediated by TtgT. In the double DOT-T1EVT mutant, no significant induction of
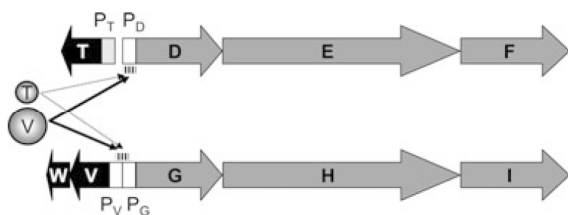
Fig. 6. Cross-regulation of *ttgDEF* and *ttgGHI* efflux pump operons and *ttgT* and *ttgVW* regulatory genes. The results obtained in this work are summarized in this scheme. TtgT and TtgV share a high degree of sequence similarity, and control the expression of three promoters (P*ttgDEF*, P*ttgGHI* and P*ttgV*) by binding to two different operator sites highly similar in sequence, located in the *ttgT-ttgDEF* and *ttgVW-ttgGHI* intergenic regions. TtgV plays a major role in the control of these promoters (thick arrows), whereas TtgT seems to be relegated to a marginal role (thin arrows). The *ttgT* promoter is constitutively expressed and does not seem to be regulated. The absence of negative autoregulation for the *ttgT* gene is a particular feature of the *ttgDEF-ttgT* system compared with *ttgGHI-ttgV*.

ttgDEF expression was detected as TtgT and TtgV were both absent. In DOT-T1E28 the low basal level expression of *ttgD* increased 10-fold after induction, which could be attributed to the accumulation of styrene within the cell due to the lack of the TtgGHI efflux pump. In DOT-T1E28T the behaviour was similar to that of DOT-T1E28, although the basal level was higher and therefore the expression of *ttgD* increased only fivefold after induction. In DOT-T1E-100, deficient in the pGRT1 plasmid, P*ttgD* was expressed at high level (80 Miller units) and increased eightfold in the presence of styrene. Overall, these results show that when the TtgGHI efflux pump is present there is no correlation between *ttgD* expression levels and the survival rate to a sudden styrene shock, which suggests that the TtgGHI efflux pump is mainly responsible for the tolerance phenotype. However, in strains lacking TtgGHI there is a clear correspondence between the level of *ttgD* expression both in the absence and in the presence of styrene and the survival rate of those cells after a styrene shock. From the results obtained with DOT-T1E28 and DOT-T1E28T, it is clear that TtgV remains bound to its operator site and repressing P*ttgD* expression even in the presence of styrene (Fig. 5). However, TtgT responds to the presence of styrene and, in the absence of TtgV, increases the expression level of the TtgDEF efflux pump, which in turn efficiently removes the organic solvent from the membranes and/or the cytoplasm. Therefore, TtgDEF/TtgT plays an important role in solvent tolerance and is responsible for the survival of cells that have lost the plasmid bearing the TtgGHI/TtgV system.

Discussion

The understanding of processes giving rise to multidrug resistance is central to fighting antibiotic resistance of

pathogenic microorganisms. Regardless of whether the primary function of a drug transport system is antimicrobial efflux or whether the export of such compounds occurs fortuitously, these proteins have been recruited by microbial pathogens in a highly successful effort to circumvent the relatively recent widespread use of antimicrobial compounds as therapeutic, prophylactic and veterinary agents. An emerging feature is that efflux pumps are often regulated by transcriptional regulators, which are usually located adjacent to the corresponding cognate-regulated gene (operons). The regulatory circuits in which these efflux pumps are integrated can be relatively simple loops, as in the case of tetracycline efflux mediated by the TetR protein (Hillen and Berens, 1994), or more complex systems, such as the control of the *Escherichia coli* MDR AcrAB pump by AcrR (Ma *et al.*, 1996). Indeed, the latter example is an exceptional case in which in addition to the local AcrR regulator, expression from the P*acrA* promoter is influenced by other proteins under different stress conditions (Ma *et al.*, 1995; Miller and Sulavik, 1996; Okusu *et al.*, 1996; Alekshun and Levy, 1997; White *et al.*, 1997).

One of the main conclusions of our study is that expression of the two efflux pumps TtgDEF and TtgGHI is regulated by local regulators without the participation of global systems, as is the case with the AcrAB pump. A second conclusion is that the key regulator of the *ttgDEF* operon is not the expected local repressor TtgT but its paralogue TtgV, the cognate regulator of the *ttgGHI* operon (Fig. 6). Our data are consistent with functional replacement of the cognate regulator and chromosomally encoded (TtgT) by a similar regulator located on a plasmid (TtgV), a situation which, in the context of the transcriptional regulation of efflux pumps, has not to our knowledge been reported in the literature and constitutes a new mode of physiological efflux pump control. TtgT seems to be relegated to a minor role, as the *in vivo* effect of TtgT on *ttgGHI* and *ttgV* expression was hardly noticeable, and the action of TtgT on *ttgDEF* expression was more evident in the absence of TtgV, at least under the conditions tested (Table 1). However, TtgT plays a central role in maintaining resistance in the strain which has lost the pGRT1 megaplasmid encoding the TtgV-TtgGHI system (Fig. 5).

In order to study whether TtgT might have evolved to exert additional functions in the cell, we scanned *P. putida* KT2440 and *P. putida* F1 genomes for TtgT/V binding sites using different algorithms and only found one possible site at the *sepABC* (similar to *ttgDEF* from DOT-T1E) promoter in F1 (S. Fillet and M.T. Gallegos, pers. comm.). The *ttgT* gene is present in the chromosome of many *Pseudomonas* strains that degrade toluene through the *tod* pathway (Phoenix *et al.*, 2003; Segura *et al.*, 2003; M.T. Gallegos, unpubl. obs.). Their role on solvent resistance has been demonstrated in *P. putida* DOT-T1E (this work) and in

P. putida F1, which harbours solely the SepABC/SepR system that is similar to TtgDEF/TtgT (Phoenix *et al.*, 2003). Therefore, TtgT and TtgV seem to be proteins specifically involved in the regulation of solvent efflux pumps and are unlikely to exert additional functions.

In vitro studies revealed that this cross-regulation is possible because both TtgT and TtgV bind to both the *ttgT-ttgDEF* and *ttgV-ttgGHI* intergenic regions. Moreover, DNase I footprinting assays showed that the binding sites of TtgT and TtgV to both promoter regions were identical: a single binding site in the *ttgT-ttgDEF* intergenic region which covers only the *ttgDEF* promoter region but not the *ttgT* region, and also a single binding site in the *ttgV-ttgGHI* intergenic region which covers *ttgV* and *ttgGHI* promoter regions. This suggests that both paralogues bind their operators and repress *ttgDEF*, *ttgGHI* and *ttgV* expression, probably by competing with the RNA polymerase for access to the promoters. The binding of effector molecules to DNA-bound TtgT and TtgV triggers dissociation of the complex, allowing the RNA polymerase to initiate transcription. It is worth noting that TtgV exhibits higher affinity than TtgT for the operator sites situated in the *ttgT-ttgDEF* and *ttgV-ttgGHI* intergenic regions. This, together with the fact that TtgV reaches higher cellular concentrations than TtgT under inducing conditions and that it seems to respond to less effectors than TtgT, explains the dominance of TtgV over TtgT observed *in vivo*.

Studies on the expression of TtgT and TtgV revealed some differences. Basal expression from the *ttgT* promoter remained constant regardless of the growth conditions and the inducers tested here (organic solvents or antibiotics); in contrast, *ttgV* expression was higher and increased in response to solvents. This indicates that the mechanisms which control TtgV and TtgT are different: TtgV controls its own expression, whereas TtgT does not. This is due to differences in the physical organization of the divergent genes. Rojas *et al.* (2003) showed that the $-10/-35$ region of the *ttgV* promoter overlaps the $-35/-10$ region of the *ttgG* promoter, so that by binding to a single site, TtgV modulates its own transcription and that of *ttgG*. In contrast, identification of the transcription initiation points of both *ttgDEF* and *ttgT* revealed that they are separated by 150 bp, a distance that allows independent transcriptional regulation of these two divergent promoters and thus differences in their expression. The absence of negative autoregulation for the *ttgT* gene is a particular feature of the TtgDEF/TtgT system compared with the TtgGHI/TtgV system. The overlapping nature of *ttgGHI* and *ttgV* promoters implies that TtgV functions as a multidrug-binding regulator that specifically modulates the expression of the *ttgGHI* efflux pump in response to effectors. This modulating role is similar to the one proposed for the AcrR repressor of the AcrAB pump of *E. coli* or TtgR from *P. putida* DOT-T1E (Ma *et al.*, 1996; Terán

et al., 2003). Negative autoregulation seems to accelerate the response of regulatory networks to reach a maximal, but controlled, level of expression in a shorter time (McAdams and Arkin, 1997; Rosenfeld *et al.*, 2002).

TtgT and TtgV repressor proteins and TtgDEF and TtgGHI efflux pumps can be considered paralogues as it appears likely that they have evolved as a result of a recent gene duplication event. Under changing environments, gene duplication can endow the microorganism with a selective advantage and thereby enable its survival and further evolution. Mutation would then provide the increased genetic diversity that drives the evolution of a diverging new protein (Aharoni *et al.*, 2005; Nies *et al.*, 2006). Soil bacteria are exposed to drastic changes in the environment, where such changes might include the appearance of new toxic compounds which are not recognized by the regulators or the pumps, and which as a consequence represent a source of evolutionary pressure. In this context, the presence of multiple copies of the same protein, such as TtgT and TtgV or TtgDEF and TtgGHI, increases the probability that a mutant protein able to handle the new threat will be generated. Contrary to other systems, where one protein of the paralogue pair is silent (Nies *et al.*, 2006), in *P. putida* DOT-T1E, regulatory genes and efflux pumps are functional and, even more, there is a good co-ordination in their expression. A possible explanation for the low but detectable regulatory activity of TtgT may be that the chromosomally encoded TtgDEF/TtgT would be the backup system responsible for the survival of cells that have lost the pGRT1 megaplasmid, especially after long exposure to solvents.

Our results show that TtgT and TtgV have similar but not identical effector profiles (Table 1, Fig. 5). For instance, in the TtgT-deficient mutant, benzonitrile caused a twofold increase in expression. In the wild type and TtgV-deficient mutant the expression was induced four- and sixfold, respectively, which reflects the action of TtgT. In the presence of other effectors, namely 2,3-dihydroxy naphthalene, indole, styrene or naphthalene, the induction of P$_{ttgD}$ expression in the wild-type strain was also greater than in the *ttgT* mutant, but lower than in the *ttgV* mutant (Table 1). Moreover, in the presence of styrene, TtgT seems to play an important role in the induction of *ttgDEF* as TtgT responds better than TtgV to that solvent (Fig. 5). Therefore, it is reasonable to suggest that the presence of both proteins allows the recognition of a wider range of effector molecules than when only one of them is present, which certainly represents an evolutionary advantage. On the other hand, in environments enriched in compounds like benzonitrile, 2,3-dihydroxy naphthalene, indole, styrene or naphthalene, it may be advantageous for *P. putida* DOT-T1E to lose the pGRT1 plasmid in order to be able to respond more readily and survive the toxic stress.

41

Table 3. Strains and plasmids used in this study.

Strains and plasmids	Relevant characteristics	Source or reference
Strains		
P. putida		
DOT-T1E	Rif^r	Ramos *et al.* (1995)
DOT-T1E-PS61	Rif^r, Km^r, *ttgV*::ΩKm	Rojas *et al.* (2001)
DOT-T1ET	Rif^r, Km^r, *ttgT*::ΩKm	This work
DOT-T1EVT	Rif^r, Km^r, Tel^r, *ttgV*::ΩKm, *ttgT*::*kilA/telAB*	This work
DOT-T1E-100	Rif^r, pGRT1$^-$ (*ttgV$^-$*, *ttgGHI$^-$*)	Rodríguez-Herva *et al.* (2007)
DOT-T1E28	Rif^r, Sm^r, *ttgH*::ΩSm	Rojas *et al.* (2003)
DOT-T1E28T	Rif^r, Sm^r, Km^r, *ttgH*::ΩSm, *ttgT*::ΩKm	This work
E. coli		
B834 (DE3)	F$^-$ *ompT hsdS$_B$* (r^-_B m^-_B) *gal dcm met* auxotroph	Novagen
Plasmids		
pET28b(+)	Km^r, protein expression vector	Novagen
pANA126	Km^r, pET28b(+) derivative vector used to produce His$_6$-TtgV	Rojas *et al.* (2001)
pTGF3	Km^r, pET28b(+) derivative vector used to produce His$_6$-TtgT	This work
pMP220	Tc^r, promoterless *lacZ* expression vector	Spaink *et al.* (1987)
pMPD1	Tc^r, *ttgD*::*'lacZ* fusion cloned in pMP220	This work
pMPT1	Tc^r, *ttgT*::*'lacZ* fusion cloned in pMP220	This work
pANA95	Tc^r, *ttgV*::*'lacZ* fusion cloned in pMP220	Rojas *et al.* (2001)
pANA96	Tc^r, *ttgG*::*'lacZ* fusion cloned in pMP220	Rojas *et al.* (2001)
pGEM-T	Ap^r, cloning vector	Promega
pHP45Ω-Km	Ap^r, carries the 2.25 kb ΩKm interposon	Fellay *et al.* (1987)
pJMT6	Ap^r, Tel^r, carries *kilA* and *telAB* tellurite resistance genes	Sánchez-Romero *et al.* (1998)
pTGFT	2744 bp chromosomal fragment bearing *ttgT* cloned into pGEM-T	This work
pTGFT-Km	pTGFT with ΩKm inserted into the EcoRI site	This work
pTGFT-Tel.	pTGFT with *kilA/telAB* genes inserted into the *Bst*Z17I site	This work

Ap^r, Km^r, Rif^r, Sm^r, Tc^r, Tel^r stand for resistance to ampicillin, kanamycin, rifampicin, streptomycin, tetracycline and tellurite respectively.

The findings reported here constitute the first evidence of cross-regulatory control of different RND efflux pumps involving their two homologous local regulators, one of them located on a megaplasmid. This is an interesting example of evolution of a simple regulatory circuit into a more complex network, and reflects the ability of bacterial regulatory systems to evolve in order to respond more efficiently to environmental signals.

Experimental procedures

Bacterial strains, plasmids and culture medium

The bacterial strains and plasmids used in this study are shown in Table 3. These strains were routinely grown in liquid Luria–Bertani (LB) medium at 30°C (Ausubel *et al.*, 1991). When required, the following antibiotics were added to the cultures to the following final concentrations: 50 μg ml^{-1} kanamycin (Km), 20 μg ml^{-1} rifampicin (Rif), 300 μg ml^{-1} streptomycin (Sm) and 20 μg ml^{-1} tetracycline (Tc).

We constructed fusions of the *ttgDEF* operon and *ttgT* gene promoters to a promoterless *lacZ* gene in the low-copy-number (two to four copies per cell) pMP220 vector (Spaink *et al.*, 1987). The *ttgT-ttgD* intergenic region (233 bp) was amplified by PCR from *P. putida* DOT-T1E chromosomal DNA, isolated according to Ausubel *et al.* (1991), with primers incorporating EcoRI and PstI restriction sites: TTG-DEcoRI (5′-NNNNGAATTCTGTAGAACTGATCTTTTGGG-3′) and TTGDPstI (5′-NNNNCTGCAGAACTGATCTTTTGGG-3′) to create a fusion of the *ttgDEF* promoter to *'lacZ*,

and TTGTEcoRI (5′-NNNNGAATTCTGATCCAGGCC-3′) and TTGTPstI (5′-NNNNCTGCAGATCCAGGCCACCG-3′) to create a fusion of the *ttgT* promoter to *'lacZ*. PCR reactions (50 μl) were carried out in PCR buffer (10 mM Tris-HCl pH 8.3, 50 mM KCl) with 2.5 U of Taq polymerase (Amersham-Pharmacia), 0.2 μM of each primer, 0.8 mM dNTPs (Roche) and about 100 ng of template DNA. Cycling parameters were 2 min incubation at 96°C, followed by 30 cycles of 96°C for 1 min, 55°C for 30 s and 72°C for 1 min, before finishing with 10 min at 72°C. Upon amplification, DNA was digested with EcoRI and PstI, and ligated to EcoRI–PstI-digested pMP220 to produce pMPD1 (P$_{ttgD}$::*'lacZ*) and pMPT1 (P$_{ttgT}$::*'lacZ*). Plasmids pMPD1 and pMPT1 were sequenced to make sure that no mutations were introduced in the corresponding promoter regions. These plasmids, together with pANA96 (P$_{ttgG}$::*'lacZ*) and pANA95 (P$_{ttgV}$::*'lacZ*) (Rojas *et al.*, 2003), were electroporated into *P. putida* DOT-T1E or its derivative mutants according to Enderle and Farwell (1998).

Construction of mutant P. putida *DOT-T1E derivatives*

We constructed the *ttgT*- and the double *ttgT/ttgV*-null mutants by gene replacement, for which we first knocked out the *ttgT* gene *in vitro*. Plasmid pTGFT is a pGEM-T derivative that carries a 2744 bp chromosomal fragment harbouring the *ttgT* gene and flanking DNA. This plasmid has a single EcoRI site around the middle of the *ttgT* ORF. Upon digestion with EcoRI, the plasmid was ligated to a 2 kb EcoRI fragment of plasmid pHP45ΩKm bearing the ΩKm interposon (Fellay *et al.*, 1987) to yield the plasmid pTGFT-Km, which was used for *in vivo*

gene replacement. The suicide plasmid pTGFT-Km encodes resistance to ampicillin (Ap)/carbenicillin (Cb) and kanamycin (Km), and was electroporated into *P. putida* DOT-T1E (Enderle and Farwell, 1998). Transformants that had acquired the inactivated gene (Km^r) were selected. Among the Km^r clones, we searched for Ap (300 µg ml^{-1})/Cb (300 µg ml^{-1})-sensitive ones, which were expected to be the result of a double-recombination event. One of the Km^r, Ap/Cb^s clones, called DOT-T1ET, was chosen and confirmed by Southern blot to have the wild-type *ttgT* gene replaced by the mutant allele *ttgT*::ΩKm (not shown). To obtain the double *ttgT/ttgV* mutant, the process was similar except that the plasmid used for gene replacement was pTGFT-Tel, in which *ttgT* was interrupted upon digestion with BstZ17I and ligation with a 3113 bp fragment bearing the tellurite resistance genes *kilA* and *telAB* from the pJMT6 plasmid (Sánchez-Romero *et al.*, 1998). The suicide plasmid pTGFT-Tel was electroporated into *P. putida* DOT-T1E-PS61 (*ttgV*::ΩKm) (Rojas *et al.*, 2003) and double mutants were selected in K$_2$TeO$_3$ (30 µg ml^{-1}) and kanamycin. One of the Tel^r, Km^r, Ap/Cb^s clones, called DOT-T1EVT, was chosen and confirmed by Southern blot to have the wild-type *ttgT* and *ttgV* genes replaced by the mutant alleles *ttgT*::Tel and *ttgV*::ΩKm respectively (not shown).

Obtaining DOT-T1E28T mutant strain was achieved through several steps. We first obtained strain DOT-T1E-100T by curing DOT-T1ET of the pGRT1 megaplasmid. For that, DOT-T1ET (pMPD1) was grown for more than 100 generations in LB medium, and then bacteria were spread onto LB plates with X-gal. Dark blue colonies were selected and the absence of the megaplasmid was checked by PCR and plasmid prep. After that, the strain was cured of the pMPD1 plasmid by the same method as before, and the Tc^s DOT-T1E-100T strain was also checked by PCR and plasmid prep. At last, we set up biparental matings as described before (Ramos-González *et al.*, 1991) between donor strain *P. putida* DOT-T1E28, which carries a mutant pGRT1 plasmid in which the wild-type *ttgH* gene has been replaced by the mutant allele *ttgH*::ΩSm, and *P. putida* DOT-T1E-100T, which is a *ttgT*-null mutant that also lacks pGRT1, as the receptor strain. The resulting strain, DOT-T1E28T, was a Sm^r and Km^r*ttgT*- and *ttgH*-null mutant.

β-Galactosidase assays

Bacterial cells were inoculated from fresh LB agar plates supplemented with the appropriate antibiotics and grown overnight at 30°C on LB medium with the appropriate antibiotics. Cultures were diluted to an initial OD$_{660}$ of 0.05 in the same medium supplemented or not with the chemicals to be tested. The organic compounds or solvents used in the β-galactosidase assays were added to a concentration of 1 mM, and were dissolved in dimethyl sulphoxide when needed (note that the latter did not interfere with the induction assays in this study). β-Galactosidase activity was determined in triplicate in permeabilized cells when cultures reached an OD$_{660}$ of 0.9–1.0 (Miller, 1972). Results are the mean of five to eight different experiments.

Overexpression and purification of TtgT and TtgV

A 807 bp fragment containing the *ttgT* gene was PCR-amplified from *P. putida* DOT-T1E chromosomal DNA, and

primers TtgT5′NdeI (5′-NNNNNNCATATGAGCGATTCGG AAGAAA-3′) and TtgT3′BamHI (5′-NNNNNNGGATCCT CATCAACCCGCAAACTCCCGA-3′), which generated NdeI and BamHI restriction sites respectively. PCR reactions were carried out as above. After digestion with these restriction enzymes, the PCR products were ligated into pET28b(+) vector (Novagen) previously digested with NdeI and BamHI. The resulting plasmid, pTGF3, contained the *ttgT* coding sequence in frame with a DNA sequence encoding a His$_6$-tag at its 5′ end. pTGF3 and pANA126 (Rojas *et al.*, 2003) were transformed into *E. coli* B834(DE3) and His$_6$-TtgT and His$_6$-TtgV purification was carried out as described previously (Rojas *et al.*, 2003).

Electrophoretic mobility shift assays (EMSAs)

The DNA probe were 295 bp fragments containing the *ttgT-ttgDEF* and *ttgV-ttgGHI* intergenic regions obtained from DOT-T1E chromosomal DNA by PCR with primers D5′E (5′-nnnnnngaattccttctgatccaggccaccg-3′) and D3′P (5′-NNNNNNCTGCAGTAACTGTCTCGCACGcaaag-3′) and G5′E (NNNNNNGAATTCGTTCATATCTTTCCTCTGCG) and G3′P (NNNNNNCTGCAGGGGGATTACCCGTAATGCAC) respectively. Cycling parameters were 5 min at 96°C followed by 30 cycles of 96°C for 1 min, 58°C for 30 s and 72°C for 1 min, before finishing with 10 min at 72°C. The PCR product was isolated from an agarose gel using the QIAquick Gel Extraction Kit (Qiagen) and radiolabelled at its 5′ ends with [γ-^{32}P]-ATP and T4 polynucleotide kinase. 1 nM (~10^4 c.p.m.) of the labelled probe was then incubated with the indicated concentrations of purified proteins in 10 µl of TAPS [50 mM Tris-acetate pH 8.0, 100 mM K-acetate, 8 mM Mg-acetate, 27 mM ammonium acetate, 3.5% (w/v) polyethylene glycol-8000 and 1 mM DTT] supplemented 15 µg ml^{-1} poly (dI-dC) and 200 µg ml^{-1} BSA. When indicated, effectors were added to the binding reaction mixture at 2 mM. Reactions were then incubated for 10 min at 30°C and samples were run on 4.5% (w/v) native polyacrylamide gels (Bio-Rad Mini-Protean II) for 2 h at 50 V at room temperature in Tris-glycine buffer (25 mM Tris-HCl pH 8.0, 200 mM glycine). Results were analysed with Personal FX equipment and Quantity One software (Bio-Rad).

Footprint assays

The DNA probes were a 218 bp and a 228 pb PCR fragment containing the *ttgT-ttgDEF* and the *ttgVW-ttgGHI* intergenic region respectively. For the footprint on the top strand, the PCR reaction was carried out with primers DEF5′ (5′-CCTTCTGATCCAGGC-3′) or GHI5′ (5′-GTTCATATGTT TCCTCTGCG-3′), the product was end-labelled with [γ-^{32}P]-ATP as described above, and DEF3′ (5′-TAGAACTGATCT TTTGG-3′) or GHI3′ (5′-GTTTGGCTCCATCTCTCTGC-3′). For the footprint on the bottom strand, the same primers were used, but DEF3′ or GHI3′ were end-labelled. Purified labelled probe (10 nM; ~10^4 c.p.m.) was incubated without or with His$_6$-TtgT or His$_6$-TtgV (1–3 µM) in 10 µl reaction volumes of STAD [25 mM Tris-acetate pH 8.0, 8 mM Mg-acetate, 10 mM KCl, 3.5% (w/v) polyethylene glycol-8000 and 1 mM DTT] supplemented with 20 µg ml^{-1} poly (dI-dC) and 200 µg ml^{-1} BSA. The mixtures were incubated for 10 min at 30°C before

being treated with 40 μl of DNase I or DMS, as described previously (Rojas *et al.*, 2003; Guazzaroni *et al.*, 2004).

Survival in response to styrene shocks

Cells were grown overnight in 30 ml of LB medium in the absence or in the presence (pre-adaptation) of styrene in the gas phase. On the following day cultures were diluted to reach a turbidity at 660 nm (OD_{660}) of 0.05, and grown under the same conditions until they reached an OD_{660} of 0.7. Then the cultures were divided into two halves; 0.3% (v/v) styrene was added to one half, and the other was used as a control. The number of viable cells was determined (before styrene addition and after 30 min of exposure to the solvent) by spreading suitable dilutions on LB plates. The assays were performed in duplicate and repeated at least three times.

Acknowledgements

References

Aharoni, A., Gaidukov, L., Khersonsky, O., McQ Gould, S., Roodveldt, C., and Tawfik, D.S. (2005) The 'evolvability' of promiscuous protein functions. *Nat Genet* **37:** 73–76.

Alekshun, M.N., and Levy, S.B. (1997) Regulation of chromosomally mediated multiple antibiotic resistance: the *mar* regulon. *Antimicrob Agents Chemother* **41:** 2067–2075.

Ausubel, F.M., Brent, R., Kingston, R.F., Moore, D.D., Seidman, J.G., Smith, J.A., and Struhl, K. (1991) *Current Protocols in Molecular Biology*. New York: Greene Publishing Associated.

Dagley, S. (1971) Catabolism of aromatic compounds by micro-organisms. *Adv Microb Physiol* **6:** 1–46.

Duque, E., Segura, A., Mosqueda, G., and Ramos, J.L. (2001) Global and cognate regulators control the expression of the organic solvent efflux pumps TtgABC and TtgDEF of *Pseudomonas putida*. *Mol Microbiol* **39:** 1100–1106.

Enderle, P.J., and Farwell, M.A. (1998) Electroporation of freshly plated *Escherichia coli* and *Pseudomonas aeruginosa* cells. *Biotechniques* **25:** 954–956.

Fellay, R., Frey, J., and Krisch, H. (1987) Interposon mutagenesis of soil and water bacteria: a family of DNA fragments designed for *in vitro* insertional mutagenesis of gram-negative bacteria. *Gene* **52:** 147–154.

Guazzaroni, M.E., Terán, W., Zhang, X., Gallegos, M.T., and Ramos, J.L. (2004) TtgV bound to a complex operator site represses transcription of the promoter for the multidrug and solvent extrusion TtgGHI pump. *J Bacteriol* **186:** 2921–2927.

Guazzaroni, M.E., Krell, T., Felipe, A., Ruiz, R., Meng, C., Zhang, X., *et al.* (2005) The multidrug efflux regulator TtgV

recognizes a wide range of structurally different effectors in solution and complexed with target DNA: evidence from isothermal titration calorimetry. *J Biol Chem* **280:** 20887–20893.

Heipieper, H.J., and de Bont, J.A.M. (1994) Adaptation of *Pseudomonas putida* S12 to ethanol and toluene at the level of fatty acid composition of membranes. *App Environ Microbiol* **60:** 4440–4444.

Heipieper, H.J., Menlenbeld, G., van Oirschot, Q., and de Bont, J.A.M. (1996) Effect of environmental factors on the *cis/trans* ratio of unsaturated fatty acids in *Pseudomonas* S12. *Appl Environ Microbiol* **62:** 2773–2777.

Hillen, W., and Berens, C. (1994) Mechanisms underlying expression of Tn*10* encoded tetracycline resistance. *Annu Rev Microbiol* **48:** 345–369.

Inoue, A., and Horikoshi, K. (1989) A *Pseudomonas* thrives in high concentrations of toluene. *Nature* **338:** 264–266.

Isken, S., and de Bont, J.A.M. (1996) Active efflux of toluene in a solvent-resistant bacterium. *J Bacteriol* **178:** 6056–6058.

Jude, F., Arpin, C., Brachet-Castang, C., Capdepuy, M., Caumette, P., and Quentin, C. (2004) TbtABM, a multidrug efflux pump associated with tributyltin resistance in *Pseudomonas stutzeri*. *FEMS Microbiol Lett* **232:** 7–14.

Junker, F., and Ramos, J.L. (1999) Involvement of the *cis-trans* isomerase CtiT1 in solvent resistance in *Pseudomonas putida* DOT T1. *J Bacteriol* **181:** 5693–5700.

Kobayashi, H., Uematsu, K., Hirayama, H., and Horikoshi, K. (2000) Novel toluene elimination system in a toluene-tolerant microorganism. *J Bacteriol* **182:** 6451–6455.

Krell, T., Molina-Henares, A.J., and Ramos, J.L. (2006) The IclR family of transcriptional activators and repressors can be defined by a single profile. *Protein Sci* **15:** 1207–1213.

Loffeld, B., and Keweloh, H. (1996) *Cis/trans* Isomerization of unsaturated fatty acids as possible control mechanism of membrane fluidity in *Pseudomonas putida* P8. *Lipids* **31:** 811–815.

Ma, D., Cook, D.N., Alberti, M., Pon, N.G., Nikaido, H., and Hearst, J.E. (1995) Genes *acrA* and *acrB* encode a stress-induced efflux system of *Escherichia coli*. *Mol Microbiol* **16:** 45–55.

Ma, D., Alberti, M., Lynch, C., Nikaido, H., and Hearst, J.E. (1996) The local repressor AcrR plays a modulating role in the regulation of *acrAB* genes of *Escherichia coli* by global stress signals. *Mol Microbiol* **19:** 101–112.

McAdams, H.H., and Arkin, A. (1997) Stochastic mechanisms in gene expression. *Proc Natl Acad Sci USA* **94:** 814–819.

Miller, J.H. (1972) *Experiments in Molecular Genetics*. Cold Spring Harbor, NY: Cold Spring Harbor Laboratory.

Miller, P.F., and Sulavik, M.C. (1996) Overlaps and parallels in the regulation of intrinsic multiple-antibiotic resistance in *Escherichia coli*. *Mol Microbiol* **21:** 441–448.

Molina-Henares, J., Krell, T., Guazzaroni, M.E., Segura, A., and Ramos, J.L. (2006) Members of the IclR family of bacterial transcriptional regulators function as activators and/or repressors. *FEMS Microbiol Rev* **30:** 157–186.

Mosqueda, G., and Ramos, J.L. (2000) A set of genes encoding a second toluene efflux system in *Pseudomonas putida* DOT-T1E is linked to the *tod* genes for toluene metabolism. *J Bacteriol* **182:** 937–943.

Nies, D.H., Rehbein, G., Hoffmann, T., Baumann, C., and Grosse, C. (2006) Paralogs of genes encoding metal resistance proteins in *Cupriavidus metallidurans* strain CH34. *J Mol Microbiol Biotechnol* **11:** 82–93.

Okusu, H., Ma, D., and Nikaido, H. (1996) AcrAB efflux pump plays a major role in the antibiotic resistance phenotype of *Escherichia coli* multiple-antibiotic-resistance (Mar) mutants. *J Bacteriol* **178:** 306–308.

Phoenix, P., Keane, A., Patel, A., Bergeron, H., Ghoshal, S., and Lau, P.C. (2003) Characterization of a new solvent-responsive gene locus in *Pseudomonas putida* F1 and its functionalization as a versatile biosensor. *Environ Microbiol* **5:** 1309–1327.

Ramos, J.L., Duque, E., Huertas, M.J., and Haidour, A. (1995) Isolation and expansion of the catabolic potential of a *Pseudomonas putida* strain able to grow in the presence of high concentrations of aromatic hydrocarbons. *J Bacteriol* **177:** 3911–3916.

Ramos, J.L., Duque, E., Godoy, P., and Segura, A. (1998) Efflux pumps involved in toluene tolerance in *Pseudomonas putida* DOT-T1E. *J Bacteriol* **180:** 3323–3329.

Ramos, J.L., Duque, E., Gallegos, M.T., Godoy, P., Ramos-González, M.I., Rojas, A., *et al.* (2002) Mechanisms of solvent tolerance in gram-negative bacteria. *Annu Rev Microbiol* **56:** 743–768.

Ramos, J.L., Martínez-Bueno, M., Molina-Henares, A.J., Terán, W., Watanabe, K., Zhang, X., *et al.* (2005) The TetR family of transcriptional repressors. *Microbiol Mol Biol Rev* **69:** 326–356.

Ramos-González, M.I., Duque, E., and Ramos, J.L. (1991) Conjugational transfer of recombinant DNA in cultures and in soils: host range of *Pseudomonas putida* TOL plasmids. *J Bacteriol* **57:** 3020–3027.

Rodríguez-Herva, J.J., García, V., Hurtado, A., Segura, A., and Ramos, J.L. (2007) The *ttgGHI* solvent efflux pump operon of *Pseudomonas putida* DOT-T1E is located on a large self-transmissible plasmid. *Environ Microbiol* **9:** 1550–1561.

Rojas, A., Duque, E., Mosqueda, G., Golden, G., Hurtado, A., Ramos, J.L., and Segura, A. (2001) Three efflux pumps are required to provide efficient tolerance to toluene in *Pseudomonas putida* DOT-T1E. *J Bacteriol* **183:** 3967–3973.

Rojas, A., Segura, A., Guazzaroni, M.E., Terán, W., Hurtado, A., Gallegos, M.T., and Ramos, J.L. (2003) *In vivo* and *in vitro* evidence shows that TtgV is the local specific regulator of the TtgGHI multidrug and solvent efflux pump of *Pseudomonas putida*. *J Bacteriol* **185:** 4755–4763.

Rosenfeld, N., Elowitz, M.B., and Alon, U. (2002) Negative autoregulation speeds the response times of transcription networks. *J Mol Biol* **323:** 785–793.

Sánchez-Romero, J.M., Díaz-Orejas, R., and de Lorenzo, V. (1998) Resistance to tellurite as a selection marker for genetic manipulations of *Pseudomonas* strains. *Appl Environ Microbiol* **64:** 4040–4046.

Segura, A., Rojas, A., Hurtado, A., Huertas, M.J., and Ramos, J.L. (2003) Comparative genomic analysis of solvent extrusion pumps in *Pseudomonas* strains exhibiting different degrees of solvent tolerance. *Extremophiles* **7:** 371–376.

Sikkema, J., de Bont, J.A.M., and Poolman, B. (1995) Mechanisms of membrane toxicity of hydrocarbons. *Microbiol Rev* **59:** 201–222.

Spaink, H.P., Okker, R.J.H., Wijffelman, C.A., Pees, E., and Lugtenberg, B.J.J. (1987) Promoters in the nodulation region of the *Rhizobium leguminosarum* Sym plasmid pRL1JI. *Plant Mol Biol* **9:** 27–39.

Terán, W., Felipe, A., Segura, A., Rojas, A., Ramos, J.L., and Gallegos, M.T. (2003) Antibiotic-dependent induction of *Pseudomonas putida* DOT-T1E TtgABC efflux pump is mediated by the drug binding repressor TtgR. *Antimicrob Agents Chemother* **47:** 3067–3072.

Terán, W., Krell, T., Ramos, J.L., and Gallegos, M.T. (2006) Effector–repressor interactions, binding of a single effector molecule to the operator-bound TtgR homodimer mediates derepression. *J Biol Chem* **281:** 7102–7109.

Wery, J., Hidayat, B., Kieboom, J., and de Bont, J.A. (2001) An insertion sequence prepares *Pseudomonas putida* S12 for severe solvent stress. *J Biol Chem* **276:** 5700–5706.

White, D.G., Goldman, J.D., Demple, B., and Levy, S.B. (1997) Role of the *acrAB* locus in organic solvent tolerance mediated by expression of *marA*, *soxS*, or *robA* in *Escherichia coli*. *J Bacteriol* **179:** 6122–6126.

Supplementary material

This material is available as part of the online article from: http://www.blackwell-synergy.com/doi/abs/10.1111/ j.1365-2958.2007.06004.x (This link will take you to the article abstract).

Please note: Blackwell Publishing is not responsible for the content or functionality of any supplementary materials supplied by the authors. Any queries (other than missing material) should be directed to the corresponding author for the article.

TtgV réprime deux promoteurs distincts en reconnaissant différentes séquences

In vivo, l'expression des opérons des pompes d'efflux *ttgDEF* et *ttgGHI* est principalement modulée par le répresseur TtgV. TtgV est un régulateur capable de reconnaître de nombreuses drogues et qui présente un domaine d'union à l'ADN dotée d'une longue hélice d'interaction comprises entre les résidus 47 et 64. Chez *Pseudomonas putida*, le modèle d'expression de ces deux pompes est distinct : en absence d'effecteurs, le promoteur du gène *ttgD* est silencieux, alors que le gène *ttgG* est exprimé à un haut niveau basal. Ce qui concorde avec le fait que TtgV présente meilleure affinité pour l'opérateur *ttgD* (K_D = 10 ± 1nM) que pour celui de *ttgG* (K_D = 19 ± 1nM). Des analyses séquentielles ont révélées que ces deux opérateurs sont identiques à 40 %, de plus, des analyses mutationnelles, combinées à des essais de retard en gel (EMSA) et expression *in vivo*, suggère que TtgV reconnaît une séquence répétée inversée avec un grand degrés de palindromicité autour de l'axe central. Nous avons généré une collection de mutants du résidu 47 au résidu 64 de TtgV, en substituant chaque acide aminé par une alanine. Le résultat de l'extensive combinaison entre les mutants des deux promoteurs et les mutants de substitution alanine ont révélé que TtgV module l'expression des promoteurs *ttgD* et *ttgG* à travers des deux : communes ou différentes, séquences des deux promoteurs. Dans cette même optique, nous avons démontré que les mutants de substitution des résidus 48, 50, 53, 54, 60 et 61 présentent un défaut d'union à *ttgG* mais sont capables de reconnaître l'opérateur *ttgD*. Les acides aminés R47, R52, L57 et T49 sont critiques pour l'union de TtgV à ses deux operateurs. En se basant sur un modèle tridimensionnel nous proposons, comme modèle d'union de TtgV, que ces résidus contactent avec les nucléotides situés au sein du sillon majeur de la double hélice de l'ADN.

TtgV reprime dos promotores distintos reconociendo secuencias distintas

In vivo, la expresion de los operones de las bombas de eflujo *ttgDEF* y *ttgGHI* está modulada fundamentalmente por el represor TtgV. TtgV es un regulador capaz de reconocer numerosas drogas y que dispone de un dominio de unión al ADN dotado de una helice de interacción entre los residuos 47 y 64. En *Pseudomonas putida*, el modelo de expresión de estas dos bombas es distincto: en ausencia de efector, el promotor del gen *ttgD* es silencioso, mientras que el del gen *ttgG* se expresa con un nivel basal alto. Lo que concuerda con el hecho que TtgV tiene mejor afinidad para el operador *ttgD* (K_D = 10 ± 1nM) que para el de *ttgG* (K_D = 19 ± 1nM). Análisis de secuencias han revelado que estos dos operadores son identicos en un 40%, además, análisis mutacionales, combinados con ensayos de retardo en gel (EMSA) y de expresion *in vivo*, suggiera que TtgV reconoce una secuencia repetida invertida con un alto grado de palindromicidad alrededor del eje central. Hemos generado

una coleccion de mutantes del residuo 47 hasta el 64 de TtgV, substituyendo cada amino acido por una alanina. El resultado de la amplia combinación entre mutantes de los dos promotores y mutantes de subtitución alanina ha revelado que TtgV modula la expresión de los promotores *ttgD* y *ttgG* mediante secuencias: comunes y differentes, en ambos promotores. En esta misma óptica, hemos demostrado que los mutantes de substitución de los residuos 48, 50, 53, 54, 60 y 61 presentan un defecto de unión en el operador *ttgG* pero son capazes de unirse a el de *ttgD*. Los aminoácidos R47, R52, L57 y T49 son críticos para la unión de TtgV a sus operadores. Basándonos en un modelo tridimensional hemos propuesto que estos residuos contactan con los nucleotidos situados en el surco mayor de la doble hélice del ADN.

TtgV Represses Two Different Promoters by Recognizing Different Sequences[∇]

Sandy Fillet,[1] Marisela Vélez,[2] Duo Lu,[3] Xiaodong Zhang,[3]
María-Trinidad Gallegos,[1] and Juan L. Ramos[1]*

*Department of Environmental Protection, EEZ-CSIC, Granada, Spain[1]; Centro de Biología Molecular,
Madrid, Spain[2]; and Imperial College, London, United Kingdom[3]*

Expression of the multidrug efflux pump *ttgDEF* and *ttgGHI* operons is modulated in vivo mainly by the TtgV repressor. TtgV is a multidrug recognition repressor that exhibits a DNA binding domain with a long interaction helix comprising residues 47 to 64. The pattern of expression of the two pumps is different in *Pseudomonas putida*: in the absence of effectors, the promoter for the *ttgD* gene is silent, whereas the *ttgG* gene is expressed at a high basal level. This correlates with the fact that TtgV exhibits a higher affinity for the *ttgD* operator ($K_D = 10 \pm 1$ nM) than for the *ttgG* ($K_D = 19 \pm 1$ nM) operator. Sequence analysis revealed that both operators are 40% identical, and mutational analysis of the *ttgD* and *ttgG* operators combined with electrophoretic mobility shift assays and in vivo expression analysis suggests that TtgV recognizes an inverted repeat with a high degree of palindromicity around the central axis. We generated a collection of alanine substitution mutants with substitutions between residues 47 and 64 of TtgV. The results of extensive combinations of promoter variants with these TtgV alanine substitution mutants revealed that TtgV modulates expression from *ttgD* and *ttgG* promoters through the recognition of both common and different sequences in the two promoters. In this regard, we found that TtgV mutants at residues 48, 50, 53, 54, 60, and 61 failed to bind *ttgG* but recognized the *ttgD* operator. TtgV residues R47, R52, L57, and T49 are critical for binding to both operators. Based on three-dimensional models, we propose that these residues contact nucleotides within the major groove of DNA.

Multidrug efflux pumps are widely distributed among prokaryotic and eukaryotic organisms and are responsible for resistance to a number of antibiotics, flavonoids, organic solvents, superoxide-generating agents, dyes, anticancer compounds, and other drugs (2, 14, 15, 16, 24).

The *Pseudomonas putida* DOT-T1E strain (Table 1) has the extraordinary capacity to withstand and even grow in the presence of high concentrations of organic solvents such as toluene, styrene, and xylenes (19). The toxicity of these aromatic hydrocarbons derives from their preferential partitioning in the cell membrane, which leads to collapse of the cell membrane potential and eventually causes cell death. The main mechanism underlying solvent resistance in this and other gram-negative bacteria lies in the action of RND (resistance-nodulation-cell division) efflux pumps (17, 18). In the DOT-T1E strain, three of these pumps, called TtgABC, TtgDEF, and TtgGHI (13, 18, 22), are involved in the concerted extrusion of organic solvents, although the TtgGHI pump is chiefly responsible, from a quantitative point of view, for the extrusion of toluene and other solvents from the cell membranes (22, 23).

Control of the expression of the *ttgABC* operon is mediated by TtgR, a member of the TetR family of regulators (1, 20), whereas expression of *ttgDEF* and *ttgGHI* is mediated mainly by the TtgV repressor, a member of the IclR family of regu-

lators (12). Expression of the last two efflux pumps is also under the side control of TtgT, another repressor that exhibits 63% identity to TtgV (27); we found that in vivo the *ttgV* gene was expressed at a higher level than the *ttgT* gene and that the TtgV protein exhibited a higher affinity than TtgT for its operators. Consequently, the TtgV protein turned out to be the main regulator of in vivo expression of the *ttgDEF* and *ttgGHI* efflux pumps (27). In a *ttgV*-deficient background, the role of TtgT as a repressor of the *ttgD* and *ttgG* promoters became measurable, as the expression of these promoters was still modulated in response to effectors. This constituted the first example of cross-regulation of two RND efflux pumps involved in the defense against toxic compounds (27).

Due to the dominant role in vivo of TtgV, its interaction with the *ttgG* promoter has been documented more widely than that of TtgT. Footprint assays revealed that TtgV protected a 42-bp region that covers the −10/−35 regions of the *ttgG* promoter and the −10 region of the divergently oriented *ttgV* promoter (5, 23). Isothermal titration calorimetry analyses showed that TtgV recognition specificity is restricted within the *ttgG* operator to a 34-nucleotide stretch, and it was proposed that TtgV recognized intercalated inverted repeats that share no significant DNA sequence similarities (4) (Fig. 1). In addition, atomic force microscopy studies of TtgV-*ttgG* operator complexes showed that TtgV induced a 57° convex bend in the DNA (4). It was therefore proposed that the mechanism of TtgV repression was based on steric occlusion of the RNA polymerase binding site, reinforced by DNA bending of the *ttgV*-*ttgG* promoter region. Early studies also showed that TtgV exhibits multidrug effector specificity and recognizes mono-

* Corresponding author. Mailing address: Estación Experimental del Zaidín, C/ Profesor Albareda 1, E-18008 Granada, Spain. Phone: 34 958 181608. Fax: 34 958 135740. E-mail: jlramos@eez.csic.es.

TABLE 1. Strains and plasmids used in this study

Strain or plasmid	Relevant characteristics[a]	Source or reference
Strains		
P. putida strains		
DOT-T1E	Rif^r	17
DOT-T1EVT	Rif^r Km^r Tel^r *ttgV*::Km *ttgT*::*kilA/telAB*	27
E. coli strains		
BL21(DE3)	Carries T7 RNA polymerase under the control of the *lacUV5* promoter	Novagen
DH5α	*supE44* Δ(*lacZYA-argF*) *U169 deoR* (φ80*lacZ*Δ*M15*) *hsdR17*(r$_K$⁻ m$_K$⁻) *recA1 endA1 gyrA* (Nal^r) *thi-1 relA1* Δ(*lacIZY*Δ-*argF*)	28
JM109	F′ *traD36 lacI*^{q} Δ(*lacZ*)M15 *proA*⁺*B*⁺/*e14* (McrA⁻) Δ(*lac-proAB*) *thi gyrA96* (Nal^r) *endA1 hsdR17*(r$_K$ m$_K$) *relA1 supE44 recA1*	29
Plasmids		
pET28b(+)	Km^r; protein expression vector	Novagen
pANA126	Km^r; pET28b(+) derivative vector used to produce His$_6$-TtgV	22
pMP220	Tc^r; promoterless *lacZ* expression vector	26
pMPD1	Tc^r; *ttgD*::'*lacZ* fusion cloned in pMP220	27
pANA96	Tc^r; *ttgG*::'*lacZ* fusion cloned in pMP220	22
pGEM-T	Ap^r; cloning vector	Promega
pMBL-T	Ap^r; cloning vector	Promega
pGG1	Ap^r; pUC18 bearing an 8-kb BamHI fragment with *ttgGHI* and *ttgVW*	22
pT1-B6	Ap^r; pUC18 bearing an 6.8-kb BamHI fragment with *ttgDEF* and *ttgT*	22
pBBRN	pBBR-MCS5 derivative with an additional NdeI restriction site	This work
pBBRN::ttgV	Gm^r; pBBRN derivative vector expressing TtgV	This work
pBBRN::R47A	Gm^r; pBBRN derivative vector expressing TtgV(R47A)	This work
pBBRN::V50A	Gm^r; pBBRN derivative vector expressing TtgV(V50A)	This work
pBBRN::Q51A	Gm^r; pBBRN derivative vector expressing TtgV(Q51A)	This work
pBBRN::E60A	Gm^r; pBBRN derivative vector expressing TtgV(E60A)	This work
pET28b(+)::R47A	Km^r; pET28b(+) derivative vector used to produce His$_6$-TtgV(R47A)	This work
pET28b(+)::S48A	Km^r; pET28b(+) derivative vector used to produce His$_6$-TtgV(S48A)	This work
pET28b(+)::T49A	Km^r; pET28b(+) derivative vector used to produce His$_6$-TtgV(T49A)	This work
pET28b(+)::V50A	Km^r; pET28b(+) derivative vector used to produce His$_6$-TtgV(V50A)	This work
pET28b(+)::Q51A	Km^r; pET28b(+) derivative vector used to produce His$_6$-TtgV(Q51A)	This work
pET28b(+)::R52A	Km^r; pET28b(+) derivative vector used to produce His$_6$-TtgV(R52A)	This work
pET28b(+)::I53A	Km^r; pET28b(+) derivative vector used to produce His$_6$-TtgV(I53A)	This work
pET28b(+)::I54A	Km^r; pET28b(+) derivative vector used to produce His$_6$-TtgV(I54A)	This work
pET28b(+)::N55A	Km^r; pET28b(+) derivative vector used to produce His$_6$-TtgV(N55A)	This work
pET28b(+)::L57A	Km^r; pET28b(+) derivative vector used to produce His$_6$-TtgV(L57A)	This work
pET28b(+)::E58A	Km^r; pET28b(+) derivative vector used to produce His$_6$-TtgV(E58A)	This work
pET28b(+)::E59A	Km^r; pET28b(+) derivative vector used to produce His$_6$-TtgV(E59A)	This work
pET28b(+)::E60A	Km^r; pET28b(+) derivative vector used to produce His$_6$-TtgV(E60A)	This work
pET28b(+)::F61A	Km^r; pET28b(+) derivative vector used to produce His$_6$-TtgV(F61A)	This work
pET28b(+)::L62A	Km^r; pET28b(+) derivative vector used to produce His$_6$-TtgV(L62A)	This work
pET28b(+)::V63A	Km^r; pET28b(+) derivative vector used to produce His$_6$-TtgV(V63A)	This work
pET28b(+)::E64A	Km^r; pET28b(+) derivative vector used to produce His$_6$-TtgV(E64A)	This work
pMBLT::pDEF	Ap^r; pMBLT derivative plasmid bearing the *ttgD* promoter	This work
pMBLT::pDEF box 1	Ap^r; pMBLT derivative plasmid bearing a mutant *ttgD* promoter in box 1	This work
pGEMT::pDEF box 3	Ap^r; pGEMT derivative plasmid bearing a mutant *ttgD* promoter in box 3	This work
pMBLT::pDEF box 4	Ap^r; pMBLT derivative plasmid bearing a mutant *ttgD* promoter in box 4	This work
pGEMT::pDEF box 5	Ap^r; pGEMT derivative plasmid bearing a mutant *ttgD* promoter in box 5	This work
pMBLT::pGHI	Ap^r; pMBLT derivative plasmid bearing the *ttgG* promoter	This work
pGEMT::pGHI box 1	Ap^r; pGEMT derivative plasmid bearing a mutant *ttgG* promoter in box 1	This work
pMBLT::pGHI box 3	Ap^r; pMBLT derivative plasmid bearing a mutant *ttgG* promoter in box 3	This work
pGEMT::pGHI box 4	Ap^r; pGEMT derivative plasmid bearing a mutant *ttgG* promoter in box 4	This work
pGEMT::pGHI box 5	Ap^r; pGEMT derivative plasmid bearing a mutant *ttgG* promoter in box 5	This work

[a] Ap^r, Gm^r, Km^r, Rif^r, Tc^r, and Tel^r stand for resistance to ampicillin, gentamicin, kanamycin, rifampin, tetracycline, and tellurite, respectively.

and biaromatic compounds. The most efficient in vivo inducers of TtgV were 1-naphthol, 2,3-dihydroxynaphthalene, and indole (3, 5). Stimulation of transcription from the *ttgD*, *ttgG*, and *ttgV* promoters occurs through a derepression mechanism such that in the absence of effectors, TtgV is bound to the target operators and represses transcription. Upon effector binding, it dissociates from the target DNA, and RNA polymerase subsequently transcribes the *ttgV*, *ttgG*, and *ttgD* promoters (3, 27).

This study was undertaken to better understand *ttgD* repression by TtgV. Initially, we expected that TtgV would recognize similar sequences in both the *ttgD* and *ttgG* operators; however, the operators share only 40% identity, as deduced from the alignment of the regions protected by TtgV in both operators (Fig. 1). It was surprising that the lowest identity was at the 5′-terminal end zone (Fig. 1, box 1), a segment that was proposed to be critical for the recognition of the *ttgG* promoter by TtgV (4) (Fig. 1). We then hypothesized that TtgV might
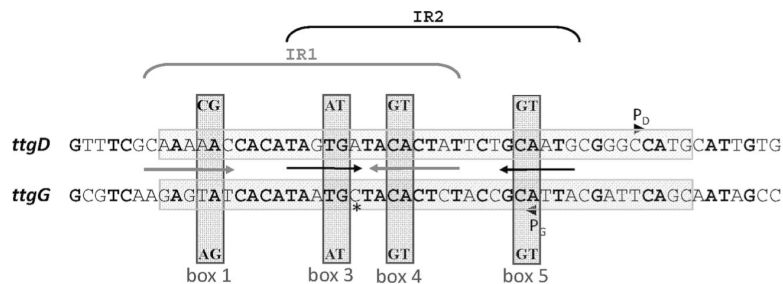
FIG. 1. Alignment of the *ttgD* and *ttgG* operators recognized by TtgV. The transcription initiation points, marked P_G and P_D, were determined in vivo by primer extension (3). The sequences shadowed in gray correspond to protected regions in the footprint. The transcription start points are indicated by arrowheads above (*ttgD*) and below (*ttgG*) the DNA sequence. The indicated overlapping inverted repeats (IR) were proposed by Guazzaroni et al. (4), based on EMSAs and isothermal titration calorimetry assays using variants of the *ttgG* operator and the TtgV protein. The dinucleotides marked boxes 1 and 4 and boxes 3 and 5 were called IR1 and IR2, respectively. The same nomenclature is used in this study to refer to the corresponding aligned sequences in *ttgD*. The dinucleotides above the *ttgD* sequence and below the *ttgG* sequence indicate the changes introduced to create mutants in the marked boxes.

recognize *ttgD* and *ttgG* differentially depending on the precise composition of the binding site. Our results support the hypothesis that TtgV modulates expression from *ttgD* and *ttgG* through the recognition of common and distinct sequences in both operators and that the importance of some residues of the TtgV DNA recognition helix also differs depending on the promoter under scrutiny.

MATERIALS AND METHODS

Bacterial strains, plasmids, and culture medium. The bacterial strains and plasmids used in this study are shown in Table 1. These strains were routinely grown in liquid Luria-Bertani (LB) medium at 30°C (*P. putida*) or 37°C (*Escherichia coli*) with shaking on an orbital platform operating at 200 rpm. *Escherichia coli* DH5α and *E. coli* JM109 were used as host strains to construct and maintain different plasmids. *Escherichia coli* BL21(DE3) was used to overproduce TtgV and its mutant variants. When required, the following antibiotics were added to the cultures to the following final concentrations: 100 μg/ml ampicillin, 10 μg/ml gentamicin, 50 μg/ml kanamycin, 20 μg/ml rifampin, and 20 μg/ml tetracycline. K_2TeO_3 (30 μg/ml) was also used to select some of the mutants.

Construction of TtgV mutants. TtgV mutants in which amino acid residues at positions 47 to 64 were replaced by alanine were generated by overlapping PCR mutagenesis, using the pANA126 plasmid (22) as a source of the *ttgV* wild-type allele. For each mutant, three PCRs were carried out. The first two PCR runs involved amplifications using an upstream primer (corresponding to the *ttgV* coding sequence), a mismatched primer that included the segment to be mutated as well as a PCR amplification using the downstream primer, and an oligonucleotide complementary to the mismatched primer. The resulting overlapping PCR products were annealed, supplemented with upstream and downstream primers, and subjected to the third PCR. The final PCR product was cloned into the pMBL-T or pGEM-T vector, which was subsequently digested with NdeI and BamHI enzymes. The digestion product was cloned into the pET28b(+) vector (Novagen).

Mutant *ttgD* and *ttgG* promoters were generated by overlapping PCR mutagenesis, using plasmids pT1-B6 and pGG1, respectively, as templates (13, 22). We used 38-bp primers mutated in each box (1 to 5) for amplification. The PCR products were cloned into pGEM-T or pMBL-T. In all cases, the introduction of site-specific changes was confirmed by DNA sequencing.

β-Galactosidase assays. Cultures were inoculated with bacterial cells from fresh LB agar plates supplemented with the appropriate antibiotics and grown overnight at 30°C on LB medium with appropriate antibiotics. Cultures were diluted to an initial optical density at 660 nm of 0.05 in the same medium supplemented or not with 1-naphthol (1 mM) dissolved in dimethyl sulfoxide (note that the latter did not interfere with the induction assays in this study). β-Galactosidase activity was determined in triplicate for permeabilized cells when cultures reached a turbidity at 660 nm of 0.5 (11). The results are reported as the means for nine different experiments.

Overexpression and purification of His-tagged TtgV and mutants. The pANA126 plasmid is a pET28b(+) derivative that was transformed into *E. coli*

BL21(DE3) and used to overproduce a His_6-TtgV-tagged protein. *ttgV* mutant alleles were cloned into the same plasmid, which was then used to overexpress *ttgV* mutant variants.

Electrophoretic mobility shift assays (EMSAs). The DNA probes were 295-bp fragments containing the *ttgT-ttgDEF* and *ttgV-ttgGHI* intergenic regions obtained from plasmid DNA (pT1-B6 or derivatives and pGG1 or derivatives, respectivley) by PCR with primers D5′E (5′-NNNNNNGAATTCCCTTCTGA TCCAGGCCACCG-3′) and D3′P (5′-NNNNNNCTGCAGTAACTGTCTCGC ACGCAAAG-3′) and with primers G5′E (5′-NNNNNNGAATTCGTTCATAT CTTTCCTCTGCG-3′) and G3′P (5′-NNNNNCTGCAGGGGGATTACCCG TAATGCAC-3′), respectively.

Cycling parameters were 2 min at 95°C followed by 30 cycles at 95°C for 1 min, 50°C for 30 s, and 72°C for 30 s, ending with 10 min at 72°C. PCR products were isolated from agarose gel by use of a Qiaquick gel extraction kit (Qiagen) and radiolabeled at the 5′ end with [γ-^{32}P]ATP and T4 polynucleotide kinase. A 1 nM concentration (~10^4 cpm) of the labeled probe was then incubated with the indicated concentrations of purified proteins in 10 μl STAD (25 mM Tris-acetate, pH 8.0, 10 mM KCl, 8 mM magnesium acetate, 3.5% [wt/vol] polyethylene glycol 8000, and 1 mM dithiothreiol) supplemented with 15 μg/ml poly(dI-dC) and 200 μg/ml bovine serum albumin. Reaction mixtures were then incubated for 10 min at 30°C, and samples were run in 4.5% (wt/vol) native polyacrylamide gels (Bio-Rad Mini-Protean II) for 2 h at 50 V at room temperature in Tris-glycine buffer (25 mM Tris-HCl, pH 8.0, 200 mM glycine). The results were analyzed with Personal FX equipment and Ouantity One software (Bio-Rad).

RESULTS

Mutational analysis of the extended DNA recognition helix of TtgV: differential effect on operator binding. Molina-Henares et al. (12) reported that the helix-turn-helix (HTH) DNA binding domain of the IclR family was relatively extended with respect to other regulators. Based on the sequence alignment of 53 IclR family members (10) and α-helix secondary structure predictions, TtgV residues 34 to 43 might form the first helix of the HTH DNA binding motif, whereas residues 47 to 64 might represent the binding helix of this domain (Fig. 2). To determine whether these residues are involved in the binding of TtgV to its operators and to explore whether TtgV interacts with the *ttgD* and *ttgG* promoters differentially depending on the precise base composition of the target sites, we mutated all residues between positions 47 and 64 to alanine. All alleles encoding mutant proteins were cloned into pET28b(+), and the proteins were purified as N-terminally His-tagged variants. Homogeneously purified mutant variants
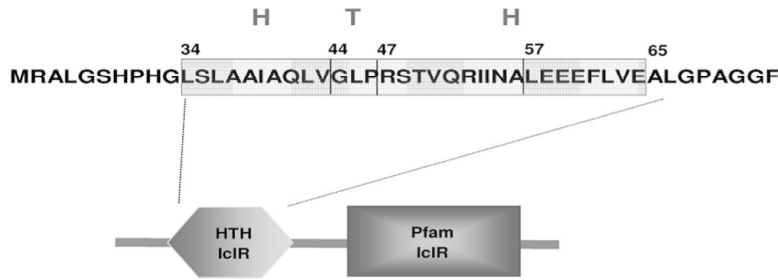
FIG. 2. Amino acid sequence at the N-terminal end of TtgV, where an extended HTH DNA binding domain is located. The proposed TtgV DNA binding protein includes a position helix (residues 34 to 43) followed by a turn and an extended recognition helix that covers residues 47 to 64. Below is the physical organization of the members of the IclR family, consisting of two domains, one involved in DNA recognition and another that includes a central segment of the proteins and extends toward the C-terminal end. The second domain seems to be involved in effector recognition and multimerization (5, 10). PFAM refers to the HMM algorithm identifying IclR members in that region.
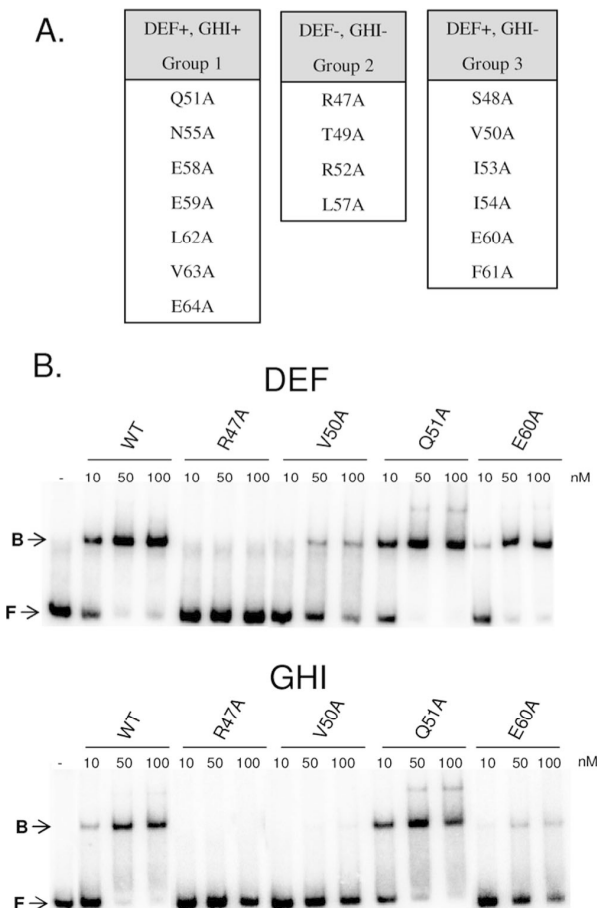

FIG. 3. TtgV mutant variants grouped according to their binding to the *ttgD* and *ttgG* operators. (A) Three groups of mutants were defined according to their ability to bind and retard (+) the *ttgD* and/or *ttgG* operator. (B) EMSA of 295-bp DNA fragments incubated in the absence (−) or presence of 10, 50, or 100 nM TtgV (WT) or the indicated mutant variant. F, free DNA; B, retarded DNA.

were used for EMSAs with similarly sized *ttgD* and *ttgG* operator regions and with the wild-type protein as a control (see Fig. 3 and 4 for examples with some of the mutants). Densitometric analysis of the amount of DNA shifted by TtgV revealed that TtgV shifted the *ttgD* operator better than the *ttgG* fragment (Fig. 3B). We also tested all mutant proteins in EMSAs with *ttgD* and *ttgG* and distinguished three types of mutant proteins. (i) Some TtgV mutants had changes that had no effect on binding to either promoter (Q51A, N55A, E58A, E59A, L62A, V63A, and E64A) (Fig. 3A and Q51A EMSA in Fig. 3B). Further support for this lack of effect was obtained when we determined that the *ttgD/ttgG* ratio of retarded DNA at a fixed concentration of TtgV (i.e., 50 nM) was close to 1 (Fig. 4). Also identified were (ii) TtgV mutants that did not bind to the *ttgG* or *ttgD* operator (R47A, T49A, R52A, and L57A) (Fig. 3A and B, R47A mutant) and (iii) TtgV variants with mutations with a more severe effect on binding to the *ttgG* operator than to the *ttgD* operator (S48A, V50A, I53A, I54A, E60A, and F61A) (Fig. 3A and E60A and V50A EMSAs in Fig. 3B). This was further supported by the fact that at a fixed concentration of TtgV mutant variants, the ratio of the amount of *ttgD*- to *ttgG*-shifted DNA was >4 (Fig. 4). We found that S48A, V50A, I53A, and I54A mutants were more severely affected in binding to *ttgG*, with ratios of 5.8- to 8.5-fold with respect to the wild-type TtgV (Fig. 4).

To quantify these effects, we carried out EMSA with a wide range of wild-type and mutant regulator concentrations and a 295-bp *ttgG* or *ttgD* promoter fragment, which allowed us to determine the apparent dissociation constant (K_D). We found that TtgV had an affinity of around 10 ± 1 nM for *ttgD* (Table 2), whereas the affinity for *ttgG* was around 19 ± 1 nM (Table 2). We also found that mutants in group 1, e.g., the Q51A mutant, bound *ttgD* and *ttgG* DNAs with K_D values similar to those of the parental protein and that TtgV mutants in the third group (e.g., V50A, I53A, I54A, E60A, and F61A mutants) exhibited reduced affinities for their target operators, with the reductions being in the range of 2.5- to 4.9-fold in the case of the *ttgD* promoter and over 35-fold in the case of *ttgG*.

To analyze the physiological relevance of the above mutations in TtgV, we decided to test their effects on expression levels from the *ttgD* and *ttgG* promoters in vivo. To this end, we constructed fusions of the promoters to a promoterless *'lacZ* gene ($P_{ttgG}::'lacZ$ and $P_{ttgD}::'lacZ$). The *ttgV* gene (or an allele
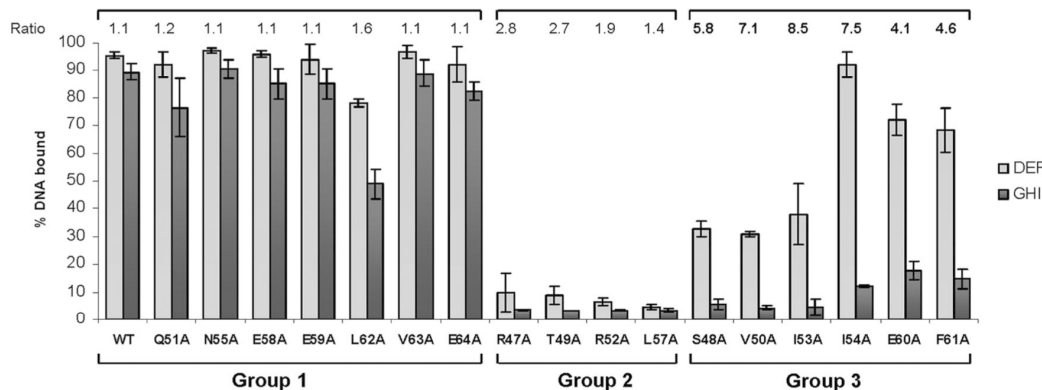
FIG. 4. Effects of mutations in the HTH DNA binding domain of TtgV on binding to the *ttgG* and *ttgD* operators. EMSAs were carried out as described in Materials and Methods and in the legend for Fig. 3, using a fixed amount of TtgV (50 nM) or its mutants. Densitometric analysis was carried out to determined the amount of protein DNA bound to each operator. The *ttgD*/*ttgG* ratio shown at the top distinguishes mutant variants that bind and retard both operators or one preferentially over the other.

encoding a mutant variant [we chose the Q51A and ES8A mutants from group 1, the R47A mutant from group 2, and the V50A and E60A mutants from group 3]) was cloned into the low-copy-number compatible pBBRN plasmid (see Materials and Methods). Expression from P_{ttgG} and P_{ttgD} was tested in a *ttgV*/*ttgT*-deficient background, and β-galactosidase activity in the absence and presence of 1-naphthol was determined (Table 3). In this background, we found that expression from the promoter was similar regardless of the presence of 1-naphthol and that the expression from *ttgG* was higher (1,900 ± 160 Miller units) than that from P_{ttgD} (around 600 Miller units). When, in addition, the cells expressed *ttgV*, we found that basal expression of *ttgD* (30 ± 5 Miller units) was lower than that of *ttgG* (750 ± 40 Miller units). As expected, in the presence of 1-naphthol, expression from the two promoters increased dramatically (550 ± 120 Miller units for *ttgD* and around 2,000 Miller units for *ttgG*) (Table 3). The V50A and E60A mutants in group 3 were not able to repress the *ttgG* promoter; consequently, high levels of β-galactosidase were seen regardless of the presence of 1-naphthol (Table 3). However, the behavior of the group 3 mutants with the *ttgD* promoter was similar to that observed for the wild-type TtgV protein, namely, basal

expression seen in the absence of effector molecules increased in the presence of 1-naphthol. This indicates that the mutation at the DNA binding domain did not interfere with effector recognition. The R47A mutant, which belongs to group 2, was not able to repress the *ttgD* or *ttgG* promoter, and no significant induction in the presence of 1-naphthol was therefore detected. In contrast, the Q51A and E58A group 1 mutants

TABLE 3. In vivo effects of TtgV and its mutant variants on the expression of *ttgD* (pMPD) and *ttgG* (pMPG) promoters fused to '*lacZ*[a]

Strain	Presence of 1-naphthol	β-Galactosidase expression (Miller units)	Mutant group
TIEVT(pMPD)	−	600 ± 60	Not relevant
	+	600 ± 100	Not relevant
TIEVT(pMPG)	−	1,900 ± 160	Not relevant
	+	2,100 ± 160	Not relevant
TIEVT(pBBRN::*ttgV*, pMPD)	−	30 ± 5	Not relevant
	+	550 ± 120	Not relevant
TIEVT(pBBRN::*ttgV*, pMPG)	−	750 ± 40	Not relevant
	+	1,850 ± 110	Not relevant
TIEVT(pBBRN-Q51A, pMPD)	−	10 ± 5	1
	+	150 ± 50	1
TIEVT(pBBRN-Q51A, pMPG)	−	100 ± 20	1
	+	2,400 ± 210	1
T1EVT(pBBRN-E58A, pMPD)	−	10 ± 10	1
	+	130 ± 5	1
T1EVT(pBBRN-E58A, pMPG)	−	30 ± 20	1
	+	1,560 ± 80	1
TIEVT(pBBRN-R47A, pMPD)	−	600 ± 80	2
	+	900 ± 30	2
TIEVT(pBBRN-R47A, pMPG)	−	2,500 ± 200	2
	+	2,800 ± 390	2
TIEVT(pBBRN-V50A, pMPD)	−	50 ± 5	3
	+	750 ± 60	3
TIEVT(pBBRN-V50A, pMPG)	−	2,250 ± 150	3
	+	2,600 ± 470	3
TIEVT(pBBRN-E60A, pMPD)	−	100 ± 10	3
	+	800 ± 100	3
TIEVT(pBBRN-E60A, pMPG)	−	2,200 ± 300	3
	+	2,800 ± 580	3

[a] *Pseudomonas putida* strains deficient in *ttgV* and *ttgT* were transformed with plasmid pMPD1 or pANA96 and pBBRN::*ttgV* or its mutant derivatives. Cells were grown on LB medium as described in Materials and Methods with rifampin, tetracycline, and kanamycin in the absence (−) and in the presence (+) of 1 mM 1-naphthol. β-Galactosidase activity was assayed in permeabilized cells as described in Materials and Methods.

TABLE 2. Determination of apparent dissociation constants of wild-type and TtgV mutants for the operators at the *ttgG* and *ttgD* promoters[a]

TtgV protein variant	K_D (nM) for *ttgD* operator	K_D (nM) for *ttgG* operator
Wild type	10 ± 1	19 ± 1
R47A	>750	>750
V50A	49 ± 11	>750
Q51A	8 ± 1	19 ± 1
I53A	42 ± 3	ND
I54A	27 ± 2	>750
E60A	26 ± 1	>750
F61A	25 ± 2	>750

[a] Data were obtained from densitometric analyses of EMSAs in the presence of concentrations of 1, 5, 10, 20, 30, 40, 50, 100, 500, and 750 nM. Results shown are the means for at least four independent assays done in duplicate. The DNA probe was 1 nM of a 295-bp fragment comprising the entire *ttgG* or *ttgD* promoter region. ND, not determined.
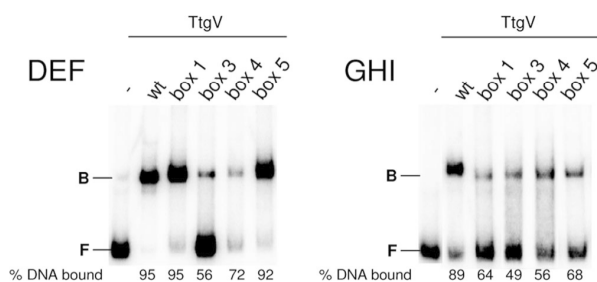
FIG. 5. Effects of nucleotide changes in the operator sequences of *ttgD* (left) and *ttgG* (right) on the binding of TtgV. EMSAs were carried out with 1 nM of the indicated wild-type or mutant operator variant (295-bp fragments) and 50 nM TtgV. Other conditions were the same as those described in the legends for Fig. 3 and 4. F and B, free and bound DNAs, respectively.

seemed to be able to bind to both promoters tightly, since basal levels of expression of *ttgD* and *ttgG* were lower than those achieved in the presence of TtgV. However, in the presence of 1-naphthol, the Q51A mutant was able to induce the expression of *ttgG* to maximum levels, but expression from *ttgD* was fourfold lower than that with the wild-type protein, which suggests that the Q51A mutant may not be as efficient as TtgV in derepressing the *ttgD* promoter.

Identification of sequences in *ttgD* important for TtgV recognition. Guazzaroni et al. (4) suggested two overlapping inverted repeats in the *ttgG* promoter (Fig. 1) as the TtgV target. Their results showed that mutations within the so-called IR1 inverted repeat (boxes 1 and 4) and IR2 inverted repeat (boxes 3 and 5) had a significant effect on recognition by TtgV. These results were corroborated in this study, as we observed that the amount of target DNA retarded by a fixed amount of TtgV decreased with the mutant operators compared to the amount of wild-type DNA (Fig. 5).

Based on the alignment of the *ttgG* and *ttgD* promoters (Fig. 1), we introduced similar double mutations in the *ttgD* operator to correspond to the inverted repeats in *ttgG*, although these sequences did not always correspond to potential inverted repeats in *ttgD*. We maintained the box 1, box 3, box 4, and box 5 nomenclature for the mutant promoters. We used EMSA to test the role of these boxes in recognition by TtgV and found that mutations in boxes 3 and 4 had a significant effect on TtgV binding to *ttgD*, since only 56% and 72%, respectively, of the DNA was retarded (Fig. 5), compared to nearly 95% of the DNA bound by the wild-type *ttgD* sequence (Fig. 5). Therefore, a clear difference between the *ttgD* and *ttgG* promoters is that boxes 1 and 5 are irrelevant for TtgV binding at *ttgD* but are important at *ttgG*, suggesting that the base composition of the binding sites is relevant.

Amino acids important for *ttgG* and *ttgD* operator recognition in the HTH DNA binding motif of TtgV. We analyzed the effects of mutations in the *ttgG* and *ttgD* operators on the binding of the whole collection of TtgV mutants. TtgV mutants in group 2 failed to bind any of the mutant promoters tested (not shown), and this was expected since the mutant proteins did not bind wild-type DNA (Fig. 3B).

TtgV mutants in group 3 (V50A, I53A, I54A, E60A, and E61A mutants) did not bind the *ttgG* wild-type operator or its

mutant variants (Fig. 6B); however, these mutants recognized *ttgD* operator variants (Fig. 6A). This indicates that TtgV can establish differential contacts with its target DNA between the two operators. Although all group 3 mutants interacted with all *ttgD* operator variants, it should be noted that in general, the amount of shifted DNA was lower than that retarded by the wild-type protein. This was particularly clear for the V50A and I53A mutants, since only approximately 30% of the total DNA was retarded (Fig. 6A).

When DNA shifts of the *ttgG* or *ttgD* operator mutant variants were assayed with TtgV mutants in group 1, e.g., the Q51A, E58A, and E59A mutants, the patterns of interactions were similar to those found with the wild-type TtgV protein (Fig. 6A and B). We also found that the group 1 L62A, V63A, and E64A mutants also bound to the *ttgG* and *ttgD* promoters and their variants. However, although none of these TtgV mutants affected binding to the *ttgD* box 1 and box 5 variants (the amount of shifted DNA was >90%), binding of these mutant proteins to *ttgG* box 1 and box 5 variants was weaker (Fig. 6A and B).

This set of results suggests that differential recognition of the promoters is influenced by specific and distinct contacts of the TtgV HTH with the two operators. This set of interactions requires resolution of the three-dimensional (3D) structure of TtgV in complex with both operators, and the nature of this structure is currently under investigation at our laboratories.

DISCUSSION

Multidrug resistance often involves the concerted action of efflux pumps, membrane permeability barriers, drug inactivation, and detoxification via metabolic conversion to less toxic molecules. The high level of tolerance to toluene in *Pseudomonas putida* DOT-T1E is mediated mainly by three efflux pumps, two of which—TtgGHI and TtgDEF—are under cross-regulation by the IclR family multidrug recognition regulators TtgV and TtgT (10, 12). Of these two repressors, TtgV has been shown to play a dominant role in the transcriptional control of these two pumps in vivo (27).

An earlier observation made by our research group was that the patterns of expression of the *ttgDEF* and *ttgGHI* operons are different, in the sense that expression of the *ttgDEF* operon is silent in the absence of aromatic hydrocarbons, whereas the *ttgGHI* operon is expressed at a relatively high basal level (13, 22). When an effector molecule is added to the culture medium, both operons are expressed at higher levels, although the maximal level of expression of the *ttgGHI* operon is superior to that of *ttgDEF* (27) (Table 3). Why does this marked difference in the expression patterns of the two operons exist if they are under the transcriptional control of the same repressors? The answer to this question is twofold. (i) The physical organizations of the genes encoding the repressors and the efflux pumps are different, and thus the access of RNA polymerase to the promoters may differ. The *ttgT* gene is adjacent to and transcribed divergently from *ttgDEF*, and the corresponding promoters are separated by 80 nucleotides (the TtgV binding site is located between positions -41 and -16 with respect to *ttgD*), whereas not only do the divergent P_{ttgV} and P_{ttgG} promoters fully overlap with each other, but the TtgV operator lies at the $-10/-35$ regions of these promoters. (ii) The DNA
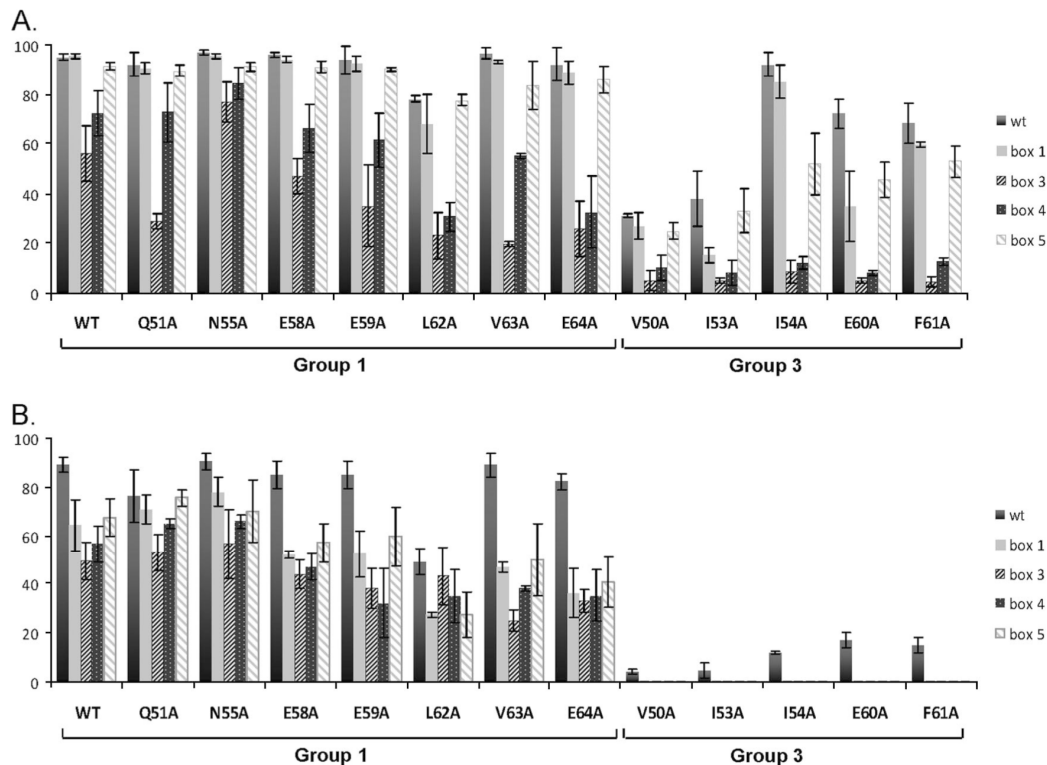
FIG. 6. Effects of nucleotide changes in the operators of *ttgD* (A) and *ttgG* (B) on the binding of TtgV and its mutants. EMSAs were carried out with 1 nM of the indicated wild-type or mutant operator variant (295-bp fragments) and 50 nM TtgV. Densitometric analysis were done to determine the amount of shifted DNA with respect to the total DNA. Data are averages for at least three independent assays plus standard errors.

sequences of the *ttgG* and *ttgD* operators show only 40% identity (Fig. 1 and 7). TtgV recognizes the *ttgD* operator with a higher affinity (twofold) than that for *ttgG*, which correlates with the lower basal expression from the *ttgD* promoter. Therefore, in vivo the different expression patterns of the two efflux pump operons seem to result from the combination of the affinity of TtgV for its target operators and the physical organization of these operators.

Previous work using TtgV and mutant variants of the *ttgG* operator revealed that TtgV binds to a region spanning about 34 nucleotides. Guazzaroni et al. (4) suggested the existence of four subsites for this interaction, called boxes 1, 3, 4, and 5, which were proposed to be organized as a set of intercalated inverted repeats. Alignment of the *ttgG* and *ttgD* operators revealed high sequence conservation at the central boxes 3 and

```
ttgD          CAAAAACCACATAGTGATACACTATTCTGCAATGCGGGCCATG
ttgG          AGAGTATCACATAATGCTACACTCTACCGCATTACGATTCAGC
Seq.consensus --A--A-CACATA-TG-TACACT-T-C-GCA-T-CG---CA--
```

FIG. 7. Proposed inverted repeat targets for TtgV, based on mutational analyses of the interactions of P*ttgG* and P*ttgD* with wild-type TtgV and its mutant variants. The conserved sequences in footprints of the *ttgG* and *ttgD* promoters are shown. The inverted repeat within the sequences protected in previous footprint assays (3, 27) is based on sequence alignment and our current mutational assays. Nucleotides in the consensus sequence were identical in the alignment, and palindromic nucleotides are shown in bold in the consensus sequence.

4, with less conservation at box 5 and large differences at box 1. In the present study, we evaluated the importance of these boxes in the binding of TtgV to the *ttgD* operator through construction of the appropriate mutants. We found that boxes 3 and 4 were critical for the recognition of *ttgD* by TtgV; however, to our surprise, boxes 1 and 5 in this promoter were dispensable (Fig. 5). To gain more insight into these observations, we reanalyzed the alignment of the *ttgD* and *ttgG* operators at the region corresponding to the footprint (Fig. 7) and found a weak inverted repeat (26 nucleotides long) centered between boxes 3 and 4 that may serve as the potential TtgV target sequence (Fig. 7). Of note is the fact that the palindromic order around the axis is higher for *ttgD* than for *ttgG* and defines a 15-bp inverted repeat. If this set of nucleotides were those directly bound by TtgV, this may explain why the affinity of TtgV for the *ttgD* operator is higher and correlates with the lower expression of the *ttgDEF* operon in vivo. Long palindromic DNA targets for IclR family members have been described recently for *Streptomyces* CcaR, a regulator involved in the control of β-lactam antibiotics in this microorganism (25), and *Acinetobacter* PcaU, a regulator involved in the metabolism of aromatic carboxylic acids (7).

To test the hypothesis that TtgV can establish different contacts in each of the two promoters, we created mutants in the recognition helix of the HTH binding domain predicted to contact DNA and searched for differential effects on the re-
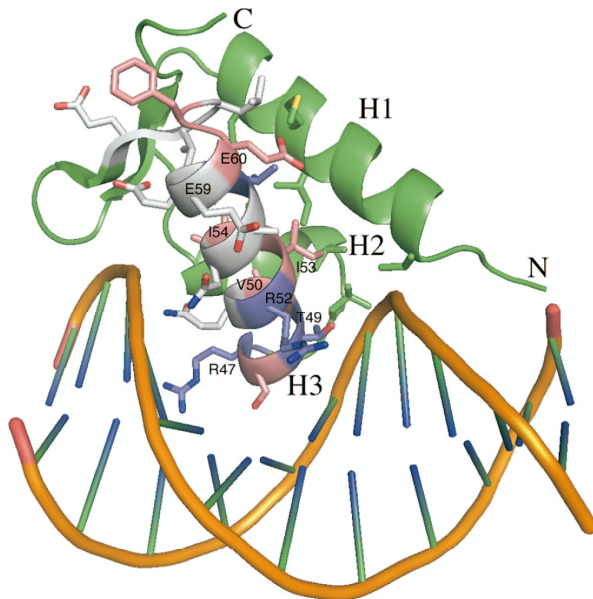
FIG. 8. Representation of the recognition helix of TtgV with B-DNA. The TtgV recognition helix is represented as a ribbon modeled on the 3D structure of the recognition helix of the IclR-TM protein (30).

pression of the *ttgG* and *ttgD* promoters and their variants. EMSA revealed that residues R47, T49, and R52 are critical for binding to *ttgD* and *ttgG* operators, whereas residues 48, 50, 53, 54, 60, and 61 in TtgV are critical for TtgV binding to the *ttgG* promoter but not to the *ttgD* promoter (compare Fig. 6A and B). To learn more about the potential role of the different amino acids, we modeled the DNA binding domain of TtgV, using the program Modeler, with *Thermotoga maritima* IclR as the template (PDB code 1MKM) (30). The DNA binding domain was then modeled onto a B-DNA, using a lambda repressor-operator complex (PDB code 1LMB). Residues R47, T49, and R52, which when mutated to A significantly reduced DNA binding, were proposed to be involved directly in DNA interaction (Fig. 8). For PobR, the positive regulator of the *pobA* gene for *p*-hydroxybenzoate metabolism and a member of the IclR family of regulators, an R56S mutant (a position that aligns with R47 in TtgV) was also unable to bind to its target sequence (9), in support of our results. Residues N55, A56, E58, and E59 (white in Fig. 8), although within the recognition helix from our model, do not appear to be involved directly in DNA interaction. Our results support this conclusion, since mutating these residues had little effect on DNA binding affinity. Residues V50, I53, and I54 (Fig. 8) were located at the interface between helices 2 and 3. Replacement of these residues by A resulted in mutant proteins that only affected DNA binding to the *ttgGHI* promoter, not to the *ttgDEF* promoter. As such, these mutations seemed to alter the conformations of helices 2 and 3, leading to a differential effect on the binding of TtgV to the two operators. Rhee et al. (21) showed that the OmpR regulator of *Salmonella* spp. can adopt different orientations depending on the precise base composi-

tion of the different binding sites that this regulator recognizes. Therefore, evidence from the present study and research with other systems support the hypothesis that HTH and DNA operators should be viewed as dynamic elements, rather than static interacting elements, in order to optimize the modulation of transcription.

In summary, we provide the first detailed study of the extended DNA recognition helix of a member of the IclR family. One conclusion from our findings is the existence of a large degree of flexibility in the interactions of the TtgV regulator with its target sequences. This flexibility may be related to the extensive interface for multimerization of monomers, as deduced from the 3D structure of IclR in *Thermotoga maritima* (30). Detailed mutational analysis of the operators recognized by TtgV showed that the central region of the zone protected in previous footprint studies (5, 23, 27) is essential for binding, whereas the border sequences are dispensable to some degree. This leads us to propose that TtgV recognizes a single inverted repeat, as shown in Fig. 7. Crystallization of TtgV in the absence and presence of target sequences is being carried out and will help to shed light on this set of complex DNA-protein interactions.

REFERENCES

1. **Duque, E., A. Segura, G. Mosqueda, and J. L. Ramos.** 2001. Global and cognate regulators control the expression of the organic solvent efflux pumps TtgABC and TtgDEF of *Pseudomonas putida*. Mol. Microbiol. **39:**1100–1106.
2. **Gottesman, M. M., and I. Pastam.** 1993. Biochemistry of multidrug resistance mediated by the multidrug transporter. Annu. Rev. Biochem. **62:**385–427.
3. **Guazzaroni, M. E., T. Krell, A. Felipe, R. Ruíz, C. Meng, X. Zhang, et al.** 2005. The multidrug efflux regulator TtgV recognizes a wide range of structurally different effectors in solution and complexed with target DNA. Evidence from isothermal titration calorimetry. J. Biol. Chem. **280:**20887–20893.
4. **Guazzaroni, M. E., T. Krell, P. Gutierrez del Arroyo, M. Vélez, M. Jiménez, G. Rivas, and J. L. Ramos.** 2007. The transcriptional repressor TtgV recognizes a complex operator as a tetramer and induces convex DNA bending. J. Mol. Biol. **369:**927–939.
5. **Guazzaroni, M. E., W. Terán, X. Zhang, M. T. Gallegos, and J. L. Ramos.** 2004. TtgV bound to a complex operator site represses transcription of the single promoter for the multidrug and solvent extrusion TtgGHI pump. J. Bacteriol. **186:**2921–2927.
6. **Isken, S., and J. A. M. de Bont.** 1996. Active efflux of toluene in a solvent-resistant bacterium. J. Bacteriol. **178:**6056–6058.
7. **Jerg, B., and U. Gerischer.** 2008. Relevance of nucleotides of the PcaV binding site from *Acinetobacter baylyi*. Microbiology **154:**756–766.
8. **Kieboom, J., J. J. Dennis, J. A. M. de Bont, and G. J. Zylstra.** 1998. Identification and molecular characterization of an efflux pump involved in *Pseudomonas putida* S12 solvent tolerance. J. Biol. Chem. **273:**85–91.
9. **Kok, R. G., D. A. D'Argenio, and L. N. Ornston.** 1998. Mutation analysis of PobR and PcaU, closely related transcriptional activators in *Acinetobacter*. J. Bacteriol. **180:**5058–5069.
10. **Krell, T., A. J. Molina-Henares, and J. L. Ramos.** 2006. The IclR family of transcriptional activators and repressors can be defined by a single profile. Protein Sci. **15:**1207–1213.
11. **Miller, J. H.** 1972. Experiments in molecular biology. Cold Spring Harbor Laboratory Press, Cold Spring Harbor, NY.

12. **Molina-Henares, A. J., T. Krell, M. E. Guazzaroni, A. Segura, and J. L. Ramos.** 2006. Members of the IclR family of bacterial transcriptional regulators function as activators and/or repressors. FEMS Microbiol. Rev. **30:** 157–186.

13. **Mosqueda, G., and J. L. Ramos.** 2000. A set of genes encoding a second toluene efflux system in *Pseudomonas putida* DOT-T1E is linked to the *tod* genes for toluene metabolism. J. Bacteriol. **182:**937–943.

14. **Nikaido, H.** 1998. Multiple antibiotic resistance and efflux. Curr. Opin. Microbiol. **1:**516–523.

15. **Poole, K.** 2000. Efflux-mediated resistance to fluoroquinolones in grampositive bacteria. Antimicrob. Agents Chemother. **44:**2233–2241.

16. **Poole, K.** 2000. Efflux-mediated resistance to fluoroquinolones in grampositive bacteria and the mycobacteria. Antimicrob. Agents Chemother. **44:**2595–2599.

17. **Ramos, J. L., E. Duque, M. T. Gallegos, P. Godoy, M. I. Ramos-González, A. Rojas, W. Terán, and A. Segura.** 2002. Mechanisms of solvent tolerance in gram-negative bacteria. Annu. Rev. Microbiol. **56:**743–768.

18. **Ramos, J. L., E. Duque, P. Godoy, and A. Segura.** 1998. Efflux pumps involved in toluene tolerance in *P. putida* DOT-T1E. J. Bacteriol. **180:**3323–3329.

19. **Ramos, J. L., E. Duque, M. J. Huertas, and A. Haïdour.** 1995. Isolation and expansion of the catabolic potential of a *Pseudomonas putida* strain able to grow in the presence of high concentrations of aromatic hydrocarbons. J. Bacteriol. **177:**3911–3916.

20. **Ramos, J. L., M. Martínez-Bueno, A. J. Molina-Henares, W. Terán, K. Watanabe, X. Zhang, M. T. Gallegos, R. Brennan, and R. Tobes.** 2005. The TetR family of transcriptional repressors. Microbiol. Mol. Biol. Rev. **69:**326–356.

21. **Rhee, J. E., W. Sheng, L. K. Morgan, R. Nolet, X. Liao, and L. J. Kenney.** 2008. Amino acids important for DNA recognition by the response regulator OmpR. J. Biol. Chem. **283:**8664–8677.

22. **Rojas, A., E. Duque, G. Mosqueda, G. Golden, A. Hurtado, J. L. Ramos, and**

A. Segura. 2001. Three efflux pumps are required to provide efficient tolerance to toluene in *Pseudomonas putida* DOT-T1E. J. Bacteriol. **183:**3967–3973.

23. **Rojas, A., A. Segura, M. E. Guazzaroni, W. Terán, A. Hurtado, M. T. Gallegos, and J. L. Ramos.** 2003. In vivo and in vitro evidence that TtgV is the specific regulator of the TtgGHI multidrug and solvent efflux pump of *Pseudomonas putida*. J. Bacteriol. **185:**4755–4763.

24. **Saier, M. J., Jr., and I. Paulsen.** 2001. Phylogeny of multidrug transporters. Cell. Dev. Biol. **12:**205–213.

25. **Santamarta, I., M. T. López-García, R. Pérez-Redondo, B. Koekman, J. F. Martín, and P. Liras.** 2007. Connecting primary and secondary metabolism: AreB, an IclR-like protein, binds the ARE(ccaR) sequence of *S. clavuligerus* and modulates leucine biosynthesis and cephamycin C and clavulanic acid production. Mol. Microbiol. **66:**511–524.

26. **Spaink, H. P., J. J. H. Okker, C. A. Wijffelman, E. Pees, and B. J. J. Lugtenberg.** 1987. Promoters in the nodulation region of the *Rhizobium leguminosarum* Sym plasmid pRL1JI. Plant Mol. Biol. **9:**27–39.

27. **Terán, W., A. Felipe, S. Fillet, M. E. Guazzaroni, T. Krell, R. Ruiz, J. L. Ramos, and M. T. Gallegos.** 2007. Complexity in efflux pump control: crossregulation by the paralogues TtgV and TtgT. Mol. Microbiol. **66:**1416–1428.

28. **Woodcock, D. M., P. J. Crowther, J. Doherty, S. Jefferson, E. DeCruz, M. Noyer-Weidner, S. S. Smith, M. Z. Michael, and M. W. Graham.** 1989. Quantitative evaluation of *Escherichia coli* host strains for tolerance to cytosine methylation in plasmid and phage recombinants. Nucleic Acids Res. **17:**3469–3478.

29. **Yanisch-Perron, C., J. Vieira, and J. Messing.** 1985. Improve M13 phage cloning vectors and host strains: nucleotide sequences of the M13mp18 and pUC19 vector. Gene **33:**103–119.

30. **Zhang, R. G., Y. Kim, T. Skarina, S. Beasley, R. Laskowski, C. Arrowsmith, A. Edwards, A. Joachimiak, and A. Savchenko.** 2002. Crystal structure of Thermotoga maritima 0065, a member of the IclR transcriptional factor family. J. Biol. **277:**19183–19190.

La structure du Crystal du tétramère TtgV en complexe avec l'ADN révèle un nouveau mécanisme de coopérativité et d'induction.

La majorité des régulateurs de gène bactérien s'unissent comme un dimère symétrique à ses séquences cibles généralement formées d'une séquence d'ADN palindromique de 12-20 paires de bases. Afin de reconnaître de longues séquences opératrices ou deux sites d'union séparés, il est commun que les protéines adoptent une conformation multimérique. Certains régulateurs de gène bactérien utilisent la conformation tétramérique pour reconnaître de manière coopérative deux sites opérateurs. Un mécanisme qui précisément restait incompris. Nous présentons dans cet article la structure complète du Crystal de la protéine d'union à de multiples drogues TtgV, un répresseur qui contrôle l'expression de pompes d'efflux, seule en solution et en complexe avec son ADN cible de 42 paires de bases. TtgV s'unit à son ADN opérateur sous forme de tétramère avec un nouvel arrangement de ses domaines sur l'ADN. Cet arrangement partage des similarités avec le modèle proposé du répresseur du bactériophage Lambda, ce qui suppose la présence d'un mode d'union commun pour les autres régulateurs de gène de conformation tétramèrique. Les structures révèlent un mécanisme d'activation unique qui implique un drastique réarrangement conformationel au niveau monomérique, dimérique et tétramérique.

La estructura del crystal del tetramero TtgV en complejo con ADN revela un nouveau mecanismo de cooperatividad y de inducción.

La mayoría de los reguladores de genes bacterianos se unen como dimeros a sus secuencias dianas que suelen ser ADN palidromicos de 12 a 20 pares de bases. Con el fin de reconocer secuencias operadoras largas o dos sitios de unión separados, es común de encontrar reguladores que presentan una conformación multimérica. Algunos regulatores de genes bacterianos solo adoptan la conformación tetramérica para reconocer de manera cooperativa dos operadores. De hecho, la forma en que eso sucede permanece sin desvelar. Presentamos en este articulo, la estructura completa del cristal de TtgV, el represor que controla la expresión de bombas de eflujo TtgGHI y TtgDEF, tanto en solución y en complejo con su ADN diana de 42 pares de bases. TtgV se une a su ADN operador de manera tetamerica con un nuevo rearreglo de sus dominios sobre el ADN. Este rearreglo comparte similaridades con el modelo propuesto del represor del bacteriofago Lambda, lo que supone la presencia de un modo de unión común con otros reguladores tetraméricos. Las estructuras revelan un mecanismo de activación único que implica un rearreglo conformacional drástico al nivel monomérico, dimérico y tetramérico.

Crystal structure of TtgV in complex with its DNA operator reveals a general model for cooperative DNA binding of tetrameric gene regulators

Duo Lu[1], Sandy Fillet[2], Cuixiang Meng[1], Yilmaz Alguel[1], Patrik Kloppsteck[1], Julien Bergeron[3], Tino Krell[2], Mari-Trini Gallegos[4], Juan Ramos[2] and Xiaodong Zhang[1*]

[1]Division of Molecular Biosciences, Centre for Structural Biology, Imperial College London, SW7 2AZ, UK
[2] Department of Environmental Protection - CSIC, Granada, Spain
[3]Current address: Department of Biochemistry and Molecular Biology, Faculty of Medicine, University of British Columbia, Canada
[4]Department of Soil Microbiology and Symbiotic Systems – CSIC, Granada, Spain

The majority of bacterial gene regulators bind as symmetric dimers to palindromic DNA operators of 12-20 base pairs. Multimeric forms of proteins, including tetramers, are able to recognize longer operator sequences in a cooperative manner, although how this is achieved is not well understood due to the lack of complete structural information. Here we present the crystal structures of the multidrug binding protein TtgV, a repressor that controls efflux pumps, alone and in complex with a 42 bp intact DNA operator. TtgV binds to its DNA operator as a tetramer and induces considerable distortions in the DNA. Upon binding to its operator, TtgV undergoes large conformational changes at the monomeric, dimeric and tetrameric levels. The structures here provide a reinterpretation of previous models for tetrameric gene regulators, that were derived from domain structures and/or incomplete DNA operator sequences, and provide mechanistic insights into how tetrameric gene regulators bind to DNA cooperatively.

Bacterial gene regulators are model systems to study protein-DNA and protein-ligand interactions as well as principles of gene regulation. The majority of bacterial gene regulators bind as symmetric dimers to palindromic DNA operators in the range of

12-20 base pairs, often acting by altering the access of RNA polymerase, in either a positive or negative fashion (Browning and Busby, 2004).These specialized gene regulators, such as the Trp repressor and the CAP activator, bind to highly conserved DNA operator sequences with high affinity through specific interactions between the protein and DNA. However, some global regulators bind to a wider range of less conserved DNA sequences and more complex regulatory systems have evolved to ensure binding specificity. One strategy is to recognize a longer region of DNA using multiple less conserved recognition sites and with reduced specificity within each individual site. The larger interaction surface between the protein and DNA compensates for the relatively weak interactions at a single interaction site. A large number of bacterial gene regulators adopt this strategy and use tetramers to recognize two DNA sites. Some of the best-studied examples include the Lac repressor (LacI or LacR), the lambda repressor (λI), members of the LysR family and a few members of the TetR and IclR regulator families (Lewis *et al*., 1996; Molina-Henares *et al*., 2006; Monferrer *et al*.; Schumacher *et al*., 2001; Stayrook *et al*., 2008). Although this mode of recognition is widespread, there is no structural information on a tetrameric protein bound to a continuous DNA operator containing two or more binding sites, which has hindered our understanding of cooperative binding by tetrameric gene regulators and the mechanism of their activation. However,

*Corresponding author: Xiaodong Zhang
Tel: +44 207 594 3151
Fax: +44 207 594 3057
Email: xiaodong.zhang@imperial.ac.uk

tetrameric models of protein/DNA complexes have been proposed based on partial domain structures and incomplete DNA sequences. One such example is the tetrameric LacI/DNA complex determined at 4.8 Å resolution, that consists of two dimers of LacI, each bound to a separate 21 bp DNA duplex (Lewis *et al*., 1996). A model for the tetrameric λI/DNA complex was extrapolated from a DNA complex structure of a λI dimer and the tetramer structure of its C-terminal domain (CTD) alone (Stayrook *et al*., 2008). The dimer DNA complex was obtained from a mutant form of λI deficient in tetramer formation in complex with a 17 bp DNA duplex. These structures provided insights into how a tetrameric gene regulator can bind to two sites. However, in both cases, a single DNA site was used instead of two continuous DNA sites and consequently the incomplete structural information required some filling in of the gaps to create plausible models (Lewis *et al*., 1996; Stayrook *et al*., 2008).

Cooperativity is observed widely in biological systems that involve protein oligomers. The general model for cooperativity in ligand binding proposes that two distinct functional states (Tense (T-state) or Relaxed (R-state)) exist in equilibrium. These two states differ in their energies and affinities for the ligand. The T-state is more stable but incompetent in ligand binding. The R-state, on the other hand, is less stable but has higher affinity for the ligand. In the absence of the ligand, the protein predominately exists in the more stable T-state. However, upon ligand binding, the favorable binding energy between the protein and the ligand can offset the higher energy cost of the R-state, switching the protein to the R-state. When the energy difference between the R and the T-state is sufficiently large, multiple cooperative binding events are required to overcome the energy barrier. Under this circumstance, ligand binding to one subunit within the protein oligomer causes conformational changes that promote further binding. The larger the energy difference is

between the T and the R-states, the higher the cooperativity is.

Pseudomonas putida DOT-T1E can grow in the presence of high concentrations of a wide variety of organic solvents and thrives in mixtures of organic solvent:water as high as 99:1 (Ramos *et al*., 1998; Ramos *et al*., 1995). The most important adaptation to permit this unusual property is the extrusion of the toxic compounds to the outer medium, an energy-dependent process that is mediated by a set of efflux pumps (reviewed by Ramos *et al*., 2002). The pumps involved in solvent extrusion are TtgGHI and TtgDEF that exhibit a wide range of substrate specificities and belong to the RND family of efflux transporters. The expression of *ttgGHI* and *ttgDEF* is regulated by the TtgV repressor (Teran *et al*., 2007), which belongs to the IclR family of regulators (Krell *et al*., 2006; Molina-Henares *et al*., 2006) and recognizes a large number of effector compounds that contain one or two aromatic rings (Guazzaroni *et al*., 2005). Effector binding releases TtgV from its operator DNA and results in an increased expression of *ttgDEG* and *ttgGHI*. The most efficient effectors *in vivo* are two-ringed aromatic compounds, such as 1-naphthol and indole, or one-ringed compounds such as 4-nitrotoluene and benzonitrile (Guazzaroni *et al*., 2005).

Analytical ultracentrifugation and DNA footprinting assays revealed that TtgV is a tetramer that protects a 42 bp long DNA sequence covering the -10 to -35 region of the *ttgG* promoter (Fillet *et al*., 2009; Guazzaroni *et al*., 2004; Rojas *et al*., 2003). In order to understand the mechanism by which TtgV binds to its long DNA operator and the mechanism of induction by effectors, we determined the crystal structures of full length TtgV alone and in a complex with its cognate 42 bp DNA operator. The structures reveal that TtgV binds to its DNA operator as a dimer of dimers with asymmetric dimer and tetramer interfaces. The binding of TtgV induces a significant distortion of the DNA that includes an overall 60° bend in the DNA. To date, models of tetrameric regulators

assembled on complete operator sequences have been constructed from partial structures using shorter DNA sequences containing a single recognition site and/or truncated protein domains. Our full length TtgV in complex with an intact DNA operator shows that binding to two continuous DNA sites imposes significant constraints on the tetramer, resulting in very different quaternary structures in the presence and absence of DNA. These structures allow us to propose a general model for cooperative binding of tetrameric gene regulators.

Results

Crystal Structure of the apo TtgV tetramer

TtgV is a tetramer in solution (Guazzaroni *et al*., 2007b) and was crystallized in space group C2 with one dimer in an asymmetric unit. The dimer has a two-fold symmetry and two dimers are related by a crystallographic two-fold axis to form a compact symmetric tetramer (Figure 1). The TtgV monomer consists of a N-terminal domain which belongs to a subgroup of the Helix-Turn-Helix family that contains a Winged Helix (WH) motif responsible for DNA binding (Gajiwala and Burley, 2000) (hence termed DNA-Binding Domain). The protein also has a linker helix, and a C-Terminal Domain (CTD) that harbours the effector binding site (Guazzaroni *et al*., 2007a; Guazzaroni *et al*., 2005) Figure 1A). The WH motif contains three a-helices (α1-α3) followed by two β-strands (β1- β2). The linker helix (α4) is continuous with the first helix in the CTD (α 5) (Figure 1A), forming a long curved helix. The CTD consists of a twisted, six-stranded, anti-parallel β-sheet sandwiched by two helices on one side and a three-helix bundle on the other. Based on structural and mutagenesis data, a hydrophobic pocket on the surface of the β-sheet is proposed to be the effector binding site (Figure 1B, white ball and stick, (Guazzaroni *et al*., 2005; Walker *et al*., 2006). Importantly, there are very few interactions between the CTD and the DBD within the same monomer (Figure 1).
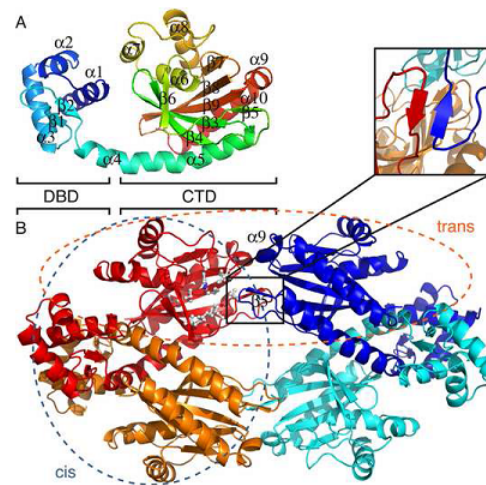
FIG. 1. The crystal structure of TtgV. A) ribbon representation of TtgV monomer colored from N (blue) to C (red) termini. B) TtgV tetramer arrangement and interactions. Each monomer is colored differently. Proposed hydrophobic residues that form the effector binding pocket are displayed as balls-and-sticks. The insert shows the b5 interactions between *trans*-dimers. Blue ellipse indicates the *cis*-dimer while orange ellipse indicates *trans*-dimer.

The CTDs between different monomers interact with one another and form a symmetric diamond shape (Figure 1B). The CTD tetramer is in the same plane of the DBDs and the tetramer is relatively flat (Figure 1B). Within the tetramer, two distinct dimer interfaces exist (Figure 1B). One dimer is stabilised mainly through interactions between the DBDs, which we term this the *cis*-dimer (Figure 1B, blue ellipse). The other dimer is formed between the α5 and α9 and we term this the *trans*-dimer (Figure 1B, orange ellipse). The *cis*-dimer has an extensive 2197 Å^2 buried surface per monomer while the *trans*-dimer has an interface of ~550 Å^2 per monomer. The *cis*-dimer is more compact with significant interactions between the DBDs while the DBDs of a *trans*-dimer are located 100 Å apart. In this configuration, TtgV must undergo conformational changes in order to bind to the two sites within the operator.

Structure of the TtgV/DNA complex

In order to understand how a TtgV binds to its operator sequence cooperatively, we determined the crystal structure of the full length TtgV tetramer bound to its cognate 42 bp *ttgG* operator. The complex was

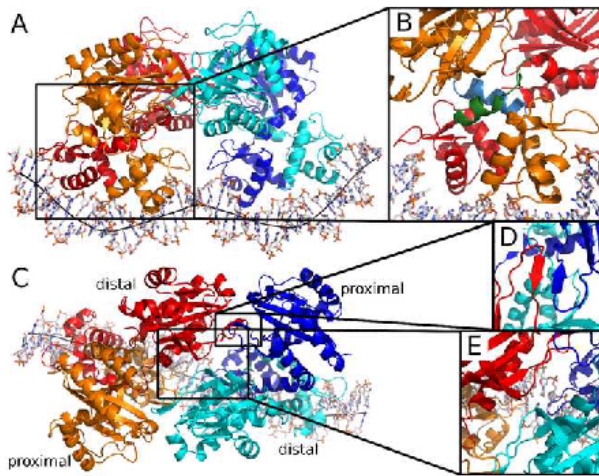**FIG. 2. The TtgV-DNA structure.** A) Viewed from the side. Each TtgV monomer is colored differently. The black line indicates the DNA axis. B) Zoom in view at one *cis*-dimer showing the different linker helix conformations. The linkers are shown in green (distal) and cyan (proximal). C) Viewed from the top highlighting the skewed diamond shape formed by the CTDs. Proximal and distal protomers are indicated. D) Zoom in view of the *trans*-dimer interface. E) Zoom in view of the interaction between the diagonal distal protomers.

crystallised in space group P6$_5$ with a complete tetramer/DNA complex in the asymmetric unit. TtgV binds to the DNA as a dimer of dimers, each bound to non-overlapping sites on the same face of the DNA duplex (Figure 2A). Two pairs of DBDs bind to a highly deformed DNA operator while the CTDs contact one another above forming an asymmetric diamond shape (Figure 2A). The tetramer contains two distinct layers of structures, one formed by the CTDs and the other by the DBDs (Figure 2A).

Within each *cis*-dimer (Figure 2, red and orange pair, blue and cyan pair), the CTDs are asymmetric in relationship to their DBDs. The asymmetry in *cis*-dimers is due to the differences in the linker helix between the DBD and the CTD (Figure 2B), with one of the linker helices adopting a bent conformation (Figure 2B, blue) and the other partially unwound (Figure 2B, green). The two *cis*-dimers interact through their CTDs to form a skewed diamond shape in the tetramer (Figure 2C). The *trans*-dimer interface is the same in the structure of both the apo and the TtgV/DNA complex involving the anti-parallel β sheet (β5) and helix α9 (Figure 1B, Figure 2C, 2D). However, there are additional hydrogen bonding interactions between the diagonal

CTDs (Figure 2E, red and cyan) near the CTD tetramer centre, through residues 134-136, adjacent to β5.

Comparisons between TtgV apo and TtgV/DNA structures

Comparison of the tetrameric structures of TtgV and TtgV/DNA reveals large conformational rearrangements at the monomeric, dimeric and tetrameric levels. At the monomeric level, the DBD and CTD have the same structure but the protomers differ in the linker between the domains. The linker between the DBD and CTD (α4) forms a continuous helix with α5 in the TtgV apo structure. However, in the TtgV/DNA complex, the protomers adopt two different conformations. In the
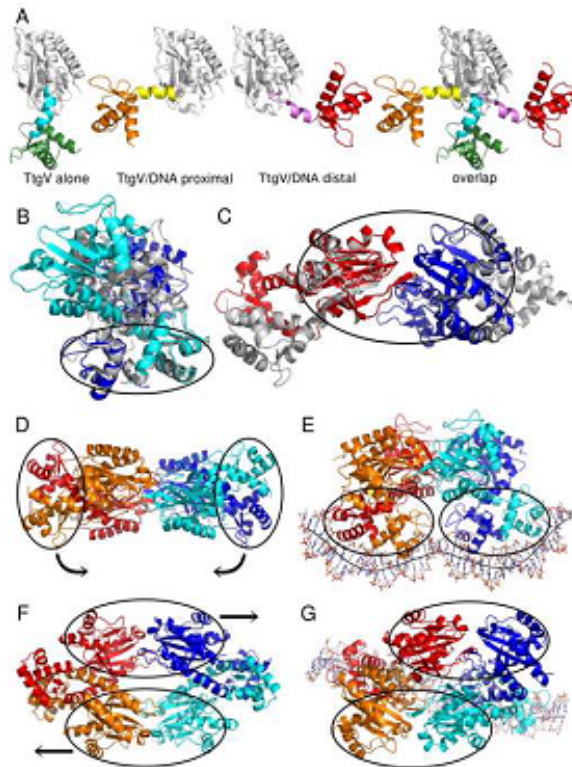
FIG. 3. Conformational changes in TtgV. A) Different monomeric conformations. From left to right: continuous linker helix (cyan) as in TtgV apo, bent linker helix (yellow) as in proximal protomer in the TtgV/DNA structure, unwound linker helix (magenta) as in distal protomers, overlay of three conformations on their CTD (white ribbon) showing different orientations of their DBDs. B) *cis*-dimer comparisons between TtgV apo (white) and TtgV/DNA (blue and cyan). Note the *cis*-DBDs (ellipse) have similar arrangements while *cis*-CTDs differ. C). *trans*-dimer comparisons between TtgV apo (white) and TtgV/DNA (red and blue). The *trans*-CTDs (ellipse) have the same arrangements in both structures. D) Side view of TtgV/DNA complex structure. Ellipses represent the *cis*-DBD units which rotate in opposite directions to (E). E) Side view of TtgV apo structure. F) Top view of TtgV/DNA structure. Ellipses represent *trans*-CTD units that slide and rotate relative to each other to (G). G) Top view of TtgV apo structure.

protomers whose DBDs are located closer to the operator centre (termed the proximal protomers), the linker helix is bent relative to α5 at residue Q86. In the protomers whose DBDs are outermost on the DNA operator (termed the distal protomers), the linker helix is partially unwound between L81 and A85 (Figure 3A). The consequences of these changes in the linker conformation are the dramatically different orientations of the DBD in relation to the CTD. In the TtgV apo structure, the DBD is located below the CTD (Figure 3A, left panel). In the TtgV/DNA proximal protomer, the DBD is positioned to the left of the CTD (Figure 3A). In the TtgV/DNA distal protomer, the unwound a4 and consequently, the DBD, stretches over to the other side of the CTD compared to the proximal protomer (Figure 3A, right).

The cis-dimer in the apo TtgV structure has a two-fold symmetry and a larger buried interface of ~4400 Å^2 than the cis-dimer in the TtgV/DNA structure, which is highly asymmetric and has a buried interface of ~3400 Å^2 (Figure 1B, 2C). In both structures, the cis-DBDs have a similar arrangement (Figure 3B, ellipse, rmsd of cis-DBD dimers is 1.29Å). However, there are few interactions between cis-CTDs and the relative orientations of the CTDs differ in the two structures. This suggests that the cis-DBDs move as a unit while the cis-CTDs move independently. Within the trans-dimer, the CTDs maintain a similar arrangement in both structures (Figure 3C, ellipse). We can, therefore, regard the trans-CTDs as a separate unit. This creates significant restrictions on the conformations within the tetramer, consisting of four rigid body units: two cis-DBD units and two trans-CTD units that are able to move independent of one another (Figure 3D, 3F, ellipses).

The transition from the symmetric apo TtgV structure to the asymmetric TtgV/DNA structure involves a ~ 40 Å sliding and ~ 60° rotation of the two trans-CTD units (Figure 3F, 3G). The two cis-DBD units, which are 180^0 and 100 Å apart from each other in the apo TtgV structure, rotate downwards and adopt a configuration capable of binding to both sites in the DNA operator (Figure 3D, 3E). Furthermore, although the cis-DBDs are similar in both structures, there are some small but significant differences (Figure 3B). In the TtgV apo structure, the distance between the a2 helices and the wings in the WH motifs within each cis-DBD unit is 2-3 Å wider than that of TtgV/DNA structure, implying that TtgV undergoes local conformational changes upon binding to the DNA.

The CTD tetramer in the DNA complex structure has a larger interaction surface (~2700 Å^2) compared to that of TtgV alone (~2200 Å^2) due to the additional interactions between the diagonal promoters, implying
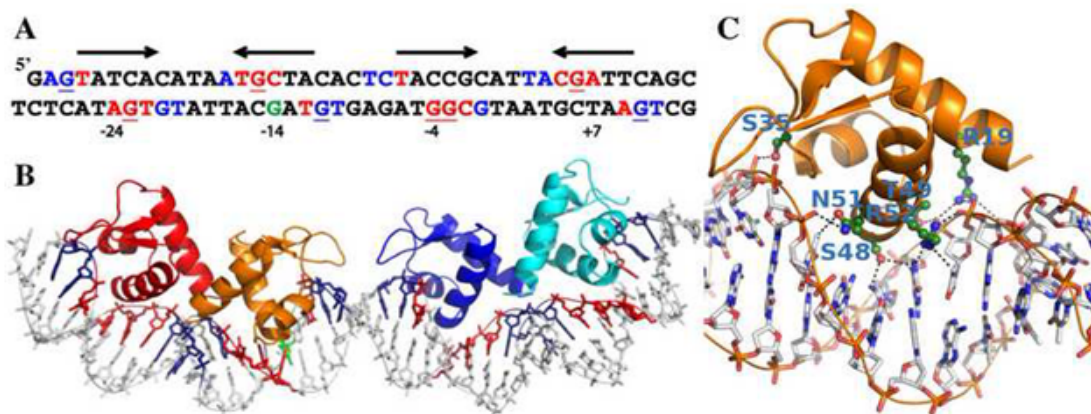
FIG. 4. TtgV-DNA interactions. A) The 42 bp ttgG operator used in the study. The major groove regions are indicated by arrows. Red bases indicate the DNA bases that interact with TtgV in the major groove while blue indicate the interacting bases in the minor grooves. Underlined bases are the sites protected by DMS methylation. Green G is the hypersensitive site. B). The corresponding structure of the DNA and WH domains with the DNA bases coloured according to A). C). Detailed interactions of one WH domain with the DNA. Residues that are involved in direct interactions are labelled.

that within isolated CTDs, the asymmetric CTD tetramer is more stable than the symmetric CTD tetramer. However, although the symmetric CTD in the apo TtgV structure has a smaller interface than the asymmetric CTD in the TtgV/DNA structure, there is a larger interface between the DBDs, a4 and the CTDs within a *cis*-dimer because the DBDs are now constrained in the apo TtgV. Consequently, the full length TtgV apo tetramer assembly is more stable with a total buried surface of ~11000 Å^2 compared to ~9500 Å^2 in the TtgV/DNA structure.

DNA interactions and distortion

The interactions between TtgV and DNA induce both conformational changes in the protein tetramer and significant distortions in the DNA. The extensive interactions between TtgV and DNA induce significant distortions in the DNA operator, with widened major grooves where the recognition helices are inserted (Figure 2, Figure 4, see also Figure S2, Figure S4). Overall, the central axis for the DNA double helix is W shaped, with inward bends at the narrowed minor grooves (~ 40°) that are A/T rich while an outward kink at the widened minor groove with a G/C pair in the middle of the operator, reducing the inward bend over the entire operator to 60° (Figure 2A, Figure 4B). This is consistent with observations in nucleosomes (Drew and Travers, 1985) where, in A/T rich sequences, the minor grooves face inwards towards the centre of the curvature while, in G/C rich sequences, the minor grooves of G/C pairs face outwards. The Widening of major and minor grooves is also observed when WH proteins such as Orc bind to DNA (Gaudier *et al.*, 2007).

The structure allows us to define pseudo-palindromic sites within the operator (Figure 4A, (Guazzaroni *et al.*, 2007b). The two sites span the entire DNA operator with a one base pair spacer in the middle. The recognition sites in the DNA major grooves are centred at positions –24, -14, -4 and +7 in the *ttgGHI* operator (Figure 4A, red bases) relative to the transcription starting

site of *ttgG*. Each major groove site spans a five base pair region (Figure 4A, arrows). There are further contacts with one or two flanking phosphate groups on the 5' end of both DNA strands (Figure 4A, blue bases). The upstream recognition site has higher palindromic symmetry (defined by the arrows) compared to the downstream recognition site. Previous biochemical studies have found that guanines at positions –27, -15, +6 on the top strand and –23, -11, -4, -3, +10 on the bottom strand are protected from DMS methylation upon TtgV binding (Fillet *et al.*, 2009; Guazzaroni *et al.*, 2007a; Guazzaroni *et al.*, 2004). Strikingly, five out of the eight bases make direct hydrogen bonds with TtgV in our TtgV/DNA structure (Figure 4A, underlined red bases), and TtgV interacts with the phosphate backbone at the other three positions (Figure 4A, underlined blue bases). The guanine at position –14 is hyper-sensitive to methylation (Figure 4A, green base (Guazzaroni *et al.*, 2004)). This site is paired with a recognized base in our structure, and is exposed by DNA distortion when TtgV binds.

TtgV interacts with the DNA major groove largely through the recognition helix (α3) of the WH motif, similar to the majority of other WH proteins (Clark *et al.*, 1993; Gajiwala and Burley, 2000). Specifically, residues S48, T49, N51, R52 interact with DNA via the major groove (Figure 4C, see also Figure S4). The wings in the WH domains lie across the minor grooves and interact with the phosphate backbones at both ends and the middle of the DNA operator sequence (Figure 4B). R19 from a1 also interacts with the phosphate backbone (Figure 4C).

Fillet *et al*. (2009) identified three groups of residues within the WH domain of TtgV based on their effects on its activity. Substitution of Group 1 residues with alanine had no effect on activity, while substitution of Group 2 residues abolished activity. Alanine substitution of Group 3 residues significantly reduced activity for the *ttgG* promoter, but had little effect on the *ttgD* promoter. The TtgV structure in complex with the *ttgG* promoter reveals that

Group 1 residues are largely located on protein surfaces and have few interactions with the rest of the protein or DNA (Figure 4, see also Figure S4, white). Group 2 residues (R47, T49 and R52) are directly involved in DNA binding and hence mutations to alanine resulted in mutant regulators that exhibit reduced affinity for the operator and a high level of expression from the target promoters. Group 3 residues are largely located at the dimer interface or interact with other parts of the protein (Figure 4, see also Figure S4). Mutations of these residues presumably affect dimerization or the conformation of the WH domain. Both could affect the orientation of one or both recognition helices, hence affecting DNA binding. Our structure also identifies an additional Group 2 residue (S35), which is involved in binding to the phosphate backbone. Mutating S35 to alanine reduced DNA binding ability significantly, without affecting its quaternary structure (Figure 5).
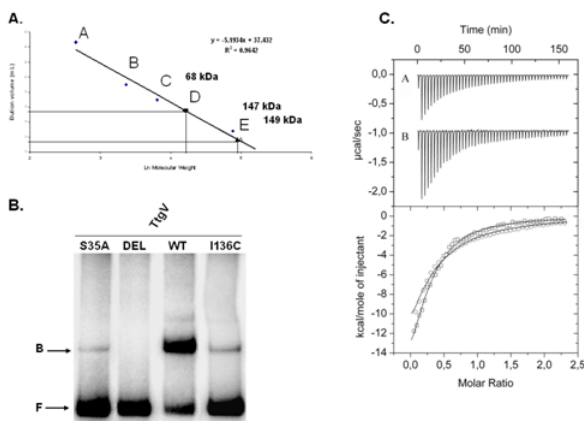

FIG. 6. A proposed cooperative binding and induction mechanism for TtgV. TtgV exists in equilibrium of straight linker helix, symmetric T-state (A) or bent/flexible linker helix, asymmetric R-state (B). The T-state is more stable while the R-state favours DNA binding. C) Upon DNA binding, the favourable interaction energy between the protein and the DNA stabilises the unstable R-state. D) Upon effector binding, the CTDs slide back to the symmetric configuration and the DBDs rotate in opposite directions, releasing from DNA and returning to the stable symmetric configuration (T state).

Our structures suggest that tetramer formation is crucial for the cooperative binding to the operator and β5 is a key component in the tetramer interface (Figure 1B, 2D). In order to test the importance of this interface, we deleted β5 (residues 129-131). The mutant protein (TtgVΔ129-131)

has a similar affinity for effectors as wild type, confirming that the mutations do not affect the overall protein structure and folding (Figure 5C). However, the deletion mutant indeed forms dimers rather than tetramers (Figure 5A) and has consequently, lost cooperativity and is no longer able to bind to DNA (Figure 5B).

Discussion
Cooperative binding of TtgV to its operator can serve as a general cooperative binding model for tetrameric gene regulators

Our structures explain how a TtgV tetramer binds cooperatively to two DNA sites within an operator. A TtgV tetramer consists of a pair of cis-dimers: each cis-dimer unit can bind to one ligand – one DNA site. There are two distinct functional states for a TtgV tetramer: a stable symmetric state, represented by the symmetric TtgV apo structure, where both cis-dimers exist in the T-state, which is more stable but unable to bind to its DNA operator, and a less stable asymmetric form, represented by the asymmetric configuration and released DBDs, where both cis-dimers exist in the R-state, which is less stable but has the correct conformation to permit simultaneous binding to two DNA sites. For simplicity, we define the symmetric apo tetramer which consists of two T-state cis-dimers the stable T-state for the tetramer, while the asymmetric form with two R-state cis-dimers the less stable R-state for the tetramer (Figure 6).

How does TtgV tetramer switch between the two states? Without any constraint, the CTD tetramer is more stable in the asymmetric R-state. However, there are increased interactions between the CTDs and the DBDs in the apo symmetric state. The net energy balance favors the symmetric apo configuration for the TtgV tetramer. In this stable T-state, the DBDs are confined in a configuration that is not competent to bind DNA (Figure 6A). This configuration is also stabilized by effectors, which are then able to bind to symmetric (equivalent) sites (Figure 6D). When DBDs are removed, the CTDs can relax to a more stable asymmetric
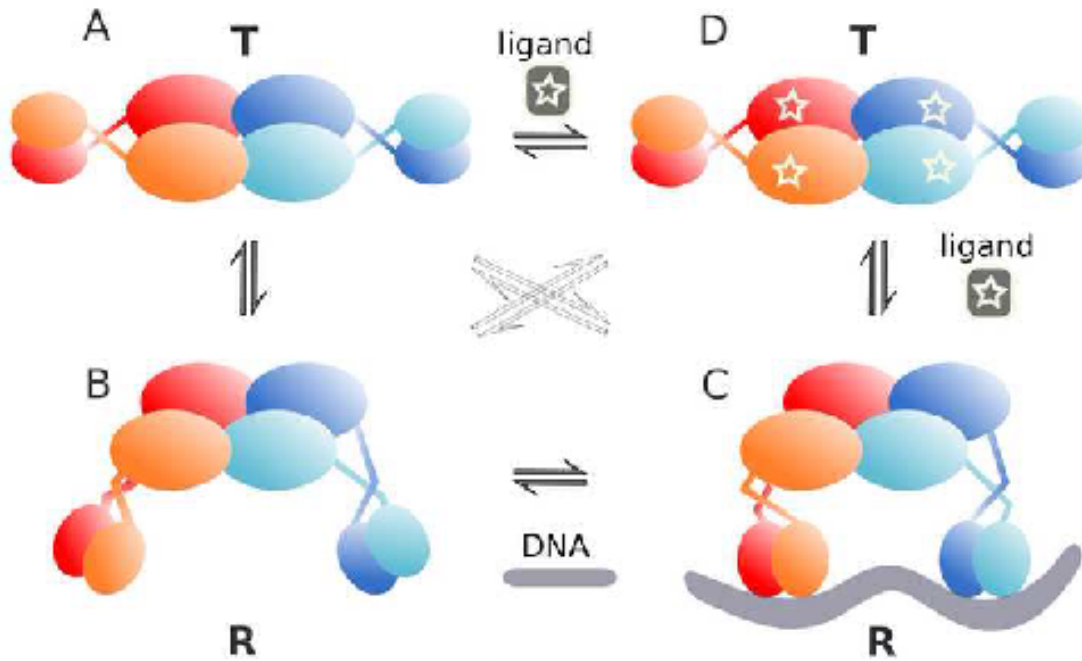
FIG. 6. A proposed cooperative binding and induction mechanism for TtgV. TtgV exists in equilibrium of straight linker helix, symmetric T-state (A) or bent/flexible linker helix, asymmetric R-state (B). The T-state is more stable while the R-state favours DNA binding. C) Upon DNA binding, the favourable interaction energy between the protein and the DNA stabilises the unstable R-state. D) Upon effector binding, the CTDs slide back to the symmetric configuration and the DBDs rotate in opposite directions, releasing from DNA and returning to the stable symmetric configuration (T state).

configuration (Figure 6B). Indeed, this is supported by structures of other IclR family proteins that are truncated to contain just the CTD (Lorca *et al.*, 2007; Zhang *et al.*, 2002), which display asymmetric arrangements.

In order to bind DNA, the symmetric tetramer (T-state) has to release the two pairs of DBDs from the CTDs (Figure 6A, 6B). This has two conflicting effects: it costs favorable interaction energy between the CTDs and the DBDs while it gains energy through the favorable asymmetric CTD arrangement. The energy values are poised so that binding to a single DNA site does not provide sufficient energy to compensate for the loss of two pairs of CTD/DBD interactions but binding to two sites does. This explains the extremely weak binding affinity of TtgV to a single site as mutating one of the two operator sites reduces the ability of TtgV binding to its operator significantly (Guazzaroni *et al.*, 2007b) while TtgV dimer (as in the form of TtgVΔ129-131 is unable to bind to DNA.

However, binding to two sites provides sufficient favorable interactions and allow the tight binding of TtgV tetramer to its operator.

Unlike DNA binding, the effectors bind to each TtgV monomer independently (Guazzaroni *et al.*, 2005) and the effector binding stabilizes the T-state. There are two types of effector binding sites in the TtgV/DNA complex: one is located near the CTD centre, the other adjacent to the linker helices (Figure 3, see also Figure S3). Effector binding to the sites near the CTD tetramer centre will weaken the favourable interactions in the asymmetric CTD tetramer involving residues 134-136. Mutating F134, which is also in the effector binding site, reduced the ability of the protein to bind to DNA (Guazzaroni *et al.*, 2007a). Mutating I136 also significantly reduced the ability in DNA binding although maintained a similar affinity in effector binding compared to wild type (Figure 5). Presumably both mutations affect the asymmetric tetramer arrangement, which is key for DNA binding. Since

residue F134 is involved in both effector binding and the asymmetric tetramer interface in the R-state, it is possible that effector binding induces conformational changes in F134, which de-stabilises the asymmetric R-state. The energy cost in the disruption of the favourable asymmetric CTDs will need to be compensated for by the increased interactions between the CTD and the DBD, therefore promoting the return to the stable symmetric T-state. Effector binding to the other sites that are located close to the linker helices would disturb the interactions of the linker helices, helping the return to the continuous helix conformation that is observed in the T-state.

Many tetrameric gene regulators contain tetrameric effector binding domains and a linker that connects the effector binding domains with the DBDs. These tetrameric gene regulators use a similar cooperative binding model irrespective of their exact domain structures. The T-state is represented by a more stable full length tetramer configuration as observed in the TtgV apo structure. In this state, both pairs of DBDs are confined and unable to bind to the DNA. In the R-state, although overall the full length tetramer is less stable, the tetramer arrangement of the effector binding domains is more stable, and the DBDs are released to permit binding to the DNA operator. DNA binding causes distortions of DNA, which are compensated for by the favourable interaction energy between the protein and two DNA sites. The degree of the cooperativity depends on the energy cost from the T to the R-state transition and the degree of distortions induced in the DNA. The larger the energy cost is to switch from the T to the R-state, and/or the larger the distortion is in the DNA, the stronger the requirement for a cooperative binding between the protein tetramer and both DNA sites is, such that favourable interactions between the protein and two DNA sites can compensate for the large energy cost. This is indeed the case for TtgV, where both DNA sites and a full tetramer are required for efficient binding. However, in some systems, where a weaker cooperativity

exists, either the tetrameric gene regulator or a dimeric form of the protein can bind to a single site albeit with a weaker affinity. These protein/DNA configurations that contain just one DNA site, however, do not represent the final R-state for the tetramer, but an intermediate state between the T and R-states.

Tetrameric models based on partial structures do not represent the assembly on continuous DNA

Lac repressor can bind to two sites separated by 92 bp and a tetramer/DNA structure is available which consists of two 21 bp DNA duplexes bound separately to two LacI dimers that form a V-shape. The ability of LacI binding to each of the two sites separately suggests that LacI binds to two sites with a relatively weak cooperativity. A DNA looping model has been proposed based on this structure, which provided invaluable insights into how LacI might regulate gene expression (Lewis *et al.*, 1996). However, computational modelling and single molecule studies suggest that the tetramer arrangement, especially the opening of the V-shape, depends on the properties of DNA between the two sites, implying that the connecting DNA sequences impose constraints on the LacI tetramer (Rutkauskas *et al.*, 2009; Swigon *et al.*, 2006). Indeed, a recent solution study on the Lac repressor suggests that tetrameric LacI adopts a different conformation in complex with DNA compared to the crystal structure (Taraban *et al.*, 2008). The LacI/DNA model most likely represents the conformation when LacI initially binds to either of the two sites. Additional conformational changes in both DNA and protein would occur upon binding to both sites to reach the final R-state, which will have a larger DNA distortion that is compensated for by further interactions between the protein and the DNA.

Recent structural studies using a mutant form of 1 repressor deficient in tetramer formation revealed an asymmetric arrangement of the *cis*-dimer in complex with its 17 bp DNA target (Stayrook *et al.*,

2008) and asymmetry was proposed to play important roles in forming the tetramer assembly (Hochschild and Lewis, 2009). Our results agree with that hypothesis and suggest that the asymmetry in the *cis*-dimer is a pre-requisite for all tetrameric gene regulators upon binding to their DNA operator containing two adjacent sites. A tetrameric arrangement of λ repressor when bound to two adjacent DNA sites was proposed based on this asymmetric dimer/DNA complex and the tetrameric arrangement of CTDs (Stayrook *et al.*, 2008). The model again provided mechanistic insights into cooperative binding of l repressor to adjacent operator sites based on the available data. However, the model used two separate, discontinuous 17 bp DNA duplexes. Consequently, in that model, although the two DNA duplexes roughly align into a continuous helix, the individual strands do not join smoothly. Furthermore, the angular alignment of the two *cis*-DBD units does not match that of the natural operators (Stayrook *et al.*, 2008). Additional distortion in DNA will be required for a full assembly of protein/DNA. The energy cost in DNA distortions will have to be compensated for by additional interactions between the protein and DNA and between protein subunits.

In summary, previous structures of tetrameric gene repressors have shed light on how they might bind to DNA cooperatively. However, due to the incomplete structural information, models of the repressor/operator complex do not necessarily represent the actual stable protein/operator assembly, or the final R-state. Our structures here provide details of a complete assembly of a tetrameric repressor with full operator sequence and reveal a general cooperative model that can be applied to explain other tetrameric regulators. We propose that the energy difference between the T-state and the R-state and the energy cost in inducing DNA distortions are key determinants for its cooperativity. To achieve the full assembly of regulator/DNA in a cooperative fashion, conformational changes must occur to allow simultaneous binding to both sites and compensate for the energy difference between the two states.

Experimental Procedures

Site-directed Mutagenesis—TtgV mutants were generated by amplification of ttgV from plasmid pANA126 using *pfu* turbo DNA polymerase (Stratagene) and 39 mer primers that incorporated the appropriate mistmaches to introduce the desired mutation. The PCR product was digested with DpnI, ligated to pET28b(+) and transformed in E. coli BL21 (DE3). The nature of each mutant allele was confirmed by DNA sequencing.

Over expression and purification of His-tagged TtgV and mutants — Escherichia coli BL21 (DE3) cells were grown in two-litre conical flasks containing 1L of 2×YT culture medium with 50 μg/ml kanamycin, incubated at 37 °C with shaking until the culture reached a turbidity of around 0.7 at 660 nm. Expression of the TtgV or its variants was induced with 1 mM isopropyl β-D-thiogalactopyranoside and the cultures were kept at 18 °C for 3 h until cells were harvested by centrifugation (10 min at 9000 × *g*). The cell pellet was resuspended in 50 ml buffer made of 25 mM sodium phosphate pH 7.0, 0.5 M NaCl, 5% (vol/vol) glycerol, 10 units lysozyme and half a tablet of COMPLETE® protease inhibitor (ROCHE). Cells were broken through two passages in a French press as described (Guazzaroni *et al*., 2007). After centrifugation at 12,000 × *g* for 45 min, the supernatant was filtered and loaded onto a 5 ml HisTrap HP column (GE Healthcare) and eluted with a imidazol gradient (45 to 500 mM). The fraction containing TtgV or its mutant variants was then dialyzed against buffer containing 15 mM Tris-HCl, pH 7,2, 10% (v/v) glycerol, 300 mM NaCl, 8 mM magnesium acetate and 1 mM dithiothreitol. Protein samples were aliquoted before freezing. All experiments were done with a single batch of each protein. Proteins aliquots were thawed for immediate use, and excess protein was discarded.

Electrophoresis Mobility Shift Assay — The DNA probes were 295-bp fragments containing the *ttgV-ttgGHI* intergenic region obtained from plasmid pGG1 by PCR with primers G5'E (5'-NNNNNNGAATTCGTTCATATCTTTCC TCTGCG-3') and G3'P (5'-NNNNNCTGCAGGGGGATTACCCGT AATGCAC-3'). Cycling parameters were 2 min at 95°C followed by 30 cycles at 95°C for 1 min, 50°C for 30 s, and 72°C for 30 s, ending with 10 min at 72°C. PCR products were isolated from agarose gel by use of a Qiaquick gel extraction kit (Qiagen) and radiolabeled at the 5' end with [γ-^{32}P] ATP and T4 polynucleotide kinase. A 1 nM concentration (~10^4 cpm) of the labeled probe was then incubated with the indicated concentrations of purified proteins in 10 µl STAD (25 mM Tris acetate, pH 8.0, 10 mM KCl, 8 mM magnesium acetate, 3.5% [wt/vol] polyethylene glycol 8000, and 1 mM dithiothreiol) supplemented with 15 µg/ml poly (dIdC) and 200 µg/ml bovine serum albumin. Reaction mixtures were then incubated for 10 min at 30°C, and samples were run in 4.5% (wt/vol) native polyacrylamide gels (Bio-Rad Mini-Protean II) for 2 h at 50 V at room temperature in Tris-glycine buffer (25 mM Tris-HCl, pH 8.0, 200 mM glycine). The results were analyzed with Personal FX equipment and Quantity One software (Bio-Rad).

Isothermal Titration Calorimetry — Measurements were performed on a VP-Microcalorimeter (MicroCal, Northampton, MA) at 25 °C. Proteins were thoroughly dialyzed against 25 mM Tris acetate, pH 8.0, 8 mM magnesium acetate, 100 mM NaCl, 10% (vol/vol) glycerol and 1 mM dithiothreitol. The protein concentration was determined using the Bradford assay. Stock solutions of 1-naphthol, and 4-nitrotoluene at a concentration of 500 mM were prepared in dimethylsulfoxide and subsequently diluted with dialysis buffer to a final concentration of 0.5 mM (1-naphthol and 4-nitrotoluene). Each titration involved a single 1.6 µl injection and a series of 4.8 µl injections of effector into the protein solution. Titration curves were fitted by a nonlinear least squares method to a function for the binding of a ligand to a macromolecule as incooperated in ORIGIN software (MicroCal).

Analytical gel filtration chromatography — We used analytical gel filtration chromatography to determine the oligomeric state of wild type and mutant TtgV in solution, using an Åkta FLPC system (Amersham Biosciences). Briefly, purified proteins were loaded onto a Superdex-200 10/300GL column (Amersham Biosciences) equilibrated in buffer A (25 mM sodium phosphate pH 7.0, 0.5 M NaCl, 5% (vol/vol) glycerol). The protein sample was eluted at a constant flow rate of 0.7 ml/min, and the absorbance of the eluate was monitored at 280 nm. The molecular mass of the protein was estimated from a plot of the elution volume against Ln of the molecular weight of standard calibration proteins, namely, α-lactalbumin from bovine milk (14.2 kDa), carbonic anhydrase from bovine erythrocytes (29 kDa), albumin from chicken egg white (45 kDa) and albumin from bovine serum (66 kDa) (Sigma).

Crystallization - DNA oligos were purchased from MWG and dissolved to a final concentration of 0.2 mM in a buffer containing 50mM HEPES pH8.0 and 40mM NaCl. To anneal into double stranded DNA (dsDNA), complementary single strand DNA fragments were mixed in equal molar ratio, heated at 95 °C for 10min and cooled slowly to room temperature. Annealed 0.1 mM dsDNA was mixed with purified protein of 50 mg/ml at a molar ratio of 1:4. The mixture was left at 4 °C for 2 hours to allow the binding between the protein and DNA. The complex was then loaded onto a superdex-200 column, which was washed with the same buffer that the DNA samples were dissolved in. The fractions of a single peak were collected containing both TtgV and DNA, and the sample was concentrated to a final concentration of 5mg/ml. Crystals were obtained by sitting drop vapour

diffusion. TtgV alone crystals were achieved accidentally from an attempt to crystallize TtgV in complex with a 43 bp DNA fragment covering *ttgGHI* operator region of -30 to +13. The crystallization buffer contained 15% PEG2000MME, 100mM BisTris Propane pH6.4, 200mM KNO_3. The Crystals appeared in 3 days at 4°C. The crystals of TtgV/42bp DNA (-29 to +13) with a 3' extruding base at the bottom strand were grown under the condition of 7% PEG4000, 50mM NaCl, 100mM Tris pH8.0. Crystals grew at 4°C for a month.

Data collection and structure determination – Crystals of TtgV alone and in complex with its DNA operator were transferred into cryo-buffers containing additional 10% or 20% ethylene glycol to their crystallization buffers, respectively, before in liquid nitrogen. Datasets were collected at beamline I04, Diamond Synchrotron Radiation Source. Diffraction data were processed in Mosflm (Leslie, 1992), scaled and truncated in Scala in CCP4 suite (COLLABORATIVE COMPUTATIONAL PROJECT, 1994). Both TtgV alone and TtgV/DNA complex structures were determined by molecular replacement method. The initial searching model for TtgV alone structure was made in Chainsaw (Stein, 2008) based on the CTD of an IclR family member protein structure (PDB code 1MKM (Zhang R.G., 2002)), and the molecular replacement solution was obtained in Phaser (McCoy A.J., 2007). The remaining of the structure was manually built in Coot (Emsley P., 2010). The refined TtgV structure was then used as the initial searching model for the complex. Solution of the CTD was obtained in Phaser. Subsequently, solutions of DBDs and small B-DNA fragments were added to the existing CTDs by using Molrep (Vagin A., 1997). The remaining of the structure was built manually in Coot. All refinements were carried out in Phenix (Adams P.D., 2010). All structure figures were made in Pymol (http://www.pymol.org/).

References

Adams P.D., A.P.V., Bunkóczi G., Chen V.B., Davis I.W., Echoo ls N., Headd J.J., Hung L.-W., Kapral G.J., Grosse-Kunstleve R.W., McCoy A.J., Moriarty N.W., Oeffner R., Read R.J., Richardson D.C., Richardson J.S., Terwilliger T.C., Zwart P.H. (2010). PHENIX: a comprehensive Python-based system for macromolecular structure solution. Acta Cryst *D66*, 213-221.

Browning, D.F., and Busby, S.J. (2004). The regulation of bacterial transcription initiation. Nat Rev Microbiol *2*, 57-65.

Clark, K.L., Halay, E.D., Lai, E., and Burley, S.K. (1993). Co-crystal structure of the HNF-3/fork head DNA-recognition motif resembles histone H5. Nature *364*, 412-420.

COLLABORATIVE COMPUTATIONAL PROJECT, N. (1994). The CCP4 Suite: Programs for Protein Crystallography. Acta Cryst *D50*, 760-763.

Drew, H.R., and Travers, A.A. (1985). DNA bending and its relation to nucleosome positioning. J Mol Biol *186*, 773-790.

Emsley P., L.B., Scott W. G., Cowtan K. (2010). Features and development of Coot. Acta Cryst *D66*, 486-501.

Fillet, S., Velez, M., Lu, D., Zhang, X., Gallegos, M.T., and Ramos, J.L. (2009). TtgV represses two different promoters by recognizing different sequences. J Bacteriol *191*, 1901-1909.

Gajiwala, K.S., and Burley, S.K. (2000). Winged helix proteins. Curr Opin Struct Biol *10*, 110-116.

Gaudier, M., Schuwirth, B.S., Westcott, S.L., and Wigley, D.B. (2007). Structural basis of DNA replication origin recognition by an ORC protein. Science *317*, 1213-1216.

Guazzaroni, M.E., Gallegos, M.T., Ramos, J.L., and Krell, T. (2007a). Different modes of binding of mono- and biaromatic effectors to the transcriptional regulator TTGV: role in

differential derepression from its cognate operator. J Biol Chem *282*, 16308-16316.

Guazzaroni, M.E., Krell, T., Felipe, A., Ruiz, R., Meng, C., Zhang, X., Gallegos, M.T., and Ramos, J.L. (2005). The multidrug efflux regulator TtgV recognizes a wide range of structurally different effectors in solution and complexed with target DNA: evidence from isothermal titration calorimetry. J Biol Chem *280*, 20887-20893.

Guazzaroni, M.E., Krell, T., Gutierrez del Arroyo, P., Velez, M., Jimenez, M., Rivas, G., and Ramos, J.L. (2007b). The transcriptional repressor TtgV recognizes a complex operator as a tetramer and induces convex DNA bending. J Mol Biol *369*, 927-939.

Guazzaroni, M.E., Teran, W., Zhang, X., Gallegos, M.T., and Ramos, J.L. (2004). TtgV bound to a complex operator site represses transcription of the promoter for the multidrug and solvent extrusion TtgGHI pump. J Bacteriol *186*, 2921-2927.

Hochschild, A., and Lewis, M. (2009). The bacteriophage lambda CI protein finds an asymmetric solution. Curr Opin Struct Biol *19*, 79-86.

Krell, T., Molina-Henares, A.J., and Ramos, J.L. (2006). The IclR family of transcriptional activators and repressors can be defined by a single profile. Protein Sci *15*, 1207-1213.

Leslie, A.G.W. (1992). Recent changes to the MOSFLM package for processing film and image plate data. Joint CCP4 + ESF-EAMCB Newsletter on Protein Crystallography, No 26 27-33.

Lewis, M., Chang, G., Horton, N.C., Kercher, M.A., Pace, H.C., Schumacher, M.A., Brennan, R.G., and Lu, P. (1996). Crystal structure of the lactose operon repressor and its complexes with DNA and inducer. Science *271*, 1247-1254.

Lorca, G.L., Ezersky, A., Lunin, V.V., Walker, J.R., Altamentova, S., Evdokimova, E., Vedadi, M., Bochkarev, A., and Savchenko, A. (2007). Glyoxylate and pyruvate are antagonistic effectors of the Escherichia coli IclR transcriptional regulator. J Biol Chem *282*, 16476-16491.

McCoy A.J., G.-K.R.W., Adams P.D., Winn M.D., Storoni L.C., Read R.J. (2007). Phaser crystallographic software. J Appl Cryst *40*, 658-674.

Molina-Henares, A.J., Krell, T., Eugenia Guazzaroni, M., Segura, A., and Ramos, J.L. (2006). Members of the IclR family of bacterial transcriptional regulators function as activators and/or repressors. FEMS Microbiol Rev *30*, 157-186.

Monferrer, D., Tralau, T., Kertesz, M.A., Dix, I., Sola, M., and Uson, I. Structural studies on the full-length LysR-type regulator TsaR from Comamonas testosteroni T-2 reveal a novel open conformation of the tetrameric LTTR fold. Mol Microbiol *75*, 1199-1214.

Ramos, J.L., Duque, E., Gallegos, M.T., Godoy, P., Ramos-Gonzalez, M.I., Rojas, A., Teran, W., and Segura, A. (2002). Mechanisms of solvent tolerance in gram-negative bacteria. Annu Rev Microbiol *56*, 743-768.

Ramos, J.L., Duque, E., Godoy, P., and Segura, A. (1998). Efflux pumps involved in toluene tolerance in Pseudomonas putida DOT-T1E. J Bacteriol *180*, 3323-3329.

Ramos, J.L., Duque, E., Huertas, M.J., and Haidour, A. (1995). Isolation and expansion of the catabolic potential of a Pseudomonas putida strain able to grow in the presence of high concentrations of aromatic hydrocarbons. J Bacteriol *177*, 3911-3916.

Rojas, A., Segura, A., Guazzaroni, M.E., Teran, W., Hurtado, A., Gallegos, M.T., and Ramos, J.L. (2003). In vivo and in vitro evidence that TtgV is the specific regulator of the TtgGHI multidrug and solvent efflux pump of Pseudomonas putida. J Bacteriol *185*, 4755-4763.

Rutkauskas, D., Zhan, H., Matthews, K.S., Pavone, F.S., and Vanzi, F. (2009). Tetramer opening in LacI-mediated DNA looping. Proc Natl Acad Sci U S A *106*, 16627-16632.

Schumacher, M.A., Miller, M.C., Grkovic, S., Brown, M.H., Skurray, R.A., and Brennan, R.G. (2001). Structural mechanisms of QacR induction and multidrug recognition. Science *294*, 2158-2163.

Stayrook, S., Jaru-Ampornpan, P., Ni, J., Hochschild, A., and Lewis, M. (2008). Crystal structure of the lambda repressor and a model for pairwise cooperative operator binding. Nature *452*, 1022-1025.

Stein, N. (2008). CHAINSAW: a program for mutating pdb files used as templates in molecular replacement. J Appl Cryst *41*, 641-643.

Swigon, D., Coleman, B.D., and Olson, W.K. (2006). Modeling the Lac repressor-operator assembly: the influence of DNA looping on Lac repressor conformation. Proc Natl Acad Sci U S A *103*, 9879-9884.

Taraban, M., Zhan, H., Whitten, A.E., Langley, D.B., Matthews, K.S., Swint-Kruse, L., and Trewhella, J. (2008). Ligand-induced conformational changes and conformational dynamics in the solution structure of the lactose repressor protein. J Mol Biol *376*, 466-481.

Teran, W., Felipe, A., Fillet, S., Guazzaroni, M.E., Krell, T., Ruiz, R., Ramos, J.L., and Gallegos, M.T. (2007). Complexity in efflux pump control: cross-regulation by the paralogues TtgV and TtgT. Mol Microbiol *66*, 1416-1428.

Vagin A., T.A. (1997). MOLREP: an automated program for molecular replacement. J Appl Cryst *30*, 1022-1025.

Walker, J.R., Altamentova, S., Ezersky, A., Lorca, G., Skarina, T., Kudritska, M., Ball, L.J., Bochkarev, A., and Savchenko, A. (2006). Structural and biochemical study of effector molecule recognition by the E.coli glyoxylate and allantoin utilization regulatory protein AllR. J Mol Biol *358*, 810-828.

Zhang, R.G., Kim, Y., Skarina, T., Beasley, S., Laskowski, R., Arrowsmith, C., Edwards, A., Joachimiak, A., and Savchenko, A. (2002). Crystal structure of Thermotoga maritima 0065, a member of the IclR transcriptional factor family. J Biol Chem *277*, 19183-19190.

Table 1. Data collection and refinement statistics

Crystal	Free TtgV	TtgV/DNA
Data process		
Space group	C2	P6$_5$
Cell parameters		
a(Å)	70.86	89.58
b(Å)	116.18	89.58
c(Å)	71.88	416.75
α	90°	90°
β	104.3°	90°
γ	90°	120°
resolution(Å)	2.9	3.4
Rsym(%)	7.9(35.4)	5.5(33.4)
I/σ<I>	7.2(2.2)	9.0(2.1)
completeness(%)	99.7	96.7
multiplicity	3.5	4.9
beamline	Diamond I04	Diamond I04
Refinement		
R(%)	20.8	21.13
Rfree(%)	27.9	29.39
RMSD bond length	0.01Å	0.03Å
RMSD bond angle	1.43°	1.68°
Ramachandran disallowed(%)	0	0.21
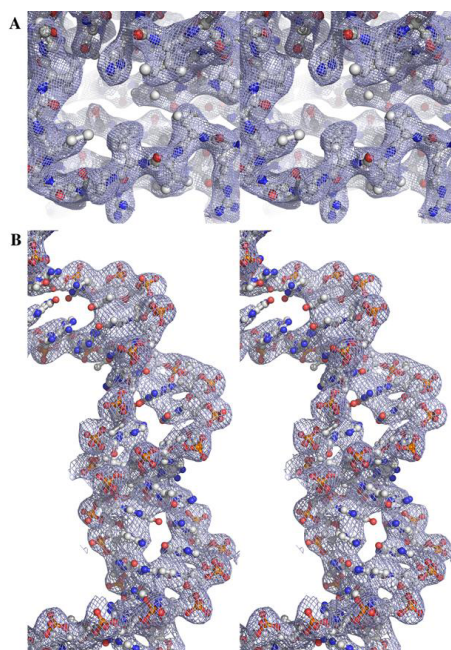
FIG. S1, related to Table1, stereo images of final 2Fo-Fc electron density maps contoured at 1σ. A) TtgV apo structure. B) TtgV/DNA complex structure.
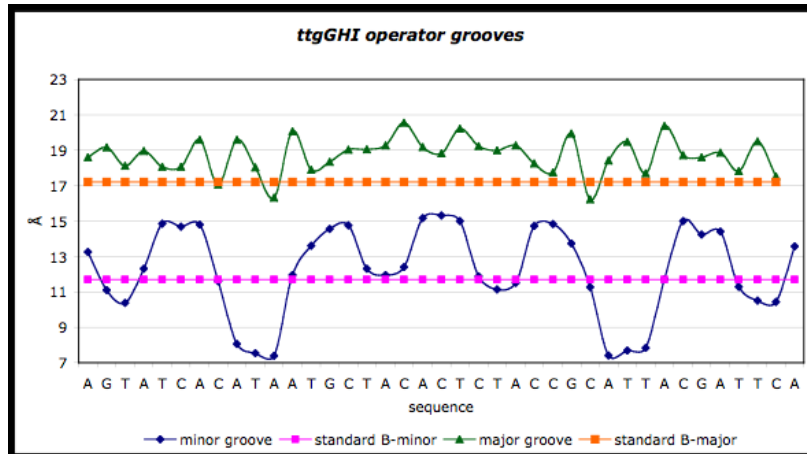
FIG. S2, related to Figure 2, the geometry of the *ttgG* operator DNA. The major groove width (green) of the operator is wider compared to that of standard B-DNA (orange). The minor groove of the operator (blue) is narrower at A/T rich regions and **Inventory of Supplemental Information** wider at the centre (C/G pairs) compared to the standard B-DNA (magenta).
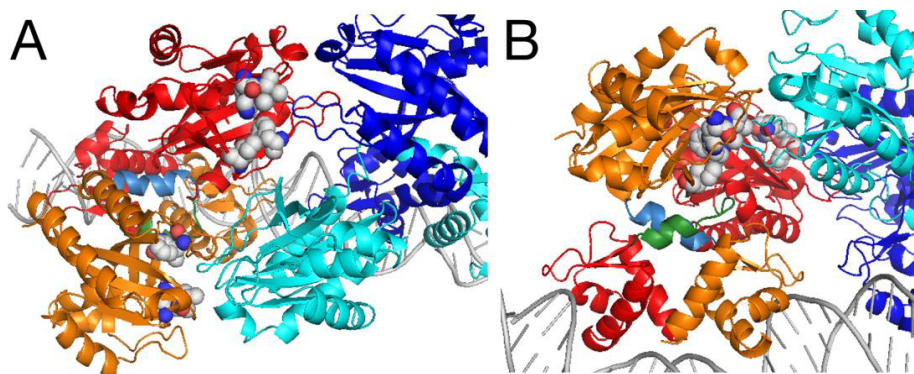
FIG. S3, related to Figure 3, Effector binding sites in the TtgV/DNA structure. A) Top view, two different type of effector binding site (spheres) for the distal protomer (red ribbon) and the proximal protomer (oranage ribbon), B) Side view highlighting the close proximity between the effector binding site and the linker he   79
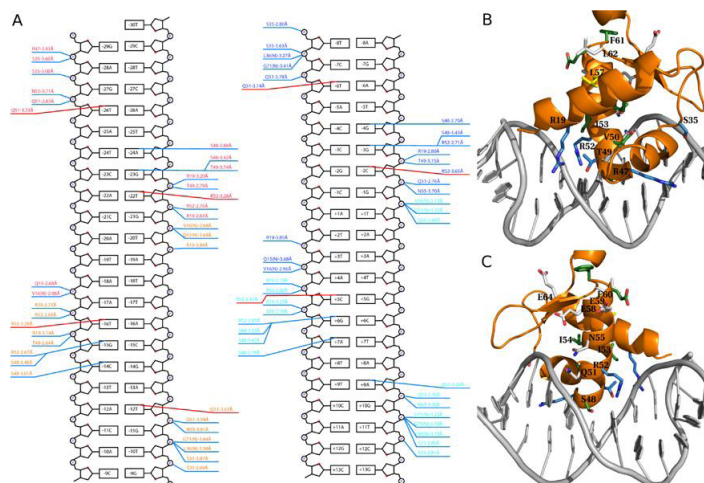
FIG. S4, related to Figure 4, TtgV-DNA interactions. A). Detailed hydrogen bonding (blue lines) and van der Waals (red lines) interactions. Residues are coloured corresponding to the individual protomers in Figure 2. B) Rit   80   esentations of TtgV/DNA interactions. The residues mutated in Fillet *et al*. were coloured differently: Group 1 in white, Group 2 in blue, and Group 3 in green. C) Viewed 180o away.

Organisation des domaines du répresseur TtgV : identification de Glu102 et Arg98 comme résidus clé dans la communication inter-domaine.

TtgV module l'expression des opérons *ttgGHI et ttgDEF*, lesquels codifient des pompes d'efflux ayant pour rôle l'expulsion de composés aromatiques. La structure 3D de TtgV révèle un domaine d'union à effecteur et un domaine d'union à l'ADN composé d'une longue hélice α. Des études de calorimétrie de scanner différentiel ont révélé que TtgV se dénaturalise en un seul événement température Tm de 47°C, indiquant que les deux domaines se dénaturalisent de manière coopérative. L'ajout d'effecteurs montre une augmentation de stabilité de 4 à 8°C. Des mutations des résidus Q51A – au sein du domaine d'union à l'ADN – et V223A – au sein du domaine d'union à effecteur – n'affectent pas l'union à l'ADN cible ; cependant, contrairement à TtgV sauvage, la libération des opérateurs est partiellement perturbée. La structure 3D de TtgV révèle que les résidus Glu98 et Asp102 sont localisés au sein d'une longue hélice α connectant les deux domaines composant TtgV et formant un pont ionique qui pourrait être impliqué dans la transmission du signal. Nous avons généré des mutants en altérant les charges des ces deux résidus. Le déploiement de TtgVE102R et TtgVR98E se déroule en deux étapes indiquant que la coopérativité de dénaturalisation entre les deux domaines est rompue au sein de ces deux mutants. En présence de 1-naphtol, la dénaturalisation thermique de ces mutants augmente la Tm du domaine d'union à effecteur uniquement, sans affecter celle du domaine d'union à l'ADN. Les doubles mutants TtgVQ51A/E102R et TtgVV223A/E102R et le triple mutant TtgVQ51A/E102R/V223A ont été construits; chacun d'eux présentes aussi une dénaturalisation dissociée en deux étapes, ce qui indique la prédominance de la mutation de l'hélice α de connexion sur les mutations des résidus situé en les deux différents domaines composant TtgV. L'ensemble de ces mutants montre aussi une configuration stabilisée en présence d'effecteur.

Organización de los dominios del represor TtgV : identificación de Glu102 y Arg98 como residuos claves en la comunicación inter dominio.

TtgV modula la expresión de los operones *ttgGHI* y *ttgDEF*, los cuales codifican bombas de eflujo que expulsan compuestos aromáticos. La estructura 3D de TtgV revela un dominio de unión al efector y un dominio de unión al ADN conectados por una larga hélice α. Estudios de calorimetría de escáner diferencial revelaron que TtgV se desnaturaliza en un evento único con una temperatura (Tm) de 47°C, lo cual indica que sus dos dominios se despliegan de manera cooperativa. El resultado de la presencia de efectores se traduce en un aumento de la estabilidad de 4 a 8°C. Mutaciones en los residuos Q51A – en el dominio de unión al ADN – y el V223A – en el dominio de unión al efector no impiden la unión al ADN de los reguladores; pero, en contraste con la proteína TtgV silvestre, la liberación del operador está en parte perturbada. La estructura 3D de TtgV ha revelado que los residuos Glu98 y Asp102 están localizados en una larga hélice α que conecta los dos dominios de

TtgV y forman un puente iónico, el cual podría estar implicado en la transmisión de señal. Hemos generados mutantes de estos dos residuos, alterando la carga de los mismos. La desnaturalización de TtgVE102R y TtgVR98E ocurre en dos etapas indicando que en estos mutantes, la cooperatividad de despliegamiento entre los dos dominios está interrumpida . En presencia de 1-naftol, la desnaturalización térmica de los mutantes aumenta la Tm del dominio de unión al efector; sin afectar la del dominio de unión al ADN. Se han construido los dobles mutantes TtgVQ51A/E102R y TtgVV223A/E102R y el triple mutante TtgVQ51A/E102R/V223A, cada uno de ellos muestran un despliegamiento desacoplado, lo cual indica la predominancia de la mutación conectando la hélice α sobre la mutación de los residuos de los dominios que componen TtgV. Estos mutantes también presentan una estabilización de su configuración en presencia de efectores.

Domain organization of the TtgV repressor: Identification of Glu102 and Arg98 as key residues in interdomain communication

Sandy Fillet[1], Tino Krell[1], Bertrand Morel[2], Duo Lu[3], Xiadong Zhang[3], and Juan L. Ramos[1*]

[1] Department of Environmental Protection, EEZ – Consejo Superior de Investigaciones Científicas, 18008 Granada, Spain
[2] Departmento de Química Física e Instituto de Biotecnología, Facultad de Ciencias, University of Granada, 18071 Granada, Spain
[3] Imperial College, London, United Kingdom

TtgV modulates the expression of the *ttgGHI* and *ttgDEF* operons, which encode efflux pumps that extrude aromatic compounds. The 3D structure of TtgV revealed an effector binding domain and a DNA binding domain bridged by a long α-helix. Differential scanning calorimetry studies revealed that TtgV unfolds in a single event with a Tm of 47 ºC, which indicates that both domains unfold cooperatively. Addition of effectors resulted in increased stability by 4 to 8 ºC. Mutants in residues Q51A – in the DNA binding domain - and V223A – in the effector binding domain, can bind target DNA; however, in contrast with the wild-type TtgV, liberation from its operators is partially impaired. The 3D structure of TtgV revealed that residues Arg98 and Asp102 are located within a long α-helix connecting the two domains and form an ion bridge that could be involved in signal transmission. We generated mutants with altered charge at these two residues. The DSC thermogram of TtgVE102R and TtgVR98E showed two events suggesting that both domains unfold individually in a non-cooperative manner. This was confirmed by thermal unfolding studies of the mutants in the presence of the effector 1-naphthol, which caused a Tm shift of the effector binding domain, without affecting the unfolding parameters of the DNA binding domain.

Additional mutations of TtgV in the DNA- or effector binding domain such as in the double mutants TtgVQ51A/E102R and TtgVV223A/E102R and the triple TtgVQ51A/E102R/V223A did not alter the sequential domain unfolding kinetics. This is indicative of the dominance of the mutation in the connecting α-helix over mutation in domain residues. A Tm upshift in only one event in the presence of effector molecules was also observed for these mutants, indicating that they preserve their capacity to bind effectors.

Pseudomonas putida DOT-T1E is a model solvent-tolerant microorganism that grows in the presence of high concentrations of extremely toxic and harmful compounds such as aromatic hydrocarbons (Ramos *et al*., 1995; Ramos *et al*., 1998). Solvent tolerance is a multifactoral process that involves the impermeabilization of the cell membranes via *cis* to *trans* isomerization of unsaturated fatty acids, as well as a series of other changes related to phospholipid headgroups and LPS composition (Bernal *et al*., 2007; Isken and de Bont, 1996; Junker and Ramos, 1999). These changes at the membrane level do not fully impermeabilize the cells and the entry of solvent leads to alterations in the respiratory chains, which result in the generation of reactive oxygen species and the denaturation of proteins (Domínguez-Cuevas *et al*., 2006). Cells respond to these changes by setting up a general stress response program, including the induction of a number of chaperones and peroxidases (Segura *et al.*, 2005). Extrusion of toxic compounds to the outer medium, an energy-dependent process mediated by a set of efflux pumps, is vital for bacteria to thrive at

*Corresponding author: Juan L. Ramos
EEZ-CSIC
C/ Profesor Albareda, 1
18008 Granada, Spain
Phone: +34 958 181608
e-mail: juanluis.ramos@eez.csic.es

high concentrations of solvents (García *et al.*, 2009; Inoue and Horikoshi, 1989; Isken and de Bont, 1996; Kieboom *et al.*, 1998; Kieboom and de Bont, 2001; Ramos *et al.*, 1998; Ramos *et al*, 2002; Rojas *et al.*, 2003; Wery *et al.*, 2001). The most relevant pumps in solvent extrusion belong to the RND family (Ramos *et al.*, 2002), although, efflux pumps belonging to other families have also been described (Endo *et al.*, 2007; García *et al.*, 2009; Kim *et al.*, 1998).

RND efflux pumps are made up of three components: an inner membrane transporter (Murakami *et al.*, 2002; Nikaido and Takatsuka, 2009; Takatsuka and Nikaido 2007; Yu *et al.*, 2003), an outer membrane channel (Koronakis *et al.*, 2000), and a fusion protein that is located in the periplasm (Ge *et al.*, 2009; Tikhonova *et al.*, 2009; Zgurskaya and Nikaido, 1999;), which likely mediates the correct assembly of all elements of the RND efflux pump. The genome of *Pseudomonas putida* DOT-T1E encodes over 20 RND efflux pumps, three of which (TtgABC, TtgDEF and TtgGHI) (Segura *et al.*, 2003) have been involved in the synergic extrusion of solvents, although from a quantitative point of view the main toluene efflux pump is TtgGHI (Rojas *et al.*, 2001). The *ttgABC* and *ttgDEF* operons are chromosomically located, whereas the *ttgGHI* genes are located on the self-transmisable pGRT1 plasmid (Rodríguez-Herva *et al*, 2007).

Expression of the *ttgABC* and *ttgGHI* operons was previously shown to be regulated by the adjacently encoded repressors TtgR and TtgV, respectively. Upstream of the *ttgDEF* operon is located a putative regulator gene named *ttgT*. Although TtgT is able to bind to the *ttgD* operator, our *in vivo* studies showed that this operon is mainly regulated by TtgV (Terán *et al.*, 2007)

The TtgV repressor belongs to the IclR family of regulators (Krell *et al.*, 2006; Molina-Henares *et al.*, 2006). Proteins of this family have two domains, an N-terminal helix-turn-helix (wHTH) DNA binding domain and an effector-binding domain, which is the trait that best defines the members of this family (Krell *et al.*, 2006; Molina-Henares *et al.*, 2006). TtgV is a tetramer in solution and it recognizes a limited number of compounds containing one or two aromatic rings, with binding K_D in the lower micromolar range. The most efficient effectors *in vivo* are two-ring aromatic compounds such as 1-naphthol (1NL) and indole (IND) and one-ring compounds such as 4-nitrotoluene (4NT) and benzonitrile (BN) (Guazzaroni *et al.*, 2005). TtgV operates according to effector-mediated derepression: namely, in the absence of effector the protein is bound at the promoter region repressing transcription, while in the presence of effector molecules TtgV is released from target sequences. Our previous studies showed that TtgV binds directly to DNA through at least three amino acids in the recognition helix of the HTH motif, namely R47, T49 and R52 (Fillet *et al.*, 2009). Effector binding to the TtgV-DNA complex is thought to produce an intramolecular stimulus that is transmitted to the DNA-binding domain, causing dissociation of TtgV from the operator. This subsequently allows RNA polymerase to accesses the promoter leading to resumption of transcription (Guazzaroni *et al.*, 2004).

ITC analysis revealed that the affinity of TtgV mutants for effectors does not correlate with the release of the mutant proteins from its target operators or with their capacity to modulate gene expression *in vivo* (Fillet *et al.*, 2009; Guazzaroni *et al.*, 2007). We show here that TtgV unfolds in a single event centred at a Tm (midpoint of protein unfolding transition) of 47 °C, indicating that the domains unfold cooperatively which is likely to be due to tight interdomain communications. The analysis of the 3D structure of TtgV (Lu *et al.*, 2010) identified a long alpha helix that connects the effector binding domain and the DNA binding domain. Within this alpha helix are residues E102 and R98, which form an ion bridge. Replacement of glutamic acid 102 with arginine and arginine 98 with glutamic acid resulted in the uncoupling of thermal unfolding of the two TtgV domains. Binding of effectors to the mutant proteins increased thermal stability of the effector binding domain, but not that of the DNA binding domain.

EXPERIMENTAL PROCEDURES

Bacterial Strains, Plasmids, and Culture Medium — The bacterial strains and plasmids

used in this study are shown in Table 1. Bacterial strains were grown in LB medium at 30 °C or 37 ºC as previously described (Abril *et al*., 1998; Duque *et al*., 2001). *Escherichia coli* BL21 (DE3) bearing appropriate plasmids was grown in 2×YT at 37 ºC for the production of the TtgV protein or its mutant variants. Liquid cultures were shaken on an orbital platform operating at 200 rpm. When required, the following antibiotics were added to the cultures: ampicillin, 100 μg/ml; gentamycin, 10 μg/ml; kanamycin, 30 μg/ml; nalidixic acid, 10 μg/ml; rifampicin, 10 μg/ml; and tetracycline, 20 μg/ml.

Site-directed Mutagenesis — TtgV mutants, in which amino acid residues at positions 98 and 102 were replaced by another amino acid, were generated by amplification of *ttgV* from plasmid pANA126 using *pfu* turbo DNA polymerase (Stratagene) and 39 mer primers that incorporated appropriate mismatches to introduce the desired mutation (Daniels *et al*., 2010). The PCR product was digested with DpnI, ligated to pET28b(+) and transformed in *E. coli* DH5α. The nature of each mutant allele was confirmed by DNA sequencing. TtgV mutants in residues 51 and 223 were generated before (Fillet *et al*., 2009; Guazzaroni *et al.*, 2007). Double mutants TtgVQ51A/E102R and TtgVV223A/E102R were generated as above but using as a template the *ttgV* mutant allele encoding the single TtgVQ51A or TtgVV223A mutant. A triple TtgVQ51A/E102R/V223A was constructed using as a template the *ttgV* mutant allele that encodes TtgVE102R/V223A mutant.

TtgV Expression and Purification — *Escherichia coli* BL21 (DE3) bearing appropriate plasmids encoding TtgV proteins cells were grown in two-litre conical flasks containing 1L of 2×YT culture medium with 30 μg/ml kanamycin, incubated at 37 °C with shaking until the culture reached a turbidity of around 0.7 at 660 nm. Then expression of TtgV or its variants was induced with 1 mM isopropyl β-D-thiogalactopyranoside and the cultures were kept at 18 °C for 3 h until cells were harvested by centrifugation (10 min at $9000 \times g$). The cell pellet was suspended in 50 ml of buffer that contained 25 mM sodium phosphate pH 7.0, 0.5 M NaCl, 5% (vol/vol)

glycerol, 10 units lysozyme (Sigma) and half a table of COMPLETE® protease inhibitor (Roche). Cells were broken through two passages in a French press as described (Guazzaroni *et al.*, 2007). After centrifugation at $12,000 \times g$ for 45 min, the supernatant was filtered and loaded onto a 5 ml HisTrap HP column (GE Healthcare) and eluted with an imidazol gradient (45 to 500 mM). The fraction containing TtgV or its mutant variants was then dialyzed against buffer containing 15 mM Tris-HCl, pH 7,2, 10% (v/v) glycerol, 300 mM NaCl, 8 mM magnesium acetate and 1 mM dithiothreitol. The purity of the protein was between 90 and 95% as judged from SDS-PAGE gels. Protein samples were aliquoted before freezing. All experiments were done with a single batch of each protein. Proteins aliquots were thawed for immediate use, and excess protein was discarded.

Electrophoresis Mobility Shift Assay — A 295-bp DNA fragment containing the P_{ttgG} or P_{ttgD} promoter was amplified by PCR from pGG1 or pT1B6 using appropriate primers, isolated from agarose gels, and end-labeled with ^{32}P as described before (Fillet *et al*., 2009). About 1 nM labeled DNA ($\sim 1.5 \times 10^4$ cpm) was incubated with the indicated amounts of purified TtgV or TtgV mutant proteins for 10 min at 30 °C in STAD binding buffer (25 mM Tris-acetate, pH 8.0; 10 mM potassium chloride; 8 mM magnesium acetate; 3.5% (w/v) polyethylene glycol 8000, and 1 mM dithiothreitol) containing 15 μg/ml poly(dI-dC) and 200 μg/ml bovine serum albumin. Electrophoresis in native polyacrylamide gels (4.5%, wt/vol) and analyses were carried out as described before (Fillet *et al*., 2009).

Isothermal Titration Calorimetry — Measurements were performed on a VP-Microcalorimeter (MicroCal, Northampton, MA) at 25 °C. Proteins were throughly dialyzed against 25 mM Tris acetate, pH 8.0, 8 mM magnesium acetate, 100 mM NaCl, 10% (vol/vol) glycerol and 1 mM dithiothreitol. The protein concentration was determined using the Bradford assay. Stock solutions of 1-naphthol, and 4-nitrotoluene at a concentration of 500 mM were prepared in dimethylsulfoxide and subsequently diluted with dialysis buffer to a final concentration of 0.5 mM (1-naphthol and

4-nitrotoluene). All chemicals were manipulated in glass vessels, and effector samples were neither degassed nor filtered, to avoid evaporation or nonspecific binding. Each titration involved a single 1.6 µl injection and a series of 4.8 µl injections of effector into the protein solution. For DNA binding studies, oligonucleotides corresponding to both strands of the TtgV operators were synthesized (5′-GCTTGCGTCAAGAGTATCACATAATGCT ACACTCTACCGCATTACGATTCAGCAAT AGCCCCC-3′ and its corresponding complementary oligonucleotide, and 5'-GGCTGTTTCGCAAAAACCACATAGTGAT ACACTATTCTGCAATGCGGGCCATGCAT TGTGATT-3' and its corresponding complementary oligonucleotide). Annealing was carried out by mixing equimolar amounts (at a concentration of 200 µM) of each complementary oligonucleotide in 10 mM phosphate buffer, pH 7.0, 1 mM EDTA and 150 mM NaCl. The mixture was incubated at 95 °C for 10 min and then chilled on ice and dialyzed in the buffer used for ITC studies. The mean enthalpies measured from injection of the ligand in the buffer were subtracted from raw titration data before data analysis with ORIGIN software (MicroCal). Titration curves were fitted by a nonlinear least squares method to a function for the binding of a ligand to a macromolecule (Wiseman *et al.*, 1989). From the curve thus fitted, the parameters ΔH (reaction enthalpy), K_A (binding constant, $K_A = 1/K_D$), and n (reaction stoichiometry) were determined. From the values of K_A and ΔH, the change in free energy (ΔG) and in entropy (ΔS) was calculated using the equation: $\Delta G = -RT \, \mathrm{Ln} K_A = \Delta H - T\Delta S$, where R is the universal molar gas constant and T is the absolute temperature.

CD Spectroscopy – CD experiments were performed using a Jasco J-715 (Tokyo, Japan) spectropolarimeter equipped with a thermostatized cell holder. Measurements of the far-UV CD spectra (260-200 nm) were made with a 0.1 cm path length quartz cuvette. The resulting spectrum was the average of 5 scans. Thermal denaturation was followed from 15 °C to 70 °C at 222 nm, which is a characteristic negative band for α-helix. The spectra were corrected using baselines obtained for samples containing only buffer.

Differential Scanning Calorimetry – Differential scanning calorimetry experiments were carried out with a VP-DSC (Valerian-Plotnikov differential scanning calorimeter) capillary-cell microcalorimeter from MicroCal (Northampton, MA) at a scan rate of 60 °C h^{-1}. Protein solutions for the calorimetric experiments were prepared by exhaustive dialysis against a buffer with 20 mM PIPES, pH 7.2, 8 mM magnesium acetate, 150 mM KCl, and 1 mM TCEP. The buffer from the last dialysis step was used in the reference cell of the calorimeter. Calorimetric cells (operating volume 0.137 ml) were kept under an excess pressure of 60 psi bar to prevent degassing during the scan and also to permit the scans to be performed at a temperature up to 80 °C. Several buffer-buffer baselines were obtained before each run with protein solution in order to ascertain proper equilibration of the instrument. Reheating runs were carried out to determine the calorimetric reversibility of the denaturation process.

RESULTS

Thermal unfolding of TtgV occurs in a single event — Multialignment of 1000 IclR family members show conserved sequence identity along the entire length of these proteins (Molina-Henares *et al.*, 2009) and a search for domains, using Provalidator and other bioinformatic tools, revealed that members of this family have a HTH DNA-binding domain at their N-terminal region and a highly conserved C-terminal region corresponding to the effector-binding domain (Krell *et al.,* 2006; Molina-Henares *et al.*, 2006; Pérez-Rueda *et al.*, 2000; Zhang *et al.*, 2002). The 3D structure of TtgV has been recently solved and the two domains were identified within the structure (Lu *et al.*, in preparation). We found that the two domains in TtgV are linked by a long extended α-helix (Figure 1).

To explore if the two domains are physically independent units we purified TtgV to homogeneity and carried out a series of physicochemical assays. The thermal unfolding properties of the protein were determined by circular dichroism (CD) by monitoring ellipticity
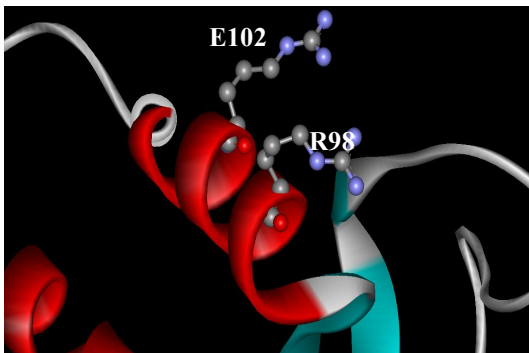
FIG. 1. Detail of the Arg98/Glu102 ion bridge in TtgV as deduced from the 3D structure of the protein. For 3D details see Lu *et al.*, 2010

at 222 nm from 15 ºC to 70 ºC at 1K/min and differential scanning calorimetry (DSC). Both approaches indicated that TtgV unfolds in a single event centred at 47º C (Figure 2A). The DSC profiles did not differ at different concentrations, what suggests that the TtgV oligomer is a stable tetramer. Rescans revealed unfolding was an irreversible process which does not depend on the protein concentration. Thermal unfolding of TtgV was also monitored by DSC in the presence of increasing concentrations of the effector molecules 1-naphthol (Figure 2B) and 4-nitrotoluene (not shown). We found that as the effector concentration increased, the thermal stability of TtgV also increased, reaching a thermal stability plateau at saturating effector concentrations. In all cases, a single unfolding event was observed with a Tm shift of 4 ºC for 4-nitrotoluene, and 8 ºC for 1-naphthol (See Figure 2B), with Tm of approximately 51 ºC

and 55 ºC, respectively. The increase in Tm was concomitant with increases in the unfolding enthalpic contribution of the system, as observed by the increase in the DSC peak height (See Figure 2B for results with increasing concentrations of 1-naphthol).

In control assays with TtgV and dimethylsulfoxide (no compound used to prepare the effector stock solutions) no change in Tm was observed (data not shown). In the assays described below results with 1-naphthol are presented as this compound caused the largest Tm shift.

Characterization of a set of TtgV mutants — We had previously generated mutants in residues Q51A (Fillet et al., 2009) and V223A (Guazzaroni et al., 2007) which, similarly to the wild-type protein, were able to bind its target DNA; however, in contrast with the wild type, the liberation of these proteins from the *ttgD* promoter in response to effectors was partially impaired. Interestingly, the former mutant is located in the DNA-binding domain, whereas the V223 residue is found in the effector-binding domain, which indicates potential inter-domain communication. To test if the defect in liberation from DNA was due to defects in effector binding, ITC assays with the protein in solution or bound to DNA targets were done. The results presented in Table 2 revealed that these proteins recognized effectors with a similar affinity to the wild-type whether in solution or complexed with DNA (see also below); therefore defects in DNA release from its targets might be due to putative deficiencies in signal transmission.

The 3D structure of TtgV identified a long α-helix connecting the effector binding domain and the HTH DNA binding domain (Lu *et al.*, 2010). In this α-helix, Glu102 and Arg98 were
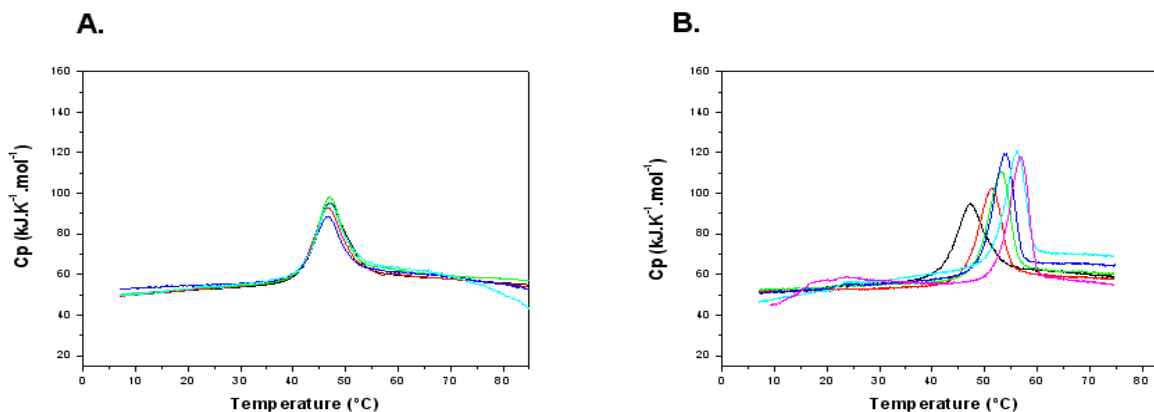
A.

B.

FIG. 2 . **A. Temperature-dependency of the apparent heat capacity of TtgV** at different concentrations in 20 mM Pipes, 8 mM magnesium acetate, 150 mM KCl, 10 mM TCEP pH 7.2. The protein concentrations are 0.17 mM (black trace), 0.1 mM (red trace), 0.06 mM (green trace), 0.03 mM (blue trace), 0.017 mM (cyan trace). **B. Analysis of TtgV by DSC** in the absence (black line) and in the presence of 1-naphthol. The protein was at a concentration of 30 µM. The ligand concentrations were 62.5 mM (red line), 125 mM (green line), 250 mM (blue line), 500 mM (cyan line), and 1250 mM (magenta line).

shown to form an ion pair that may be important to protein stability by helix capping, suggesting that these residues are relevant for the functioning of the protein. We choose to further explore the importance of these residues by generating Ala mutants at residues E102 and R98. Additionally, point mutants replacing Glu102 with either Asp or Arg were also generated to maintain or alter the charge of the residue. At position 98 a mutant in which Arg was replaced by Glu was also generated. All mutant alleles were cloned into pET28b(+) (Table 1) for expression of the His-tagged TtgV mutant variants, which were purified to homogeneity. All mutants exhibited similar far UV CD spectra (Suppl. Table 1), indicating that the mutation points did not affect the overall secondary structure of the protein.

Subsequently, the mutant proteins were submitted to unfolding assays: Mutants Q51A, V223A, E102D, R98A and E102A unfolded in a single event, as the wild-type protein, with thermal parameters similar to those of wild-type TtgV, both in the absence and in the presence of effectors (See Suppl. Figure 1 for TtgVQ51A). Interestingly, mutant TtgVE102R and TtgVR98E exhibited an altered denaturation pattern, with unfolding

TtgEV102A (Figure 3B) and 42ºC and 48.5ºC for TtgVR98E (Suppl. Figure 2). The two unfolding events are likely to represent individual unfolding of the DNA-binding and effector binding domains. Therefore, the mutations at residues 98 and 102 appear to have uncoupled the cooperative unfolding of both domains observed in the wild-type protein. We also tested whether the presence of effectors influenced the thermal stability of the seen with E102R and R98A in this series of assays we used 33 μM 1-naphthol. We found an upshift of the initial event, whereas the other unfolding event showed an unaltered Tm value (Figure 3). This is indicative that the first event is related to the unfolding of the effector binding domain, whereas the second event corresponded to the unfolding of the DNA binding domain. Because a mutation in the long α-helix connecting the two domains in TtgV affected thermal stability, we decided to combine mutations in each of the domains and one mutation in the connecting helix. For this reason we constructed double mutants TtgVQ51A/E102R and

TABLE II
Affinity of TtgV in solution or complexed to target for 1-naphthol as determined from ITC titrations.

Protein -DNA	Effector	K_D	K_A	ΔH	$T\Delta S$	ΔG
		μM	M^{-1}	kcal/mol	kcal/mol	kcal/mol
WT	1 naphthol	18,7 ± 1,33	(5,4 ± 0,38) x10⁴	- 40,4 ± 8,11	- 33,9± 8,11	- 6,5 ± 0,04
WT-DEF	1 naphthol	16,8 ± 0,42	(5,9 ± 0,15) x10⁴	- 23,9 ± 1,33	- 17,4 ± 1,34	- 6,5 ± 0,02
WT-GHI	1 naphthol	24,7 ± 0,61	(4,1 ± 0,10) x10⁴	- 53,3 ± 7,31	- 47,0 ± 0,74	- 6,3 ± 0,02
Q51A	1 naphthol	17,5 ± 1,32	(5,7 ± 0,43) x10⁴	- 41,0 ± 8,32	- 34,5 ± 8,31	- 6,5 ± 0,05
Q51A-DEF	1 naphthol	16,5 ± 1,52	(6,1 ± 0,56) x10⁴	- 4,9 ± 0,32	1,6 ± 0,33	- 6,5 ± 0,06
Q51A-GHI	1 naphthol	22,6 ± 1,22	(4,4 ± 0,24) x10⁴	- 30,1 ± 3,6	- 23,8 ± 3,64	- 6,3 ± 0,03
R98E	1 naphthol	10,3 ± 1,02	(9,7 ± 0,96) x10⁴	- 41,4 ± 8,31	- 34,6 ± 8,31	- 6,8 ± 0,06
R98E-DEF	1 naphthol	13,1 ± 1,19	(7,7 ± 0,70) x10⁴	- 33,0 ± 1,07	- 26,3 ± 1,07	- 6,7 ± 0,05
R98E-GHI	1 naphthol	19,6 ± 1,81	(5,1 ± 0,47) x10⁴	- 24,0 ± 5,03	- 17,6 ± 5,03	- 6,4 ± 0,06
E102A	1 naphthol	18,3 ± 1,14	(5,5 ± 0,34) x10⁴	- 41,4 ± 6,54	- 35,0 ± 6,54	- 6,5 ± 0,04
E102A-DEF	1 naphthol	15,2 ± 0,76	(6,6 ± 0,33) x10⁴	- 26,4 ± 2,85	- 19,8 ± 2,85	- 6,6 ± 0,03
E102A-GHI	1 naphthol	13,7 ± 1,28	(7,3 ± 0,68) x10⁴	- 21,9 ± 2,78	- 15,3 ± 2,78	- 6,6 ± 0,06
E102R	1 naphthol	22,3 ± 0,60	(4,5 ± 0,12) x10⁴	- 74,6 ± 7,67	- 68,3 ± 7,67	- 6,3 ± 0,02
E102R-DEF	1 naphthol	15,0 ± 0,52	(6,7 ± 0,23) x10⁴	- 113,6 ± 3,78	- 107,0 ± 3,78	- 6,6 ± 0,02
E102R -GHI	1 naphthol	22,1 ± 0,64	(4,5 ± 0,13) x10⁴	- 73,0 ± 10,30	- 66,5 ± 10,30	- 6,4 ± 0,02
V223A	1 naphthol	5,4 ± 0,68	(18,4 ± 2,30) x10⁴	-14,8 ± 1,73	- 25,6 ± 5,81	- 7,2 ± 0,07
V223A-DEF	1 naphthol	11,3 ± 0,33	(8,8 ± 0,26) x10⁴	- 20,4 ± 0,90	- 13,7 ± 0,90	- 6,7 ± 0,02
V223A-GHI	1 naphthol	10,3 ± 0,37	(9,7 ± 0,35) x10⁴	- 16,9 ± 0,63	- 10,1 ± 0,63	- 6,8 ± 0,02

occurring in two events, characterized by Tm of 48.5 and 56 ºC for TtgVE102R (Figure 3A) and 49 and 56 ºC for

TtgVV223A/E102R and a triple mutant Q51A/E102R/V223A and submitted the mutant proteins to several assays. CD

90

spectra of the double mutants and the triple mutant revealed a lower α-helix content and the proteins started to precipitate at a concentration of 150 μM, a concentration at which wild-type TtgV is fully soluble. For thermal unfolding assays we used 33 μM of the double and triple mutants. We found that the double mutants and the triple mutant showed two thermal unfolding events as seen with the single TtgVE102R mutant. Furthermore, as expected, the unfolding event corresponding to the effector binding domain was stabilized in the presence of effector molecules in the double and triple mutant. To elucidate the relevance of the above set of findings regarding the mechanism of derepression of target promoters, we designed a series of *in vitro* and *in vivo* assays that are described below.

In Vitro and in vivo responses of TtgV and its mutants to effectors — From a mechanistic point of view, it has been proposed that TtgV functions by sterically preventing RNA polymerase from accessing the promoter region (Guazzaroni *et al*., 2004). Therefore, TtgV achieves up-regulation of gene expression via effector-mediated dissociation from its operators. We found that TtgVV223A, TtgVQ51A and TtgVE102R bound to target DNA promoters, while the TtgVR98E did not. To determine how well effectors were recognized by TtgV mutants (TtgVV223A, TtgVQ51A, TtgVE102R) we undertook different approaches. *In vivo*, we used a

$P_{ttgG}::'lacZ$ (pANA96) and a $P_{ttgD}::'lacZ$ fusion (pMPD1) to measure β-galactosidase activity in *P. putida* DOT-T1EΔVT bearing the mutant TtgV when grown in the absence and in the presence of 1 mM of 4-nitrotoluene and 1-naphthol (Table 3). As a control the wild-type TtgV was used (Table 3). The basal level of expression from the *ttgG* promoter in cells bearing TtgV was 745 ± 10 Miller units, and expression increased at least 2-fold in response to 1 mM 1-naphthol or 4-nitrotoluene (Table 3). Basal expression from the *ttgD* promoter was lower (30 ± 5 Miller Units) than that seen with *ttgG*, indicating more efficient repression. Consistently, the level of induction from P_{ttgD} was higher with effectors (about 5 to 15-fold induction, Table 3). However, when TtgV was replaced by cells expressed TtgVQ51A, TtgVE102R, or TtgVV223A we found that the basal level of expression from P_{ttgG} and P_{ttgD} was 2- to 18-fold lower indicating that these mutants were more efficient repressors than the wild-type protein (Table 3).

For the P_{ttgG} promoter, all of the mutants responded to 4-nitrotoluene and 1-naphthol allowing significant derepression with maximal expression levels similar to those measured for wild-type TtgV (Table 3). With P_{ttgD} not all the mutants behaved like the wild-type protein, and upon addition of effectors did not exactly follow the pattern seen with the wild-type protein, i.e., the increase of β-gal activity with TtgVV223A in response to 1-naphthol or 4-nitrotoluene was very low, and with mutants Q51A and E102R the response to effectors was

TABLE III

In vivo effects of TtgV and its mutant variant on the expression from *ttgD* (pMPD1) and *ttgG* (pMPG) promoters fused to *'lacZ.*

	pMPD ($P_{ttgD}::'lacZ$)			
Effector	TIEVT (pBBRN::*ttgV*)	TIEVT (pBBRN-Q51A)	TIEVT(pBBRN-E102R)	TIEVT (pBBRN-V223A)
None	30 ± 5	15 ± 5	10 ± 5	10 ± 5
1-naphthol	440 ± 135	160 ± 50	140 ± 30	30 ± 10
4-nitrotoluene	140 ± 45	60 ± 15	50 ± 20	20 ± 10

	pANA96 ($P_{ttgG}::'lacZ$)			
Effector	TIEVT (pBBRN::*ttgV*)	TIEVT (pBBRN-Q51A)	TIEVT (pBBRN-E102R)	TIEVT (pBBRN-V223A)
None	745 ± 10	130 ± 25	40 ± 5	320 ± 70
1-naphthol	1750 ± 130	2400 ± 5	1870 ± 25	1735 ± 140
4-nitrotoluene	1400 ± 170	1960 ± 350	2390 ± 240	1880 ± 170

A *Pseudomonas putida* strain deficient in *ttgV* and *ttgT* (TIEVT) was transformed with plasmid pMPD1 or pANA96 and pBBRN::*ttgV* or derivatives bearing the indicated TtgV mutant. Cells were grown as described under Experimental Procedures in the absence (none) or in the presence of 1 mM 1-naphthol or 4-nitrotoluene. β-galactosidase was measured in permeabilized cells as described in Experimental Procedures.

about 30% of that measured for wild-type TtgV. This suggests that the release of TtgV mutants from target operators depends on the DNA sequence of the operator site. This may be due to differential recognition of effectors by TtgV mutants when bound to the two different operators, or that the efficiency in transmission of signals from the effector binding domain to the DNA-binding domain is influenced by the nature of the TtgV mutant DNA complex.

To clarify whether interactions between effector and TtgV mutants, as well as whether binding affinities between TtgV mutants and the operator DNA sequences differ from wild-type TtgV, we carried out isothermal titration calorimetry and EMSA. We have previously shown that TtgV binds 1-naphthol and 4-nitrotoluene in an enthalpy-driven process. First we tested the binding of effector molecules to TtgVV223A, TtgVE102R, TtgVE102A, TtgVR98A and TtgVQ51A. The results showed that the mutants in solution bound 1-naphthol and 4-nitrotoluene with an affinity equivalent to that of the wild-type protein (see Table 2). To test if mutant proteins recognized effectors when complexed with target DNAs, we annealed complementary synthetic 63-bp oligonucleotides spanning the TtgV target sequences in P_{ttgD} and P_{ttgG} (See Experimental Procedures). Experiments were designed so that the protein concentration after saturation with DNA corresponded exactly to the protein concentration used for the titration of unliganded protein with 1-naphthol or 4-nitrotoluene. After saturation, the wild-type TtgV-DNA and mutant TtgV (Q51A, R98E, E102A, E102R, and V223A)-DNA complex was titrated with effectors in a similar fashion to the titration of free TtgV protein in solution.

We found that, when complexed, the affinity of wild-type TtgV and Q51A, E102A and E102R mutants for 1-naphthol was similar, with an affinity in the range of 17 to 22 µM (Table 2). The affinity of TtgVV223A when complexed with P_{ttgG} promoter was around 10 µM. Therefore, the affinity of TtgV and its mutants for effectors either unligated or affinity complexed with DNA recognize effector molecules with a similar.

We then reasoned that the differences seen *in vivo* with β-galactosidase activity cannot be due to differences in effector recognition and hypothesized that it might be possible that the efficiency of different effectors is influenced by the TtgV mutant/DNA complex formed with either the *ttgG* or *ttgD* promoter. To explore this hypothesis, we conducted EMSA with constant amounts of *ttgG* and *ttgD* promoter DNA and TtgV or its mutants in the presence of 1 mM of effector. Our ITC studies have shown that at this concentration (around 50-fold higher than the K_D), TtgV (or its mutants) either free or when complexed with DNA was entirely saturated with effector. Differences in effector-mediated protein release can thus be assumed to reflect differences in the efficiency of intramolecular domain – domain cross-talk, since no significant differences in affinity for effectors were measured by ITC.

The densitometric analysis of the gels revealed that TtgV binds slightly better to the *ttgD* promoter (83%) than to *ttgG* promoter (74%). We then analysed in EMSA the series of mutants generated in this study. We found that all TtgV mutants bound to the *ttgD* and *ttgG* promoters with an affinity similar to that of TtgV and retarded similar amounts of DNA (Figure 4).

Subsequently, a series of assays were done to evaluate the efficiency of ligands to induce

A. **B.**
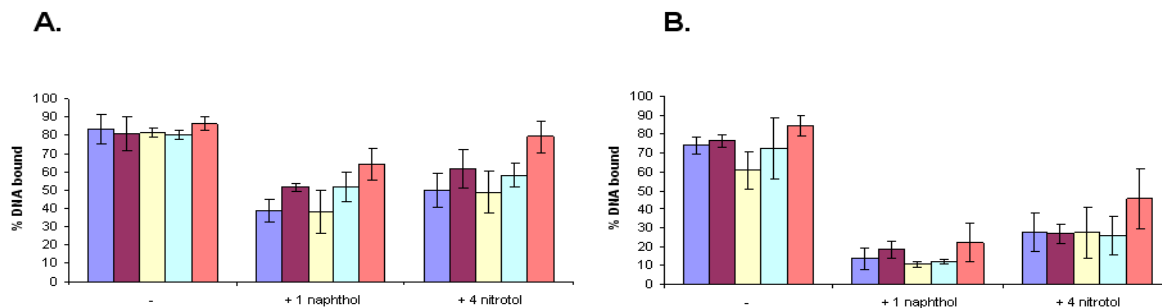
FIG. 4. Effects of TtgV mutant variants on the binding to the *ttgD* and *ttgG* operators. EMSAs were carried out with 1 nM of the indicated operator DEF (panel A) or GHI (panel B) (295-bp fragments) and 50 nM TtgV or its mutants and incubated in the absence (−) or presence of 1 naphthol (1 mM) or 4 nitrotoluene (1 mM). Densitometric analyses were done to determine the amount of shifted DNA with respect to the total DNA. Data are averages for at least three independent assays plus standard errors. TtgV variants were: wild type (dark blue), Q51A (purple), E102A (yellow), E102R (cyan), and V223A (pink).

protein/DNA dissociation. We found that 1-naphthol and 4-nitrotoluene induced the release of TtgV wild-type protein from both *ttgD* and *ttgG* promoters as expected, although the release was more efficient with 1-naphthol, which correlates to the higher level of expression achieved from the *ttgG* promoter when induced with this compound. The addition of 1-naphthol to each of the TtgV mutants in complex with P_{ttgG} was able to efficiently release them from the operator, while release from the P_{ttgD} operator was not as dramatic. It is of interest to note that the inefficient release of TtgVV223A from P_{ttgD} with 32% of the protein remaining bound while less than 10% of the TtgVV223A was bound in the case of *ttgG* promoter. With 4-nitrotoluene the release of TtgV and its mutants was less efficient when bound to either operator (Figure 4). We also found that the TtgVQ51A, TtgVE102R and TtgVV223A mutants were barely released from the *ttgD* promoter with this effector. Since TtgV mutants recognized effector with similar affinities but yielded different levels and patterns of induction than the wild-type protein, the data are consistent with the notion that different effectors exhibit differring efficiencies in their ability to mediate inter- domain signal transmission, and that this signal transmission is influenced by mutations in TtgV.

DISCUSSION

Bacteria are exposed to a wide range of chemicals produced through their own metabolism, as well as those present in the surrounding environment. Some of the endogenously generated chemicals are waste products of cellular metabolism that are exported to the outer medium via a wide series of transporters (Ramos *et al.*, 2002). The TtgGHI and TtgDEF RND pumps preferentially extrude one- and two-ring aromatic compounds such as BTEX, naphthol and others (Rojas *et al.*, 2001). The *P. putida* DOT-T1E TtgDEF efflux pump is chromosomically encoded (Mosqueda and Ramos, 2000), whereas the genes encoding *ttgGHI* are on a self-transmissible plasmid (Rodríguez-Herva *et al.*, 2007). Expression of these pumps is regulated by the concerted action of two repressors of the IclR family of regulators, which are encoded by the chromosomal *ttgT* gene and the plasmid-borne *ttgV* gene (Guazzaroni *et al.* 2004; Rojas *et al.*, 2003; Terán *et al.*, 2007). Our previous studies have shown that TtgV is the main regulator of both efflux pumps *in vivo* (Terán *et al.*, 2007) and hence we have concentrated our efforts in the characterization of the TtgV repressor protein.

DSC data available on multidomain protein show that frequently the individual domains unfold independently in a consecutive manner. Due to those reasons DSC has been used in the past to study the domain arrangement and domain interaction of multidomain proteins (Beldarraín *et al.*, 2001; Ruiz-Arribas *et al.*, 1994; Krell *et al.*, 2003). However, transcriptional regulators which are typically composed of an effector binding domain and a DNA binding domain (Pabo and Sauer, 1992) do not appear to follow this trend since for example the two domain regulators NmrA (Lamb *et al.*, 2003), TetR (Kedracka-Krok and Wasylewski (2003), and Crp (Blaszczyk and Wasylewski, 2003; Won *et al.*, 2008) were found to unfold in a single event. In analogy to these results the thermal unfolding of TtgV is also characterized by a single unfolding event. The tendency of these two-domain transcriptional regulators to have a single unfolding event can be considered a result of the tight functional communication between domains. Our DSC data showed that the binding of 1-naphthol stabilized TtgV denaturation by 8 °C, although denaturation also occurred as a single event (Figure 3), confirming the cooperativity that exists between the domains of TtgV.

Guazzaroni and collaborators (2007) suggested that valine-223, situated in the effector binding domain may be involved in some kind of intramolecular communication in TtgV since this mutant was less efficient than the wild-type protein in its ability to dissociate from DNA in the presence of mono- or bi-aromatic effectors. Later, we found that glutamine 51, located in the DNA binding domain, could also be involved in interdomain communication because the TtgVQ51A mutant

was less efficiently freed from the operator (Fillet *et al*, 2009).

Deficiencies in signal transmission that result in defects in the release of a repressor from its target promoter have been reported in the case of the FapR regulator. Schujman and collaborators (2006) proposed that binding of the malonyl-CoA effector to FapR provoked a disorder-to-order transition of a loop that modified the orientation of α-helix linker that bridges both domains, thus separating the DNA binding domain and the effector binding region. Ligand binding induces modifications that are propagated by the helical linker to the HTH motif, impairing binding to the operator region. In the case of FapR, the high flexibility and the orientation of the α-helix serves as a conector between the malonyl-CoA (effects) domain and the DNA binding site. Mutation in the connecting α-helix that lead to loss of protein flexibility result in FapR mutants being deficient in the DNA binding (Schujman et al., 2006).

We have solved the 3D structure of TtgV and showed that the two domains are linked by an extended α-helix (Lu *et al*., 2010). In the present study we have further characterized mutants in both domains, as well as constructed mutants in residues 98 and 102 that form an ion bridge between glutamic acid and arginine within the extended α-helix. ITC experiments demonstrated that none of these mutations significantly altered effector binding affinity, whether the protein was in solution or bound to DNA. However, EMSA in the presence of effectors showed that certain mutants (TtgVV223A, TtgVQ51A and TtgVE102R), were less efficiently released from the to *ttgD* operator. In terms of protein evolution, this observation is consistent with mutations having primarily an effect on the mechanism of inter-domain communication rather than on the recognition of effectors and the target DNA itself.

Therefore, in TtgV inter-domain communication is a multifactorial process since mutations in any of the three structural parts of TtgV (effector binding domain, DNA binding domain and the linker region) influence of hamper interdomain signal transfer.

Interestingly, we have found that replacement of Glu102 by Arg or Arg98 by Glu caused an uncoupling of the thermal unfolding of the two domains of TtgV. This resulted in opposite effects - while R98E mutant did not bind to DNA, the E102R mutant still was able to bind to target operators and the protein remained functional, as shown by β-galactosidase assays *in vivo* and *in vitro* by EMSA. *In vivo* we also showed that the TtgVE102R protein repressed gene expression from *ttgD* and *ttgG* promoters in the absence of ligands, and that addition of effectors to the culture medium lead to a modest induction as compared to the TtgV wild-type protein. Double mutants that combines a mutation in the linker α-helix with mutations in the effector binding pocket (i.e., V223A/E102R) and the DNA binding domain (i.e., Q51A/E102R) unfolded in two steps. This substantiates the independent nature of the folding of the two domains and the essential role of the interconnecting α-helix in the response to effectors.

Regarding the interconnecting α-helix it is worth to note that helix stability is determined by helix capping and also by the intrinsic propensities of the individual amino acids to form helices. R98 and E102 form a helix cap and its mutation results in the breaking of this helix cap. However among all the 20 natural amino acids alanine is the strongest helix former and has the highest propensity to form α-helices, whereas arginine and glutamate can be considered as helix breaker (Chakrabartty et al., 1994, Baldwin, 2007). Mutants R98A and E102A lead to the rupture of the ion pair, but the mutant unfolds in a single event. This might indicate that although the helix cap is broken, an amino acid replacement with the helix-forming alanine stabilizes the alpha helical conformation of the linker. In contrast replacement of R98 and E102 with E and R, respectively, firstly break the helix cap and the introduced amino acid is considered as helix breaker which most likely results in an at least partial loss of the helical conformation of the linker, which is likely to cause the altered unfolding behavior. This interpretation is also supported by cd measurements: the TtgVE102A mutant has 3 % more alpha helix than the TtgVE102R mutant.

In summary, this study presents relevant new results for the IclR family of regulators, showing that the two domains of TtgV are tightly associated but can be uncoupled via mutations in the α-helix that link them. Furthermore, this uncoupling does not necessarily result in loss of function but leads to differential responses to ligand as deduced from *in vitro* and *in vivo* data, illustrating the importance of intra-molecular domain cross-talk to TtgV function.

REFERENCES

Abril MA, Michán C, Timmis KN, Ramos JL (1989) Regulator and enzyme specificities of the TOL plasmid-encoded upper pathway for degradation of aromatic hydrocarbons and expansion of the substrate range of the pathway. *J Bacteriol* 171:6782-6790.

Baldwin RL (2007) Energetics of protein folding. *J Mol Biol* 371:283-301.

Beldarraín A, Lopez-Lacomba JL, Kutyshenko VP, Serrano R, Cortijo M (2001) Multidomain structure of a recombinant strptokinase. A differentia lscanning calorimetry study. *J Protein Chem* 20:9-17.

Bernal P, Segura A, Ramos JL (2007) Compensatory role of the *cis-trans*-isomerase and cardiolipin synthase in the membrane fluidity of *Pseudomonas putida* DOT-T1E. *Environ Microbiol* 9:1658-1664.

Bkaszczyk U, Wasylewski Z (2003) Interaction of cAMP receptor protein from *Escherichia coli* with cAMP and DNA studied by differential scanning calorimetry. *J Protein Chem* 22:285-293.

Chakrabartty A, Kortemme T, Baldwin RL (1994) Helix propensities of the amino acids measured in alanine-based peptides without helix-stabilizing side-chain interactions. *Protein Sci* 3:843-852f.

Daniels C, Daddaoua A, Lu D, Zhang X, Ramos JL (2010) Domain cross-talk during effector binding to the multidrug binding TtgR regulator. *J Biol Chem* doi/10.1074/jbc.M110.113282.

De Smet MJ, Kingma J, Witholt B (1978) The effect of toluene on the structure and permeability of the outer and cytoplasmic membranes of *Escherichia coli*. *Biochim Biophys Acta* 506:64-80

Domínguez-Cuevas P, González-Pastor JE, Marqués S, Ramos JL, de Lorenzo V (2006) Transcriptional tradeoff between metabolic and stress-response programs in *Pseudomonas putida* KT2440 cells exposed to toluene. *J Biol Chem* 281:11981-11991.

Duque E, Segura A, Mosqueda G, Ramos JL (2001) Global and cognate regulators control the expression of the organic solvent efflux pumps TtgABC and TtgDEF of *Pseudomonas putida*. *Mol Microbiol* 39:1100-1106.

Endo, R, Ohtsubo, Y, Tsuda, M, and Nagata, Y (2007) Identification and characterization of genes encoding a putative ABC-type transporter essential for utilization of γ-hexachlorocyclohexane in *Sphingomonas japonicum* UT26. *J Bacteriol* 189:3712-3720

Fillet S, Vélez M, Lu D, Zhang X, Gallegos MT, Ramos JL (2009) TtgV represses two different promoters by recognizing different sequences. *J Bacteriol* 191:1901-1909.

Ge Q, Yamada Y, Zgurskaya H (2009) The C-terminal domain of AcrA is essential for the assembly and function of the multidrug efflux pump AcrAB-TolC. *J Bacteriol* 191:4365-4371.

García V, Godoy P, Daniels C, Hurtado A, Ramos JL, Segura A (2009) New transporters involved in stress tolerance in *Pseudomonas putida* DOT-T1E: from proteomic and transcriptomic data to functional analysis. Environ. *Microbiol Reports* doi:10.1111/j1758-222-9 00092.

Guazzaroni ME, Gallegos MT, Ramos JL, Krell T (2007) Different modes of binding of mono- and bioaromatic effectors to the transcriptional regulator TtgV. Role in differential derepression from its cognate operator. *J Biol Chem* 282:16308-16316.

Guazzaroni ME, Krell T, Felipe A, Ruiz R, Meng C, Zhang X, Gallegos MT, Ramos JL (2005) The multidrug efflux regulator TtgV recognizes a wide range of structurally different effectors in solution and complexed with target DNA: evidence from isothermal titration calorimetry. *J Biol Chem* 280:20887-20893.

Guazzaroni ME, Krell T, Gutierrez del Arroyo P, Vélez M, Jiménez M, Rivas G, Ramos JL (2007) The transcriptional repressor TtgV recognizes a complex operator as a tetramer and induces convex DNA bending. *J Mol Biol* 369:927-939.

Guazzaroni ME, Terán W, Zhang X, Gallegos MT, Ramos JL (2004) TtgV bound to a complex operator site represses transcription of the promoter for the multidrug and solvent extrusion TtgGHI pump. *J Bacteriol* 186:2921-2927.

Inoue A, Horikoshi K (1989) A *Pseudomonas* thrives in high concentrations of toluene. *Nature* 338: 264−266.

Isken S, de Bont JAM (1996) Active efflux of toluene in a solvent-resistant bacterium. *J Bacteriol* 178:6056-6058.

Junker F, Ramos JL (1999) Involvement of the *cis/trans* isomerase Cti in solvent resistance of *Pseudomonas putida* DOT-T1E. *J Bacteriol* 181:5693-700.

Kedracka-Krok S, Wasylewski Z (2003) A differential scanning calorimetry study of tetracycline repressor. *Eur J Biochem* 270:4564-4573

Kieboom J, de Bont JAM (2001) Identification and molecular characterization of an efflux system involved in *Pseudomonas putida* S12 multidrug

resistance. *Microbiology* 147:43-51

Kieboom J, Dennis JJ, Zylstra GJ, de Bont JAM (1998) Active efflux of organic solvents by *Pseudomonas putida* S12 is induced by solvents. *J Bacteriol* 180:6769-6772

Kim K, Lee S, Lee K, Lim D (1998) Isolation and characterization of toluene-sensitive mutants from the toluene-resistant bacterium *Pseudomonas putida* GM73. *J Bacteriol* 180:3692-3696

Koronakis V, Sharff A, Koronakis E, Luisi B, Hughes C (2000) Crystal structure of the bacterial membrane protein TolC central to multidrug efflux and protein export. *Nature* 405:914-919.

Krell T, Molina-Henares AJ, Ramos JL (2006) The IclR family of transcriptional activators and repressors can be defined by a single profile. *Protein Science* 15:1207-1213.

Krell T, Renauld-Mongénie G, Nicolaï MC, Fraysse S, Chevalier M, Bérard Y, Oakhill J, Evans RW, Gorringe A, Lissolo L (2003) Insight into the structure and function of the transferrin receptor from Neisseria meningitidis using microcalorimetric techniques. *J Biol Chem* 278:14712-14722.

Lamb HK, Leslie K, Dodds AL, Nutley M, Cooper A, Johnson C, Thompson P, Stammers DK, Hawkins AR (2003) The negative transcriptional regulator NmrA discriminates between oxidized and reduced dinucleotides. *J Biol Chem* 278:32107-32114.

Lu D, Fillet S, Meng C, Alguel Y. Kloppsteck P, Bergeron J, Krell T, Gallegos MT, Ramos JL, Zhang X. (2010) Crystal structures of tetrameric TtgV in complex with DNA reveal a novel cooperative binding and induction mechanism. *Cell* Submited.

Molina-Henares AJ, Godoy P, Duque E, Ramos JL (2009) A general profile for the MerR family of transcriptional regulators constructed based on the semi-automated Provalidator tool. *Environ Microbiol Reports* 1:518-523.

Molina-Henares AJ, Krell T, Guazzaroni ME, Segura A, Ramos JL (2006) Members of the IclR family of bacterial transcriptional regulators function as activators and/or repressors. *FEMS Microbiol Rev* 20:157-186.

Mosqueda G, Ramos JL (2000) A set of genes encoding a second toluene efflux system in *Pseudomonas putida* DOT-T1E is linked to the tod genes for toluene metabolism. *J Bacteriol* 182:937-943.

Murakami S, Nakashima R, Yamashita E, Yamaguchi A (2002) Crystal structure of bacterial multidrug efflux transporter AcrB. *Nature* 419:587-593.

Nikaido H, Takatsuka Y (2009) Mechanisms of RND multidrug efflux pumps. *Biochim Biophys Acta* 1794:769-781.

Pabo CO, Sauer RT (1992) Transcription factors: structural families and principles of DNA recognition. Ann Rev Biochem 61:1053-1095.

Pérez-Rueda E, Collado-Vides J (2000) The repertoire of DNA-binding transcriptional regulators in *Escherichia coli* K-12. *Nucl Acids Res* 28:1838-1847.

Ramos JL, Duque E, Gallegos MT, Godoy P, Ramos-González MI, Rojas A, Terán W, Segura A (2002) Mechanisms of solvent tolerance in gram-negative bacteria. *Ann Rev Microbiol* 56:743-768.

Ramos JL, Duque E, Godoy P, Segura A (1998) Efflux pumps involved in toluene tolerance in *Pseudomonas putida* DOT-T1E. *J Bacteriol* 180:3323-3329.

Ramos JL, Duque E, Huertas M-J, Haïdour A (1995) Isolation and expansion of the catabolic potential of a *Pseudomonas putida* strain able to grow in the presence of high concentrations of aromatic hydrocarbons. *J Bacteriol* 177:3911-3916.

Rodríguez-Herva JJ, García V, Hurtado A, Segura A, Ramos JL (2007) The *ttgGHI* solvent efflux pump operon of *Pseudomonas putida* DOT-T1E is located on a large self-transmissible plasmid. *Environ Microbiol* 9:1550-1561.

Rojas A, Duque E, Mosqueda G, Golden G, Hurtado A, Ramos JL, Segura A (2001) Three efflux pumps are required to provide efficient tolerance to toluene in *Pseudomonas putida* DOT-T1E. *J Bacteriol* 183:3967-3973.

Rojas A, Segura A, Guazzaroni ME, Terán W, Hurtado A, Gallegos MT, Ramos JL (2003) *In vivo* and *in vitro* evidence that TtgV is the specific regulator of the TtgGHI multidrug and solvent efflux pump of *Pseudomonas putida*. *J Bacteriol* 185:4755-4763.

Ruiz-Arribas A, Santamaria RI, Zhadan GG, Villar E, Shnyrov VL /1994) Differential scanning calorimetric study of the thermal stability of xylanase from Streptomyces halstedii JM8. *Biochemistry* 33:13787-13791.

Schujman GE, Guerin M, Buschiazzo A, Schaeffer F, Llarrull L, Reh G, Vila AJ, Alzari PM, de Mendoza D (2006) Structural basis of lipid biosynthesis regulation in Gram-positive bacteria. *EMBO J* 25:4074-4083.

Segura A, Godoy P, van Dillewijn P, Hurtado A, Arroyo N, Santacruz S, Ramos JL (2005) Proteomic analysis reveals the participation of energy- and stress-related proteins in the response of *Pseudomonas putida* DOT-T1E to toluene. *J Bacteriol* 187:5937-5945.

Segura A, Rojas A, Hurtado A, Huertas MJ, Ramos JL (2003) Comparative genomic analysis of solvent extrusion pumps in *Pseudomonas* strains exhibiting different degrees of solvent tolerance. *Extremophiles* 7:371-376.

Spaink HP, Okker JJH, Wijffelman CA, Pees E, Lugtenberg BJJ (1987) Promoters in the nodulation region of the *Rhizobium leguminosarum* Sym plasmid pRL1JL. *Plant Mol Biol* 9:27-39.

Takatsuka Y, Nikaido H (2007) Site-directed disulfide cross-linking shows that cleft flexibility in the periplasmic domain is needed for the multidrug efflux pump AcrB of *Escherichia coli*. *J Bacteriol* 189:8677-8684.

Terán W, Felipe A, Fillet S, Guazzaroni ME, Krell T, Ruiz R, Ramos JL, Gallegos MT. (2007) Complexity in efflux pump control: cross-regulation by the paralogues TtgV and TtgT. *Mol Microbiol* 66:1416-1428.

Tikhonova EB, Dastidar V, Rybenkov VV, Zgurskaya HI (2009) Kinetic control of TolC recruitment by multidrug efflux complexes. *Proc Natl Acad Sci USA* 106:16416-16421

Wery J, Hidayat B, Kieboom J, de Bont JAM (2001) An insertion sequence prepares *Pseudomonas putida* S12 for severe solvent stress. *J Biol Chem* 276:5700-5706

Wiseman T, Williston S, Brandts JF, Lin LN (1989) Rapid measurement of binding constants and heats of binding using a new titration calorimeter. *Anal Biochem* 179:131-137.

Won HS, Seo MD, Ko HS, Choi WS, Lee BJ (2008) Thermal denaturation of the apocyclic AMP receptor protein and noncovalent interactions beween its domains. *Mol Cells* 26:61-66.

Woodcocke DM, Crowther PJ, Doherty J, Jefferson S. DeCruz E, Noyer-Weidner M, Smith SS, Michael MZ, Graham MW (1989) Quantitative evaluation of *Escherichia coli* host strains for tolerance to cytosine methylation in plasmid and phage recombinants. *Nucleic Acids Res* 17:3469-3478.

Yu EW, McDermott G, Zgurskaya HI, Nikaido H, Koshland DE Jr (2003) Structural basis of multiple drug-binding capacity of the AcrB multidrug efflux pump. *Science* 300:976-980.

Zgurskaya HI, Nikaido H (1999) AcrA is a highly asymmetric protein capable of spanning the periplasm. *J Mol Biol* 285:409-420.

Zhang RG, Kim Y, Skarina T, Beasley S, Laskowski R, Arrowsmith C, Edwards A, Joachimiak A, Savchenko A (2002) Crystal structure of *Thermotoga maritima* 0065, a member of the IclR transcriptional factor family. *Proc Natl Acad Sci USA* 99:4638-4643.

Strains and plasmids	Characteristics	Relevant source or references
P. putida DOT-T1E	Rif[r], Tol[r]	Ramos *et al.*, 1995
P. putida DOT-T1EVT	Rif[r] Km[r] Tel[r] *ttgV*::Km *ttgT::kilA/telAB*, Tol[r]	Terán *et al.*, 2007
E. coli BL21 (DE3)	F[-], *ompI hsdS_B (r⁻ _B m⁻ _B) gal dem met*	Novagen
E. coli DH5α	*supE44* Δ(*lacZYA-argF*) *U169 deoR* (φ80*lacZ* Δ*M15*) *hsdR17*(r_K⁻ m_K⁻) *recA1 endA1 gyrA* (Nal[r]) *thi-1 relA1* Δ(*lacIZY* Δ-*argF*)	Woodcock *et al.*, 1989
pMP220	Tc[r], promoterless *lacZ* expression vector	Spaink *et al.*, 1987
pMPD1	Tc[r], *ttgD* promoter cloned in pMP220	Terán *et al.*, 2007
pANA96	Tc[r], *ttgG* promoter cloned in pMP220	Rojas *et al.*, 2001
pT1-B6	Ap[r], pUC18 bearing an 8-kb BamHI fragment with *ttgDEF* and *ttgT*	Rojas *et al.*, 2001
pGG1	Ap[r], pUC18 bearing an 8-kb BamHI fragment with *ttgGHI* and *ttgVW*	Rojas *et al.*, 2001
pANA126	Km[r], pET28b(+) derivative vector used to produce His_6-TtgV	Rojas *et al.*, 2001
pET28b(+)	Km[r], protein expression vector	Novagen
pET28b(+)::Q51A	Km[r], pET28b(+) derivative used to produce TtgVQ51A	Fillet *et al.*, 2009
pET28b(+)::E102A	Km[r], pET28b(+) derivative used to produce TtgVE102A	this work
pET28b(+)::E102D	Km[r], pET28b(+) derivative used to produce TtgVE102D	this work
pET28b(+)::E102R	Km[r], pET28b(+) derivative used to produce TtgVE102R	this work
pET28b(+)::V223A	Km[r], pET28b(+) derivative used to produce TtgVV223A	Guazzaroni *et al.*, 2007
pET28b(+)::Q51A/E102R	Km[r], pET28(+) derivative used to produce TtgVQ51A/E102R	this work
pET28b(+)::V223A/E102R	Km[r], pET28b(+) derivative used produce TtgVV223A/E102R	this work
pET28b(+)::Q51A/E102R/V223A	Km[r], pET28b(+) derivative used to produce TtgVQ51A/E102R/V223A	this work
pBBRN	pBBR-MCS5 derivative with an additional NdeI restriction site	Fillet *et al.*, 2009
pBBRN::TtgV	Gm[r]; pBBRN derivative vector expressing TtgV	Fillet *et al.*, 2009
pBBRN::Q51A	Gm[r]; pBBRN derivative vector expressing TtgVQ51A	Fillet *et al.*, 2009
pBBRN::E102R	Gm[r]; pBBRN derivative vector expressing TtgVE102R	this work
pBBRN::V223A	Gm[r]; pBBRN derivative vector expressing TtgVV223A	this work

Ap[r], Cm[r], Km[r], Tc[r],Tel[r], Rif[r], Tol[r] correspond to resistance to ampicillin, chloramphenicol, kanamycin, tetracycline, tellurite, rifampicin, and toluene, respectively.
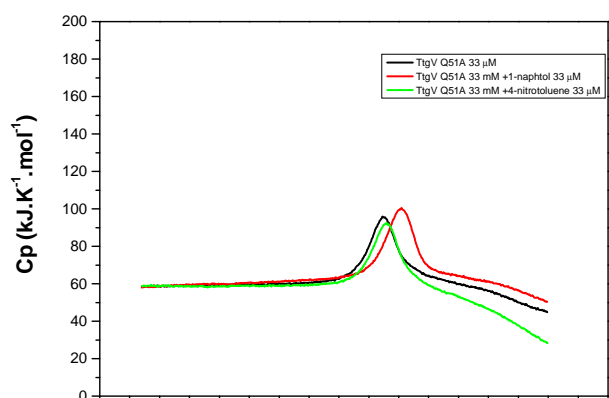
Suppl FIG. 1. Effect of 1-naphthol and 4-nitrotoluene on the thermal unfolding of TtgV. The assays were done in 20 mM Pipes, 8 mM magnesium acetate, 150 mM KCl, 1 mM TCEP pH 7.2. The protein concentration was 30 μM for all experiments.
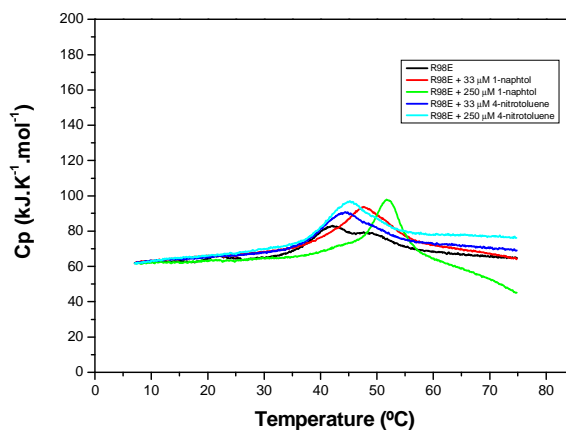
Suppl. FIG. 2. DSC with mutant TtgVR98E proteins. Temperature-dependence of the apparent heat capacity of R98E in 20 mM Pipes, 8 mM magnesium acetate, 150 mM KCl, 1 mM TCEP pH 7.2. The protein concentration was 33 μM for all assays and the concentration of 1-naphthol or 4-nitrotoluene is indicated.

Supplementary Table 1
Table representing the α-helical content of WT and TtgV mutants.

	% α-helix content
WT TtgV	31.0
TtgV Q51A	31.5
TtgVR98E	27.7
TtgVE102A	27.1
TtgV E102R	24.3
TtgV V223A	29.0
TtgVQ51A/E102R	23.6
TtgVQ51A/E102R/V223A	27.3
TtgV E102R/V223A	25.5

Discussion

Pseudomonas putida DOT-T1E was isolated in 1995 by the scientific personnel at the Department of Environmental Protection in Granada. This strain became a model organism in solvent tolerance because of its ability to grow in presence of high concentrations of solvents (Huertas *et al,* 1998; Ramos *et al,* 1998). Studies of the of *Pseudomonas putida* DOT-T1E genome has allowed the identification of three efflux pumps TtgABC, TtgDEF and TtgGHI (Rojas *et al.*, 2001; Segura *et al.,* in preparation) as the main components of solvent tolerance in *P. putida* DOT-T1E (Segura *et al.*, 2003). From a quantitative point of view, TtgGHI plays the major role in solvent removal. The simple presence of this pump in several *P. putida* strains confers high resistance to toluene and other aromatic compounds (Rodríguez-Herva *et al.*, 2007). Despite the high basal expression level of the *ttgGHI* operon, exposure to aromatic compounds increases dramatically its transcription rate. The TtgV repressor modulates the expression of this efflux pump and is released from its cognate operator in the presence of effectors leading to a higher level of transcription.

Along my PhD work, our genetic and physiological data have shown that TtgV is not only the regulator of the TtgGHI efflux pump; it is also the key repressor of the *ttgDEF* operon (Terán *et al.,* 2007). The *ttgDEF/ttgT* system is encoded on the *P. putida* DOT-T1E chromosome and plays a role in resistance to solvents. This was particularly seen in a TtgGHI pump deficient background (Mosqueda and Ramos, 1999). Surprisingly, *ttgGHI* and *ttgV* are borne on the pGRT1 megaplasmid (Rodríguez-Herva, *et al.,* 2007), whereas *ttgDEF* is chromosomally-encoded. Footprint assays have demonstrated that TtgV and TtgT bind to the same *ttgT-ttgDEF* and *ttgV-ttgGHI* intergenic regions, showing a clear cross-regulation by the paralogues, and even between both efflux pumps (Terán *et al.,* 2007). These data reported in the *Mol. Microbiol.* by our group (Terán et al., 2007) represented the first example of a new way of efflux pumps control. As with a large number of transcriptional repressors, TtgV and TtgT control gene expression through the physical occlusion of the RNA polymerase (Rojo *et al.,* 2001; Teràn *et al.,* 2003; Yamamoto and Ishihama, 2003, Molina-Henares *et al.*, 2006). When TtgV binds its effectors, a series of conformational changes occur in the regulator leading to the release of the repressor from the target DNA.

TtgV is able to bind a wide range of aromatic compounds and consequently *P. putida* DOT-T1E can survive in the presence of many different toxic chemicals (Guazzaroni *et al.,* 2004 and 2005). As other members of the IclR family, like AllR (Walker *et al.,* 2006) or IclR (Yamamoto and Ishihama, 2003), TtgV presents a ligand binding site in its C-terminal domain. The structure of the C-terminal domain of AllR has allowed us to identify potential amino acids involved in binding to effectors (Walker *et al.*, 2006). Guazzaroni and

collaborators generated mutants in the putative effector binding pocket of TtgV and found that TtgV binds one- or two-ring aromatic compounds with high affinity (µM range, see Guazzaroni *et al.,* 2007a). It was also surprising to see that the regions corresponding to the effector binding pockets were relatively similar, which is probably why Molina-Henares *et al*. (2006) identified this region as part of the motif that defines the IclR family of regulators.

In my thesis, I have initially focused on the characterization of TtgV binding to its DNA targets. TtgV binds DNA thanks to a wing Helix-Turn-Helix (wHTH) motif (Krell *et al.,* 2006). The second helix is known to be involved in the direct recognition of the DNA sequence. Mutations in each amino acid of this α-helix enabled us to identify four amino acids: R47, T49, R52, and L57 as responsible for the direct interaction with nucleotic acids on both promoters (Fillet *et al.,* 2009). The R47 residue is highly conserved within the IclR family. These data were confirmed with the resolution of the crystal structure of TtgV that identified a residue outside the recognition helix and that we overlooked in our bioinformatics analysis. This residue corresponded to Serine 35 (Lu *et al*., in preparation). We then generated mutants at residue 35 and found that replacement of serine by alanine resulted in a mutant that was also defective in DNA binding. We deduced from the protein/DNA co-crystals, that the extensive interactions between TtgV and DNA induced significant distortion within the DNA major groove resulting in a ~ 90° overall bend (Lu *et al*., in preparation). Mobility shift assays revealed that the binding to the *ttgGHI* operator required a perfect conservation of the DNA sequence, whereas only the central part of the target sequence was critical for the binding of *ttgDEF* operator (Fillet *et al.,* 2009). Interestingly, the greater homology between the two promoters is located exactly in the middle of the 42 pb of the target sequence, corresponding to the critical region for the two promoters (Fillet *et al.,* 2009). This set of data support that TtgV exhibits a large degree of flexibility in interactions with both intergenic regions.

The TtgV crystal structure, free and bound to its DNA operator in *ttgGHI,* added value to our genetic data and, together with our biochemical and biophysical studies, has allowed us a better understanding of the TtgV mechanism of action. We deduced that the regulator requires communication between its two domains. TtgV is a tetramer in solution (Guazzaroni *et al.,* 2007b; Lu *et al.,* in preparation), which takes the form of a symmetric diamond thanks to its C- terminal domains. When TtgV is bound to the DNA, we observed a large rearrangement of the tetramer in two asymmetric dimers (Lu *et al*., in preparation). We identified the amino acids crucial for the success of this drastic re-organisation, as I136, and a loop that comprised residues 129 to 131 (Lu *et al*., in preparation). When comparing the TtgV structure free in solution with the structure of TtgV in complex with DNA, we observed a clear break in the long α-helix that connects the DNA binding domain with the ligand binding domain (Figure 1A). This break is exactly located at residue Q86 (Lu *et al*., in preparation). The two domains in each monomer of TtgV exhibit very few interactions and we hypothesized that the α4 helix linker could be the communicating element between the TtgV domains. To confirm this hypothesis, we decided to construct mutants in two amino acids in this helix, namely E102R and R98E. When we studied the thermal unfolding of TtgV we found that the regulator was unfolded in one event. Interestingly, this cooperative

phenomenon can be uncoupled via mutations in the connecting α-helix (Figure 1B) (Fillet *et al.,* in preparation). Moreover, *in vivo* studies demonstrated that the E102mutant is unable to release the DNA promoter in presence of the effector, resulting in strong repression of the promoter (Fillet *et al.,* in preparation). *In vitro* and *in vivo* data strongly suggest the importance of intra-molecular domain cross-talk to TtgV function.

   Data obtained in this thesis, not only provide relevant information on TtgV, but also adds solid grounds to understand how proteins of the IclR family work in general terms, and also provides new information to understand the mechanism of action of a large number of tetrameric gene regulators.

A.   B.

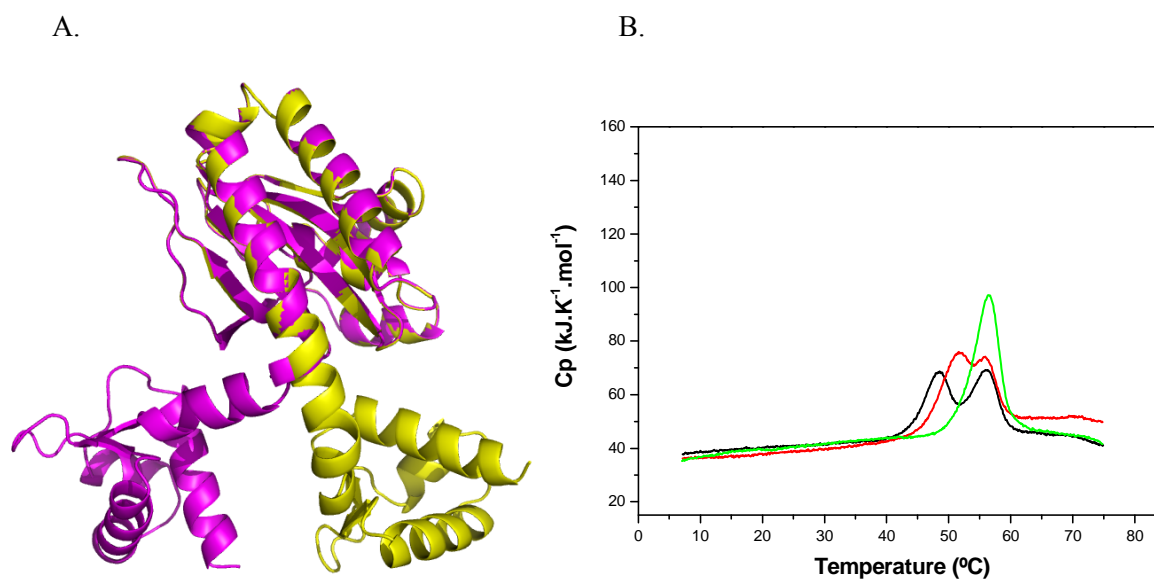**Figure 1. A, superpose of DNA binding domain,** yellow represents TtgV and magenta represents the TtgV/DNA complex (see for details Lu *et al.,* in preparation). **B, Effect of 1-naphthol on the thermal unfolding of TtgVE102R.** The DSC experiments of the TtgV mutants were done without effector (black line) and in the presence of 33 μM (red) and 250 μM (green) 1-naphthol (for details see Fillet *et al.,* in preparation).

1. From a quantitative point of view TtgGHI is the main efflux pump for solvent tolerance in *P. putida* DOT-T1E. Expression of this operon is regulated by TtgV. The *ttgGHI* and *ttgV* genes are borne on the pGRT1 plasmid, but TtgV also controls expression of the chromosomally-encoded TtgDEF efflux system. Adjacent to the *ttgDEF* operon lays a gene encoding a regulator of the IclR family and which shares 63 % sequence identity with TtgV. This regulator is called TtgT.

2. TtgV and TtgT bind the same operators at the *ttgDEF* and *ttgGHI* promoters. However, *in vivo*, TtgV is the dominant repressor of both operons and the regulatory activity of TtgT is only detectable in a TtgV-deficient background.

3. TtgV and TtgT are multidrug-binding regulators that recognize a wide range of aromatic compounds. However, TtgV and TtgT do not exhibit the same effector profile, which results in a wider repertoire of responses to solvents.

4. Effector binding to TtgV or TtgT complexed to target operators leads to the release of the repressor from the promoters.

5. The HTH DNA-binding domain of TtgV and TtgT are almost identical, but residue 44 is different, i.e. aspartic acid in TtgT instead of leucine in TtgV. TtgV has higher affinity than TtgT for the *ttgGHI* operator, which suggests that residue 44 could be partly, responsible for the difference in binding affinity to target DNA.

6. Four amino acids located in the recognition helix of TtgV are decisive for its binding to the *ttgDEF* and *ttgGHI* operators, namely R47, T49, R52, and L57. The replacement of these residues by alanine resulted in mutants defective in DNA binding.

7. TtgV establishes different contacts in each of its two operators. Six amino acids, S48, V50, I53, I54, E60 and F61, are relevant for binding to the *ttgGHI* operator, but are not essential for *ttgDEF* recognition.

8. The operator region at *ttgG* and *ttgD* promoters is made up of 42 bp. Base composition of operator sequences is important for TtgV recognition. While the regulator needs a palindromic central sequence for most favourable binding, the sequences at the ends of the operator are more permissible.

9. The 3D structure of TtgV revealed that it is a tetramer and that each monomer is made up of two distinctive domains: an N-terminal domain responsible for DNA binding, and a C-terminal domain that contains the ligand binding site. Both domains are linked by a long α helix (helix α4). No apparent interactions between the different domains within each monomer were found. The linker helix plays a role in the contacts between monomers and serves to stabilize a dimer. TtgV can be defined as a dimer of dimers organized in a symmetric diamond. Adjacent dimers interact with each others through two loops that are only a a few amino acids long and which act as crossing hands.

10. The thermal unfolding of free TtgV or in complex with 1-naphthol, one of its effectors, is characterized by a single event; although binding of 1-naphthol stabilizes TtgV by 8°.

11. Amino acids R98 and E102 located in the extended helix linker α4 form an ion bridge. Mutation of either one of these two amino acids leads to the unfolding of the protein in two events, indicating the loss of cooperativity between the TtgV domains.

12. The structure of TtgV in complex with its 42 pb *ttgG* operator showed that TtgV self reorganizes in a complex structure characterized by a break in the long helix α4. This drastic rearrangement leads to a change in the orientation of the ligand binding domain with respect to the DNA binding domain.

13. The extensive interactions between TtgV and DNA induce significant distortions in the DNA and provoke a of 90ºDNA bend. The tetrameric interface between the β-strands formed by the ligand binding domain is important for the maintenance of the tetramer conformation when it is bound to DNA.

Bibliography

Akama H., Matsumura T., Kashiwagi S., Yoneyama H., Narita S., Tsukihara T., Nakagawa A., Nakae T. 2004. Crystal structure of the membrane fusion protein, MexA, of the multidrug transporter in *Pseudomonas aeruginosa. J Biol Chem* 279: 25939-25942.

Alekshun M.N., Levy S.B., Mealy T.R., Seaton B.A., Head J.F. 2001. The crystal structure of MarR, a regulator of multiple antibiotic resistance, at 2.3 A resolution. *Nat Struct Biol* 8: 710-714.

Alguel Y., Meng C., Terán W., Krell T., Ramos J.L., Gallegos M.T., Zhang X. 2007. Crystal structures of multidrug binding protein TtgR in complex with antibiotics and plant antimicrobials. *J Mol Biol* 369: 829-840.

Aono R., Ito M., Inoue A., Horikoshi H. 1992. Isolation of a novel toluene-tolerant strain of *Pseudomonas aeruginosa. Biosci Biotechnol Biochem* 1:145-146.

Aono R. 1998. Improvement of organic solvent tolerance level of *Escherichia coli* by overexpression of stress-responsive genes. *Extremophiles* 2: 239-248.

Arias-Barrau E., Olivera E.R., Luengo J.M., Fernández C., Galán B., García J.L., Díaz E., Miñambres B. 2004. The homogentisate pathway: a central catabolic pathway involved in the degradation of *L*-phenylalanine, *L*-tyrosine, and 3-hydroxyphenylacetate in *Pseudomonas putida*. *J Bacteriol* 186: 5062-5077.

Brown M.H., Skurray R.A. 2001. Staphylococcal multidrug efflux protein QacA. *J Mol Microbiol Biotechnol* 3: 163-170.

Bernal P., Muñoz-Rojas J., Hurtado A., Ramos J.L., Segura A. 2007a. A *Pseudomonas putida* cardiolipin synthase mutant exhibits increased sensitivity to drugs related to transport functionality. *Environ Microbiol* 9: 1135-1145.

Bernal P., Segura A., Ramos J.L. 2007b. Compensatory role of the *cis-trans*-isomerase and cadiolipin synthase in the membrane fluidity of *Pseudomonas putida* DOT-T1E. *Environ Microbiol* 9: 1658-1664.

Chen Y.J., Pornillos O., Lieu S., Ma C., Chen AP., Chang G. 2007. X-ray structure of EmrE supports dual topology model. *Proc Natl Acad Sci USA* 104: 18999-19004.

Costerton J.W., Stewart P.S., Greenberg E.P. 1999. Bacterial biofilms: a common cause of persistent infections. *Science* 284: 1318-1322.

Cruden D.L., Wolfram J.H., Rogers R.D., Gibson D.T. 1992. Physiological properties of a *Pseudomonas* strain which grows with *p*-xylene in a two-phase (organic-aqueous) medium. *Appl Environ Microbiol* 58: 2723-2729.

Daniels C., Daddaoua A., Lu D., Zhang X., Ramos J.L. 2010. Domain cross-talk during effector binding to the multidrug binding TtgR regulator. *J Biol Chem* In press.

Daniels C., Michán C., Krell T., Roca A., Ramos J.L. 2009. The heat, drugs and knockout systems of *Microbial Biotechnonolgy*. *Microbial Biotechnology* 2: 598-600.

De Smet M.J., Kingma J., Witholt B. 1978. The effect of toluene on the structure and permeability of the outer and cytoplasmic membranes of *Escherichia coli*. *Biochim Biophys Acta* 506: 64-80

DiMarco A.A., Averhoff B.A., Kim E.E., Ornston L.N. 1993. Evolutionary divergence of *pobA*, the structural gene encoding *p*-hydroxybenzoate hydroxylase in an *Acinetobacter calcoaceticus* strain well-suited for genetic analysis. *Gene* 125: 25-33.
DiMarco A.A., Ornston L.N. 1994. Regulation of p-hydroxybenzoate hydroxylase synthesis by PobR bound to an operator in *Acinetobacter calcoaceticus*. *J Bacteriol* 176: 4277-4284.

Domínguez-Cuevas P., Gonzáles-Pastor J.E., Marqués S., Ramos J.L., de Lorenzo V. 2006. Transcriptional tradeoff between metabolic and stress-response programs in *Pseudomonas putida* KT2440 cells exposed to toluene. *J Biol Chem* 281: 11981-11991.

Duque E., Segura A., Mosqueda G., Ramos J.L. 2001. Global and cognate regulators control the expression of the organic solvent efflux pumps TtgABC and TtgDEF of *Pseudomonas putida*. *Mol Microbiol* 39: 1100-1106.

Espinosa-Urgel M., Kolter R., Ramos J.L. 2002. Root colonization by *Pseudomonas putida*: love at first sight. *Microbiology* 148: 341-343.

Eswaran J., Koronakis E., Higgins M.K., Hughes C., Koronakis V. 2004. Three's company: component structures bring a closer view of tripartite drug efflux pumps. *Curr Opin Struct Biol* 14: 741-747.

Gerischer U., Segura A., Ornston L.N. 1998. PcaU, a transcriptional activator of genes for protocatechuate utilization in *Acinetobacter*. *J Bacteriol* 180: 1512-1524.

Gibson, D.T., and Subramanian, V. 1984. Microbial degradation of aromatic hydrocarbons. In : Gibson D. T. (ed). Microbial degradation of organic compounds (pp 361-369) Marcel Dekker. New York.

Grkovic S., Brown M.H., Skurray R.A. 2001. Transcriptional regulation of multidrug efflux pumps in bacteria. *Semin Cell Dev Biol* 12: 225-37.

Grogan D.W., Cronan J.E. 1997. Cyclopropane ring formation in membrane lipids of bacteria. *Microbiol Mol Biol Rev* 61: 429-441.

Guazzaroni M.E., Terán W., Zhang X., Gallegos M.T., Ramos J.L. 2004. TtgV bound to a complex operator site represses transcription of the promoter for the multidrug and solvent extrusion TtgGHI pump. *J Bacteriol* 186: 2921-2927.

Guazzaroni M.E., Krell T., Felipe A., Ruiz R., Meng C., Zhang X., Gallegos M.T., Ramos J.L. 2005. The multidrug efflux regulator TtgV recognizes a wide range of structurally different effectors in solution and complexed with target DNA: evidence from isothermal titration calorimetry. *J Biol Chem* 280: 20887-20893.

Guazzaroni M.E., Gallegos M.T., Ramos J.L., Krell T. 2007a. Different modes of binding of mono- and biaromatic effectors to the transcriptional regulator TtgV: role in differential derepression from its cognate operator. *J Biol Chem* 282: 16308-16316.

Guazzaroni M.E., Krell T., Gutiérrez del Arroyo P., Vélez M., Jiménez M., Rivas G., Ramos J.L. 2007b. The transcriptional repressor TtgV recognizes a complex operator as a tetramer and induces convex DNA bending. *J Mol Biol* 369: 927-939.

Heipieper H.J., Diefenbach R., Keweloh H. 1992. Conversion of *cis* unsaturated fatty acids to *trans*, a possible mechanism for the protection of phenol-degrading *Pseudomonas putida* P8 from substrate toxicity. *App Environ Microbiol* 58: 1847-1852.

Higgins M.K., Bokma E., Koronakis E., Hughes C., Koronakis V. 2004. Structure of the periplasmic component of a bacterial drug efflux pump. *Proc Natl Acad Sci U S A* 101: 9994-9999.

Hobman J.L. **2007.** MerR family transcription activators: similar designs, different specificities. *Mol Microbiol* 63: 1275-1278.

Huertas M.J., Duque E., Marques S., Ramos J.L. 1998. Survival in soil of different toluene-degrading *Pseudomonas* strains after solvent shock. *Appl Environ Microbiol* 64: 38-42.

Isken S., de Bont J.A. 1996. Active efflux of toluene in a solvent-resistant bacterium. *J Bacteriol* 178: 6056-6058.

Jerg B., Gerischer U. 2008. Relevance of nucleotides of the PcaU binding site from *Acinetobacter baylyi.* *Microbiology* 154: 756-766.

Junker F., Ramos J.L. 1999. Involvement of the *cis/trans* isomerase Cti in solvent resistance of *Pseudomonas putida* DOT-T1E. *J Bacteriol* 181: 5693-5700.

Kieboom J., Bruinenberg R., Keizer-Gunnink I., de Bont J.A. 2001. Transposon mutations in the flagella biosynthetic pathway of the solvent-tolerant *Pseudomonas putida* S12 result in a decreased expression of solvent efflux genes. *FEMS Microbiol Lett* 198: 117-122.

Kim K., Lee S., Lee K., Lim D. 1998. Isolation and characterization of toluene-sensitive mutants from the toluene-resistant bacterium *Pseudomonas putida* GM73. *J Bacteriol* 180: 3692-3696.

Koronakis V., Sharff A., Koronakis E., Luisi B., Hughes C. 2000. Crystal structure of the bacterial membrane protein TolC central to multidrug efflux and protein export. *Nature* 405: 914-919.

Krell T., Molina-Henares A.J., Ramos J.L. 2006. The IclR family of transcriptional activators and repressors can be defined by a single profile. *Protein Sci* 15: 1207-1213.

Krulwich T.A., Lewinson O., Padan E., Bibi E. 2005. Do physiological roles foster persistence of drug/multidrug-efflux transporters? A case study. *Nat Rev Microbiol* 3: 566-572.

Kumari S., Beatty C.M., Browning D.F., Busby S.J., Simel E.J., Hovel-Miner G., Wolfe A.J. 2000. Regulation of acetyl coenzyme A synthetase in *Escherichia coli*. *J Bacteriol* 182: 4173-4179.

Lau P.C., Wang Y., Patel A., Labbé D., Bergeron H., Brousseau R., Konishi Y., Rawling M. 1997. A bacterial basic region leucine zipper histidine kinase regulating toluene degradation. *Proc Natl Acad Sci USA* 94: 1453-1458.

Lee S.W., Cooksey D.A. 2000. Genes expressed in *Pseudomonas putida* during colonization of a plant-pathogenic fungus. *Appl Environ Microbiol* 66: 2764-2772.

Lobedanz S., Bokma E., Symmons M.F., Koronakis E., Hughes C., Koronakis V. 2007. A periplasmic coiled-coil interface underlying TolC recruitment and the assembly of bacterial drug efflux pumps. *Proc Natl Acad Sci U S A* 104: 4612-4617.

Lorca G.L., Ezersky A., Lunin V.V., Walker J.R., Altamentova S., Evdokimova E., Vedadi M., Bochkarev A., Savchenko A. 2007. Glyoxylate and pyruvate are antagonistic effectors of the *Escherichia coli* IclR transcriptional regulator. *J Biol Chem* 282: 16476-16491.

Martins dos Santos V.A., Fouts D.E., Gill S.R., Pop M., Holmes M., Brinkac L., Beanan M., DeBoy R.T., Daugherty S., Kolonay J., Madupu R., Nelson W., White O., Peterson J., Khouri H., Hance I., Chris Lee P., Holtzapple E., Scanlan D., Tran K., Moazzez A., Utterback T., Rizzo M., Lee K., Kosack D., Moestl D., Wedler H., Lauber J., Stjepandic D., Hoheisel J., Straetz M., Heim S., Kiewitz C., Eisen J.A., Timmis K.N., Düsterhöft A., Tümmler B., Fraser C.M. 2002. Complete genome sequence and comparative analysis of the metabolically versatile *Pseudomonas putida* KT2440. *Environ Microbiol* 4: 799-808.

Mikolosko J., Bobyk K., Zgurskaya H.I., Ghosh P. 2006. Conformational flexibility in the multidrug efflux system protein AcrA. *Structure* 14: 577-587.

Molina L., Ramos C., Ronchel M.C., Molin S., Ramos J.L. 1998. Construction of an efficient biologically contained pseudomonas putida strain and its survival in outdoor assays. *Appl Environ Microbiol* 64: 2072-2078.

Molina L., Duque E., Gomez-Rodríguez M.J., Krell T., Lacal J., García-Puente A., Matilla M., Ramos J.L., Segura A. 2010. The pGRT1 plasmid confers extremophile properties to Pseudomonas. *Submitted in ISMES Journal.*

Molina-Henares A.J., Krell T., Guazzaroni M.E., Segura A., Ramos J.L. 2006. Members of the IclR family of bacterial transcriptional regulators function as activators and/or repressors. *FEMS Microbiol Rev* 30: 157-186.

Morita Y., Kataoka A., Shiota S., Mizushima T., Tsuchiya T. 2000. NorM of *Vibrio parahaemolyticus* is a Na$^+$-driven multidrug efflux pump. *J Bacteriol* 182: 6694-6697.

Mosqueda G., Ramos-González M.I., Ramos J.L. 1999. Toluene metabolism by the solvent-tolerant *Pseudomonas putida* DOT-T1E strain, and its role in solvent impermeabilization. *Gene* 232: 69-76.

Mosqueda G., Ramos J.L. 2000. A set of genes encoding a second toluene efflux system in *Pseudomonas putida* DOT-T1E is linked to the *tod* genes for toluene metabolism. *J Bacteriol* 182: 937-943.

Muñoz-Rojas J., Bernal P., Duque E., Godoy P., Segura A., Ramos J.L. 2006. Involvement of cyclopropane fatty acids in the response of *Pseudomonas putida* KT2440 to freeze-drying. *Appl Environ Microbiol* 72: 472-477.

Murakami S., Nakashima R., Yamashita E., Yamaguchi A. 2002. Crystal structure of bacterial multidrug efflux transporter AcrB. *Nature* 419: 587-593.

Murakami S. 2008. Multidrug efflux transporter, AcrB—the pumping mechanism *Curr Opin Struct Biol* 18: 459–465.

Niepold F., Anderson D., Mills D. 1985. Cloning determinants of pathogenesis from *Pseudomonas syringae* pathovar *syringae.* *Proc Natl Acad Sci U S A* 82: 406-410.

Nikaido H., Takatsuka Y. 2009. Mechanisms of RND multidrug efflux pumps. *Biochim Biophys Acta* 1794: 769-781.

Pabo C.O., Sauer R.T. 1992. Transcription factors: structural families and principles of DNA recognition. *Annu Rev Biochem* 61: 1053-1095.

Paulsen I.T. 2003. Multidrug efflux pumps and resistance: regulation and evolution. *Curr Opin Microbiol* 6: 446-451. Review.

Paulsen I.T., Brown M.H., Skurray R.A. 1996. Proton-dependent multidrug efflux systems. *Microbiol Rev* 60: 575-608.

Pellequer J.L., Wager-Smith K.A., Kay S.A., Getzoff E.D. 1998. Photoactive yellow protein: a structural prototype for the three-dimensional fold of the PAS domain superfamily. *Proc Natl Acad Sci* 95: 5884-5890.

Phoenix P., Keane A., Patel A., Bergeron H., Ghoshal S., Lau P.C. 2003. Characterization of a new solvent-responsive gene locus in *Pseudomonas putida* F1 and its functionalization as a versatile biosensor. *Environ Microbiol* 5: 1309-1327.

Piddock L.J. 2006. Multidrug-resistance efflux pumps - not just for resistance. *Nat Rev Microbiol* 4: 629-636.

Pinkart H.C., White D.C. 1997. Phospholipid biosynthesis and solvent tolerance in *Pseudomonas putida* strains. *J Bacteriol* 179: 4219-4226.

Pini C.V., Bernal P., Godoy P., Ramos J.L., Segura A. 2009. Cyclopropane fatty acids are involved in organic solvent tolerance but not in acid stress resistance in *Pseudomonas putida* DOT-T1E. *Microbial Biotech* 2: 253-261.

Poelarends G.J., Konings W.N. 2002. The transmembrane domains of the ABC multidrug transporter LmrA form a cytoplasmic exposed, aqueous chamber within the membrane. *J Biol Chem* 277: 42891-42898.

Popp R., Kohl T., Patz P., Trautwein G., Gerischer U. 2002. Differential DNA binding of transcriptional regulator PcaU from *Acinetobacter sp.* strain ADP1. *J Bacteriol* 184: 1988-1997.

Preston G.M., Bertrand N., Rainey P.B. 2001. Type III secretion in plant growth-promoting *Pseudomonas fluorescens* SBW25. *Mol Microbiol* 41: 999-1014.

Rainey P.B. 1999. Adaptation of *Pseudomonas fluorescens* to the plant rhizosphere. *Environ Microbiol* 1: 243-257.

Ramos J.L., Duque E., Huertas M.J., Haïdour A. 1995. Isolation and expansion of the catabolic potential of a *Pseudomonas putida* strain able to grow in the presence of high concentrations of aromatic hydrocarbons. *J Bacteriol* 177: 3911-3916.

Ramos J.L., Duque E., Rodríguez-Herva J.J., Godoy P., Haïdour A., Reyes F., and Fernández-Barrera A. 1997. Mechanisms for solvent tolerance in bacteria. *J Biol Chem* 272: 3887-3890.

Ramos J.L., Duque E., Godoy P., Segura A. 1998. Efflux pump involved in toluene tolerance in *Pseudomonas putida* DOT-T1E. *J Bacteriol* 180: 3323-3329.

Ramos J.L., Duque E., Gallegos M.T., Godoy P., Ramos-Gonzalez M.I., Rojas A., Teran W., Segura A. 2002. Mechanism of tolerance in gram-negative bacteria. *Annu Rev Microbiol* 56: 743-768.

Ramos J.L, Martínez-Bueno M., Molina-Henares A.J., Terán W., Watanabe K., Zhang X., Gallegos M.T., Brennan R., Tobes R. 2005. The TetR family of transcriptional repressors. *Microbiol Mol Biol Rev* 69: 326-356.

Ramos, J.L., Daniels, C., Krell, T., Duque, E., Godoy, P., De la Torre, J., Fernández-Escamilla, A.M., Daddoua, A., Navarro-Avilés, G., Fillet, S., Pini, C., Molina-Henares, M.A., Lacal, J., Busch, A., Silva-Jiménez, H., Rodríguez, S., Molina, L., Bursakov, S.A, Roca, A., and Segura, A. 2010. Sovent tolerance in Pseudomonas. *Encyclopedia of extremophiles* In press.

Ramos-González M.I., Campos M.J., Ramos J.L. 2005. Analysis of *Pseudomonas putida* KT2440 gene expression in the maize rhizosphere: *in vivo* expression technology capture and identification of root-activated promoters. *J Bacteriol* 187: 4033-4041.

Rodríguez-Herva J.J., García V., Hurtado A., Segura A., Ramos J.L. 2007. The *ttgGHI* solvent efflux pump operon of *Pseudomonas putida* DOT-T1E is located on a large self-transmissible plasmid. *Environ Microbiol* 9:1550-1561.

Rojas A., Duque E., Mosqueda G., Golden G., Hurtado A., Ramos J.L., Segura A. 2001. Three efflux pumps are required to provide efficient tolerance to toluene in *Pseudomonas putida* DOT-T1E. *J Bacteriol* 183: 3967-3973.

Rojas A., Segura A., Guazzaroni M.E., Terán W., Hurtado A., Gallegos M.T., Ramos J.L. 2003. In vivo and in vitro evidence that TtgV is the specific regulator of the TtgGHI multidrug and solvent efflux pump of *Pseudomonas putida.* *J Bacteriol* 185: 4755-4763.

Rojo F. 2001. Mechanisms of transcriptional repression. *Curr Opin Microbiol* 4: 145-51. Review.

Schell M.A. 1993. Molecular biology of the LysR family of transcriptional regulators. *Annu Rev Microbiol* 47: 597-626.

Schumacher M.A., Miller M.C., Grkovic S., Brown M.H., Skurray R.A., Brennan R.G. 2001. Structural mechanisms of QacR induction and multidrug recognition. *Science* 294: 2158-2163.

Schumacher M.A., Miller M.C., Grkovic S., Brown M.H., Skurray R.A., Brennan R.G. 2002. Structural basis for cooperative DNA binding by two dimers of the multidrug-binding protein QacR. *EMBO J* 21: 1210-1208.

Segura A., Duque E., Hurtado A., Ramos J.L. 2001. Mutations in genes involved in the flagellar export apparatus of the solvent-tolerant *Pseudomonas putida* DOT-T1E strain impair motility and lead to hypersensivity to toluene shocks. *J bacteriol* 183: 4127-4133.

Segura A., Rojas A., Hurtado A., Huertas M.J., Ramos J.L. 2003. Comparative genomic analysis of solvent extrusion pumps in *Pseudomonas* strains exhibiting different degrees of solvent tolerance. *Extremophiles* 7: 371-376.

Segura A., Godoy P., van Dillewijn P., Hurtado A., Arroyo N., Santacruz S., Ramos J.L. 2005. Proteomic analysis reveals the participation of energy- and stress-related proteins in the response of Pseudomonas putida DOT-T1E to toluene. *J Bacteriol* 187: 5937-5945.

Setubal J.C., Moreira L.M., da Silva A.C. 2005. Bacterial phytopathogens and genome science. *Curr Opin Microbiol* 8: 595-600.

Sikkema J., De Bont J.A. M., Poolman B. 1995. Mechanisms of membrane toxicity of hydrocarbons. *Microbiol Rev* 59: 201-222.

Singh P.K., Schaefer A.L., Parsek M.R., Moninger T.O., Welsh M.J., Greenberg E.P. 2000. Quorum-sensing signals indicate that cystic fibrosis lungs are infected with bacterial biofilms. *Nature* 407: 762-764.

Stover C.K., Pham X.Q., Erwin A.L., Mizoguchi S.D., Warrener P., Hickey M.J., Brinkman F.S., Hufnagle W.O., Kowalik D.J., Lagrou M., Garber R.L., Goltry L., Tolentino E., Westbrock-Wadman S., Yuan Y., Brody L.L., Coulter S.N., Folger K.R., Kas A., Larbig K., Lim R., Smith K., Spencer D., Wong G.K., Wu Z., Paulsen I.T., Reizer J., Saier M.H., Hancock R.E., Lory S., Olson M.V. 2000. Complete genome sequence of *Pseudomonas aeruginosa* PAO1, an opportunist pathogen. *Nature* 406: 959-964.

Sudip K. S., Om V. Singh and Rakesh K. Jain. 2002. Polycyclic aromatic hydrocarbons: environmental pollution and bioremediation. *TRENDS in Biotechnology* 20: 243-248.

Sunnarborg A., Klumpp D., Chung T., LaPorte D.C. 1990. Regulation of the glyoxylate bypass operon: cloning and characterization of iclR. *J Bacteriol* 172: 2642-2649.

Tamura N., Murakami S., Oyama Y., Ishiguro M., Yamaguchi A. 2005. Direct interaction of multidrug efflux transporter AcrB and outer membrane channel TolC detected *via* site-directed disulfide cross-linking. *Biochemistry* 44: 11115-11121.

Terán W., Felipe A., Segura A., Rojas A., Ramos J.L., Gallegos M.T. 2003. Antibiotic-dependent induction of *Pseudomonas putida* DOT-T1E TtgABC efflux pump is mediated by the drug binding repressor TtgR. *Antimicrob Agents Chemother* 47: 3067-3072.

Terán W., Krell T., Ramos J.L., Gallegos M.T. 2006. Effector-repressor interactions, binding of a single effector molecule to the operator-bound TtgR homodimer mediates derepression. *J Biol Chem* 281: 7102-7109.

Tobes R., Ramos J.L. 2002. AraC-XylS database: a family of positive transcriptional regulators in bacteria. *Nucleic Acids Res* 30: 318-321.

Tropel D., van der Meer J.R. 2004. Bacterial transcriptional regulators for degradation pathways of aromatic compounds. *Microbiol Mol Biol Rev* 68: 474-500.

Velamakanni S., Lau C.H., Gutmann D.A., Venter H., Barrera N.P., Seeger M.A., Woebking B., Matak-Vinkovic D., Balakrishnan L., Yao Y., U E.C., Shilling R.A., Robinson C.V., Thorn P., van Veen H.W. 2009. A multidrug ABC transporter with a taste for salt. *PloS One* 4: e6137.

Walker J.R., Altamentova S., Ezersky A., Lorca G., Skarina T., Kudritska M., Ball L.J., Bochkarev A., Savchenko A. 2006. Structural and biochemical study of effector molecule recognition by the *E.coli* glyoxylate and allantoin utilization regulatory protein AllR. *J Mol Biol* 358: 810-828.

Volkers R.J., de Jong A.L., Hulst A.G., van Baar B.L., de Bont J.A., Wery J. 2006. Chemostat-based proteomic analysis of toluene-affected *Pseudomonas putida* S12. *Environ Microbiol* 8: 1674-1679.

Weber F.J., Isken S., de Bont J.A. 1994. *Cis/trans* isomerization of fatty acids as a defence mechanism of *Pseudomonas putida* strains to toxic concentrations of toluene. *Microbiology* 140: 2013-2017.

White D.G., Goldman J.D., Demple B., Levy S.B.1997. Role of the *acrAB* locus in organic solvent tolerance mediated by expression of *marA*, *soxS*, or *robA* in *Escherichia coli*. *J Bacteriol* 179: 6122-6126.

Yamamoto K., Ishihama A. 2003. Two different modes of transcription repression of the *Escherichia coli* acetate operon by IclR. *Mol Microbiol* 47: 183-194.

Yerushalmi H., Lebendiker M., Schuldiner S. 1995. EmrE, an *Escherichia coli* 12-kDa multidrug transporter, exchanges toxic cations and H+ and is soluble in organic solvents. *J Biol Chem* 270: 6856-6863.

Yousef-Coronado F., Travieso M.L., Espinosa-Urgel M. 2008. Different, overlapping mechanisms for colonization of abiotic and plant surfaces by Pseudomonas putida. *FEMS Microbiol Lett* 288: 118-124.

Zhang R. G., Kim Y., Skarina T., Beasley S., Laskowski R., Arrowsmith C. 2002. Crystal structure of Thermotoga maritime 0065, a member of the IclR transcriptional factor family. *J Biol Chem* 277: 19183-19190.